Stony Brook University

OFFICIAL COPY

The official electronic file of this thesis or dissertation is maintained by the University Libraries on behalf of The Graduate School at Stony Brook University.

© All Rights Reserved by Author.

Using Quantitative SILAC Proteomics to Identify Mek1 Substrates During Yeast Meiosis

A Dissertation Presented

by

Raymond Theodore Suhandynata

to

The Graduate School

in Partial Fulfillment of the

Requirements

for the Degree of

Doctor of Philosophy

in

Biochemistry and Structural Biology

Stony Brook University

August 2016

Stony Brook University

The Graduate School

Raymond Theodore Suhandynata

We, the dissertation committee for the above candidate for the

Doctor of Philosophy degree, hereby recommend

acceptance of this dissertation.

Nancy M. Hollingsworth, Ph.D.-Dissertation Advisor
Professor, Department of Biochemistry and Cell Biology

Aaron Neiman, Ph.D-Chairperson of Defense
Professor, Department of Biochemistry and Cell Biology

Ed Luk, Ph.D.
Assistant Professor, Department of Biochemistry and Cell Biology

Bruce Futcher, Ph.D.
Professor, Department of Molecular Genetics and Microbiology

This dissertation is accepted by the Graduate School

Nancy Goroff

Interim Dean of the Graduate School

Abstract of the Dissertation

Using Quantitative SILAC Proteomics to Identify Mek1 Substrates During Yeast Meiosis

by

Raymond Theodore Suhandynata

Doctor of Philosophy

in

Biochemistry and Structural Biology

Stony Brook University

2016

The exchange of reciprocal information between homologous chromosomes in conjunction with sister chromatid cohesion ensures proper segregation of homologous chromosomes during Meiosis I. Improper segregation of homologous chromosomes during meiosis leads to chromosomal imbalance, which in humans can lead to genetic disorders such as Down syndrome (Trisomy 21) and Turner syndrome (monosomy of the X chromosome).

Meiotic recombination begins with the initiation of double-strand breaks (DSBs) and the biased repair of these breaks by the homologous chromosome. This inter-homolog (IH) bias is upheld by the meiotic recombination checkpoint kinase Mek1. Mek1 is a meiosis specific serine/threonine kinase that prevents cells from progressing through meiosis I with unrepaired DSBs and also places a bias for meiotic DSBs to be repaired using the homologous chromosome. Although Mek1 has been previously shown to be necessary for proper chromosome segregation via its promotion of IH bias and checkpoint functions, non-phosphorylatable mutants of Mek1 substrates, with the exception of Mek1 itself, do not pheno-copy a *mek1*Δ. This suggests that there are other Mek1 substrates that promote IH bias as well as the meiotic recombination checkpoint.

To identify novel substrates of Mek1, a method for sporulating yeast out of synthetic medium was developed. This method allows the application of quantitative stable isotope labeling by amino acids in cell culture (SILAC) phosphoproteomics to meiosis, thereby allowing identification of novel Mek1 substrates in a global and

unbiased manner. An analog sensitive allele of *MEK1* (*mek1-as*) was used to conditionally inactivate Mek1 in *dmc1*Δ-arrested cells containing heavy isotopes of arginine and lysine. Mek1 phosphosites are underrepresented in the heavy culture, resulting in light/heavy (L/H) phosphopeptide ratios ≥2. Known substrates of Mek1, including Rad54 and Mek1 itself, were identified as proof of principle.

Phosphopeptides from the *dmc1*Δ *mek1-as* experiments were divided into three classes based on their L/H ratio. Motif analysis of the different classes revealed that the Mek1 consensus motif, RXXT, was specifically enriched in the Mek1 active culture. Thus, 16 RXXT proteins were identified as candidate Mek1 substrates, with Spp1 and Rad17 having the most functional relevance to the known functions of Mek1.

Motif analysis of the phosphorylation events that become enriched in the Mek1 inactivated culture revealed a D/EXS/Tψ motif that matches the known consensus motif of Polo-Like Kinase or Cdc5 in budding yeast, leading to the identification of 10 candidate Cdc5 substrates.

Finally, SILAC experiments using *mek1-as* and *ntd80*-arrested cells indicated that phosphorylation of the synaptonemal complex protein Zip1 protein is dependent upon Mek1. My main contribution to this collaboration with Dr. Xiangyu Chen were identifying the Zip1 phosphorylation sites characterized in (Chen et al., 2015).

Table of Contents

List of Figures vii

List of Tables ix

List of Abbreviations x

CHAPTER ONE Introduction 1

Meioic Chromosome segregation and its significance 2

Using Saccharomyces cerevisiae to study meiosis 2

Meiotic Recombination in *Saccharomyces cerevisiae* 5

Rad51 and Dmc1 are necessary for proper interhomolog recombination 8

Meiotic recombination occurs in the context of a meiosis-specific structure formed between homologs called the synaptonemal complex 9

Regulation of Meiotic DSB repair by Mek1 14

Quantitative SILAC Proteomics and the synthetic sporulation problem 17

Using Phosphoproteomics to Identify Kinase Substrates 18

CHAPTER TWO A method for sporulating budding yeast cells that allows for unbiased identification of kinase substrates using stable isotope labeling by amino acids in cell culture 20

Abstract 21

Introduction 22

Materials and Methods 24

Results 35

Discussion 47

CHAPTER THREE Identifying novel substrates of Mek1 at the *dmc1*Δ arrest using quantitative phosphoproteomics 50

Introduction 51

Results 51

CHAPTER FOUR 78

Identifying the synaptonemal complex protein, Zip1, as a Mek1-dependent substrate using SILAC 78

Introduction 79

Methods 80

Results 83
CHAPTER FIVE Discussion 93
References 99

List of Figures

Figure 1-1 Meiotic chromosome segregation

Figure 1-2 Molecular pathways of meiotic DSB processing

Figure 1-3 SC assembly in meiotic prophase I

Figure 1-4 Initiation of meiotic DSBs

Figure 1-5 Activation of the meiotic recombination checkpoint

Figure 2-1 Comparison of various meiotic parameters in cultures grown in either YPA or RPS-L prior to sporulation

Figure 2-2 Fate of meiotic DSBs in *dmc1*Δ *mek1-as* diploids with or without inhibitor

Figure 2-3 Relative abundance of total and phosphorylated peptides from a *dmc1*Δ *mek1-as* SILAC experiment

Figure 2-4 Location of phosphopeptides on Mek1, Rad54 and Rec8

Figure 2-5 Distribution of phosphorylated peptides and their light:heavy (L/H) ratios for Mek1, Rad54 and Rec8

Figure 3-1 Integrated light/heavy (L/H) ratios of phosphopeptides obtained from the merged non-redundant phosphopeptide datasets from two SILAC experiments using *dmc1*Δ *mek1-as* diploids

Figure 3-2 Motif analysis of the *dmc1*Δ *mek1-as* SILAC phosphopeptides

Figure 3-3 Graphical representation of RXXT phosphorylation sites identified in *dmc1*Δ *mek1-as cells*

Figure 3-4 Distribution of phosphosites on Class 1 proteins containing at least one RXXT motif

Figure 4-1 Zip1 staining can be broken down into three distinct patterns

Figure 4-2 Identification of putative Mek1-regulated phosphosites on Zip1

Figure 4-3 Integrated light/heavy (L/H) ratios of phosphopeptides obtained from the merged non-redundant phosphopeptide datasets from two SILAC experiments using *mek1-as ndt80*Δ

List of Tables

Table 2-1 *S. cerevisiae* strains

Table 2-2 Sporulation and spore viability under various conditions after pregrowth in either YPA, RPS-L or RPS-H.

Table 3-1 Number of phospho-peptides containing consensus motifs in *dmc1*Δ *mek1-as* phosphopeptides with different L/H ratios

Table 3-2 Proteins containing RXXT motifs from the subset of *dmc1*Δ *mek1-as* phosphopeptides with L/H ratios >2.

Table 3-3 Class 1 proteins containing the SQ Mec1/Tel1 motif.

Table 3-4 Proteins containing D/EXS/Tψ motif and the Polo Box binding motif from the subset of *dmc1*Δ *mek1-as* phosphopeptides with L/H ratios <0.5.

Table 4-1 Scoring of *mek1-as ndt80*Δ chromosome spreads for Zip1 staining

Table 4-2 Zip1 phosphopeptides and their Light/Heavy (L/H) ratios from a *mek1-as ndt80*Δ SILAC experiment

List of Abbreviations

μg: microgram

μL: microliter

1-NA-PP1: 4-amino-1-tert-butyl-3-(1'naphthyl) pyrazolo [3,4-d] pyrimidine

AE: Axial element

as: analog sensitive

ATM/ATR: Ataxia Telangiectasia Mutated/Ataxia Telengiectasia and Rad3 related

ATP: Adenosine 5'-triphosphate

CO: Crossover

DAPI: 4'6-diamidino-2-phenylindole

dHJ: Double Holliday junction

DNA: Deoxyribonucleic acid

DSB: Double strand break

EDTA: Ethylenediamine tetraacetic acid

FHA: Forkhead associated domain

HCl: Hydrochloric acid

HILIC: Hydrophilic interaction liquid chromatography

HORMA: Hop1 Rev7 Mad2

HPLC: High pressure/performance liquid chromatography

hr: hour

IH: Interhomolog

IMAC: Immobilized Metal Affinity Chromatography

JM: Joint molecule

LC-MS/MS: Liquid chromatography tandem mass spectrometry

mg: milligram

List of Abbreviations continued

MI: Meiosis I

MII: Meiosis II

min: minute

mL: milliliter (this is how you wrote this in Chapter 4—make sure it is consistent

NCO: Noncrossover

OD: optical density

PCR: Polymerase chain reaction

RPA: Replication Protein A

RPS: Ray's pre-sporulation medium

SC: Synaptonemal complex

SD: Synthetic dextrose

SDSA: Synthesis dependent strand annealing

SILAC: Stable isotope labeling by amino acids in cell culture

SPM: sporulation medium (2% potassium acetate)

Spo: Sporulation medium (2% potassium acetate)

ssDNA: single strand DNA

TBS: Tris base aaline

TFA: Trifluoroacetic acid

WT: wild-type

YPA: yeast extract-peptone-acetate (Pre-sporulation medium)

YPD: yeast extract-peptone-dextrose

CHAPTER ONE

Introduction

Meiotic chromosome segregation and its significance

Down syndrome (Trisomy 21), Turner syndrome (monosomy of the X chromosome), and a significant percentage of spontaneous abortions are caused by an imbalance in chromosome number, or aneuploidy, resulting from mistakes during human meiosis (Eichenlaub-Ritter, 2012). Meiosis is a specialized type of cell division that produces gametes necessary for sexual reproduction. In meiosis, one round of DNA replication is followed by two rounds of chromosome segregation **(Fig 1-1)**. The first division (Meiosis I or MI) is reductional, meaning that homologous chromosomes separate to opposite poles, while the second division (Meiosis II or MII) is equational, in that sister chromatids segregate to opposite poles. The result is four haploid cells, each containing half the chromosome number of the parental diploid cell. Aneuploidy is typically caused by improper chromosome segregation termed non-disjunction, and in human pregnancies, is mostly attributable to errors at MI in mothers (Nagaoka et al., 2012). Proper segregation at MI requires connections between homologous chromosomes that are comprised of a combination of sister chromatid cohesion and interhomolog recombination (Petronczki et al., 2003). Therefore defects in the regulation and execution of meiotic recombination can lead to non-disjunction in MI, resulting in aneuploidy.

Using *Saccharomyces cerevisiae* to study meiosis

The budding yeast, *Saccharomyces cerevisiae*, has been used for the last 50 years as a model organism for studying meiosis (Liu and West, 2004). Meiosis is an evolutionarily conserved process and *S. cerevisiae* is more amenable to genetic approaches than metazoans. Furthermore, mutations in mammalian genes that are

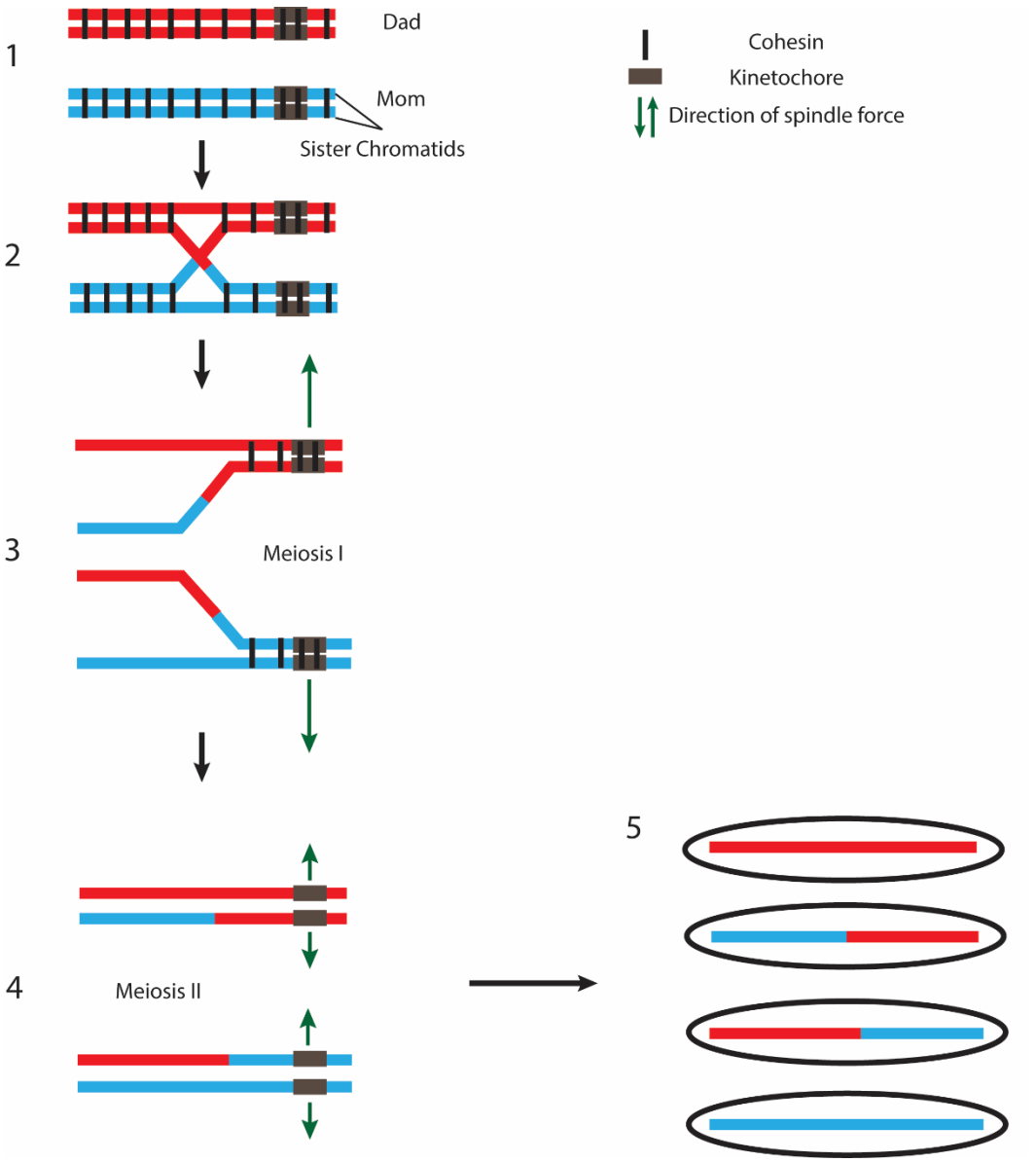

Figure 1-1: **Meiotic chromosome segregation.** 1) Following premeiotic DNA replication, sister chromatids are held together by meiosis-specific cohesin complexes. 2) Recombination between non-sister chromatids generates crossovers, which together with sister chromatid cohesion, physically connect the homologs. 3) At MI, cohesion is lost on chromosome arms but not the centromeres, allowing homologous chromosomes to separate to opposite poles. 4) At MII, cohesion at centromeres is lost allowing sister chromatids to segregate to opposite poles. 5) This generates four haploid meiotic products. In yeast the gametes are called spores and are packaged together in a sac called an ascus or tetrad.

orthologous to genes found in *S. cerevisiae* exhibit phenotypes similar to the equivalent budding yeast mutants, indicating that studying meiosis in *S. cerevisiae* should lead to insights into the biology of human meiosis (Villeneuve and Hillers, 2001).

The life cycle of *S. cerevisiae* can be broken into three distinct stages. The first is cell proliferation, where one cell gives rise to a second cell that is genetically identical by mitotic growth. The second and third stages result in a change in ploidy of a cell, by either two haploids mating to form a diploid or a diploid undergoing meiosis to form four haploid spores (Herskowitz, 1988). Budding yeast has two distinct mating types known as *MATα* and *MAT***a**, which can either proliferate as haploids through mitotic growth, or mate together to form a diploid *MAT***a** / *MATα* cell. Diploid cells can divide mitotically and can also be induced to undergo meiosis by nitrogen starvation in the presence of a nonfermentable carbon source. Sporulation begins with meiosis, which leads to the production of four haploid nuclei. These nuclei are then individually packaged within *de novo*-formed plasma membranes to form spores within the mother cells. Sporulated cells containing the four haploid spores are called tetrads or asci (singular, ascus) (Neiman, 2011).There are many advantages for using budding yeast as a model organism for meiotic research. (1) The SK1 strain undergoes efficient and relatively synchronous meiosis (Primig et al., 2000). (2) Tetrad dissection of the spores in an ascus allows analysis of the four meiotic products from the same meiosis, either genetically or by sequencing of entire genomes to precisely look at recombination products at the nucleotide level (Chen et al., 2008; Malkova et al., 2004). (3) Physical assays exist to detect intermediates at different steps in recombination, including double strand breaks (DSBs), single end invasion intermediates (SEIs), double Holliday

junctions (dHJs), crossovers (COs) and noncrossovers (NCOs) (see below) (Cao et al., 1990; Collins and Newlon, 1994; Hunter and Kleckner, 2001; Schwacha and Kleckner, 1994; Storlazzi et al., 1995; Thacker et al., 2014). (4) Genetic assays can be used to measure CO interference, the probability that a crossover at one locus reduces the probability of a second crossover nearby, as can whole genome sequencing (Chen et al., 2008; Malkova et al., 2004; Muller, 1916; Sturtevant, 1913; Sym and Roeder, 1994). (5) Cytological assays combining chromosome spreads with immunostaining or fluorescently tagged proteins can reveal where proteins localize on meiotic chromosomes (Dresser and Giroux, 1988; Tung and Roeder, 1998; White et al., 2004). (6) The ability to obtain large numbers of cells facilitates biochemical experiments.

Meiotic recombination in *Saccharomyces cerevisiae*

In addition to generating genetically diverse gametes, meiotic recombination has an important mechanical role in establishing physical connections between homologous chromosomes. Recombination is initiated by the introduction of programmed double strand breaks (DSBs) catalyzed by a meiosis-specific endonuclease called Spo11 at discrete regions of the genome known as hotspots (**Fig 1-2**) (Keeney et al., 1997; Pan and Keeney, 2007). After cleavage, Spo11 covalently attached to the 3' ends of a break is removed by endonucleolytic cleavage to release "Spo11-oligonucleotides" (Neale and Keeney, 2009; Pan and Keeney, 2009). Upon removal of Spo11, DSBs are resected in a 5' to 3' direction (Cao et al., 1990; Sun et al., 1991). The resulting 3' ends are then bound by the mitotic recombinase Rad51, as well as the meiosis-specific recombinase Dmc1, to form nucleoprotein filaments that mediate strand invasion of homologous chromosomes (Brown et al., 2015; Cloud et al., 2012; Kurzbauer et al., 2012) (**Fig 1-2**).

Extension of the invading 3' end by DNA polymerase displaces the strand of like polarity to form a displacement or D-loop (**Fig 1-2**). In some cases, the extended strand is disassembled from the D-loop by a protein complex comprised of the Sgs1 helicase, Top3 topisomerase and RmiI (called the STR complex) (Kaur et al., 2015; Tang et al., 2015). The extended strand can then anneal to the other side of the break, such that the breaks are repaired without exchange to create NCOs in a process called synthesis-dependent strand annealing (SDSA) (Allers and Lichten, 2001; McMahill et al., 2007; Nassif et al., 1994). Crossover formation requires that the D-loop be extended by DNA synthesis of the invading strand until the displaced single strand anneals to the other side of the DSB in a process known as second end capture. When the two ends are covalently attached by ligation, a dHJ intermediate is formed (**Fig 1-2**) (Schwacha and Kleckner, 1995). In wild-type meiosis, most of the dHJs are resolved in a biased way by the Mlh1-Mlh3-Exo1 complex to generate COs that are distributed throughout the genome by interference (Allers and Lichten, 2001; Argueso et al., 2004; Zakharyevich et al., 2010; Zakharyevich et al., 2012). In addition, a small fraction of COs and NCOs is formed by the unbiased resolution of dHJs by structure-specific endonucleases such as Mus81-Mms4 and Yen1 (Jessop and Lichten, 2008; Zakharyevich et al., 2012) (**Fig 1-2**). In addition, NCOs may be formed by dissolution of dHJs via the Sgs1-Top3-Rmi1 complex (Kaur et al., 2015; Tang et al., 2015).

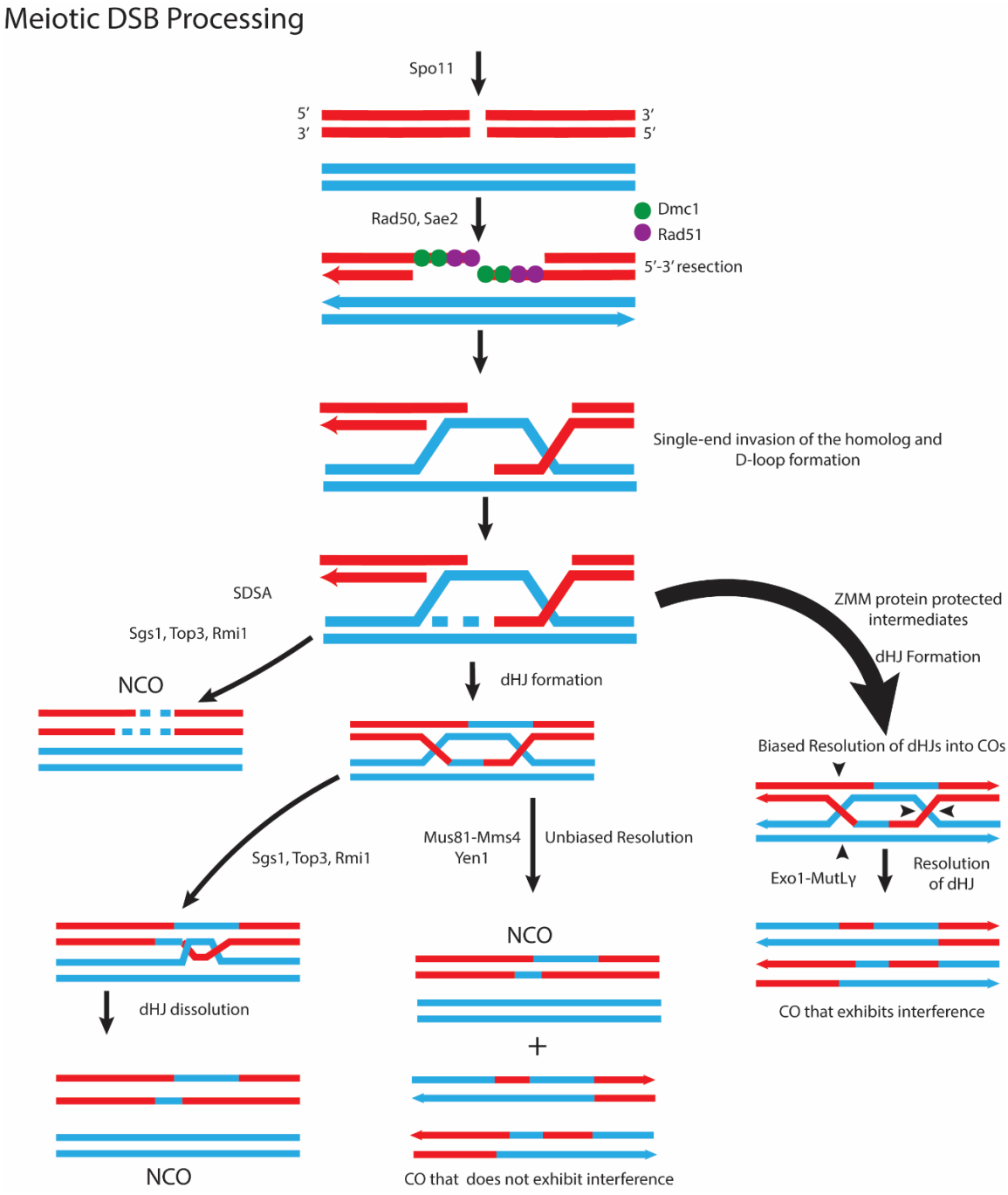

Figure 1-2: **Molecular pathways of meiotic DSB processing**. Following pre-meiotic DNA replication and Spo11 induced DSB formation, DSB repair can be directed down 4 pathways. The major pathway involves the ZMM proteins, and directs dHJs to be resolved into the majority of meiotic COs that are observed. Alternatively, COs and NCOs can be generated via a minor pathway that utilized the structure selective nucleases to generate COs that do not exhibit interference. Finally NCOs are generated via the SDSA and dissolution pathways that require the STR complex.

Analysis of meiotic DSBs successfully mapped a majority of hotspots in yeast (Pan and Keeney, 2007). In addition, artificial hotspots on chromosome III have been used extensively to analyze recombination (Goldfarb and Lichten, 2010; Hunter and Kleckner, 2001; Jessop et al., 2005). DNA isolated from cells at different times in meiosis are digested with enzymes that cut at polymorphic restriction sites flanking the hotspots. Probing of the DNA using Southern blots can be used to detect DSBs, SEIs, dHJs, COs, and NCOs, (Hunter and Kleckner, 2001; Kaur et al., 2015).

Rad51 and Dmc1 are necessary for proper interhomolog recombination

Rad51 and the meiosis specific protein, Dmc1, are RecA orthologs that are both required for interhomolog bias (**Fig 1-2**) (Cloud et al., 2012; Kurzbauer et al., 2012; Lao et al., 2008; Schwacha and Kleckner, 1997). These two proteins form filaments on the 3' ends of meiotic DSBs, which catalyze strand invasion of homologous chromosomes (Brown et al., 2015). Rad51 strand exchange activity is dispensable for meiotic interhomolog recombination, although the presence of Rad51 is necessary for the interhomolog bias mediated by Dmc1 (Cloud et al., 2012; Lao et al., 2008; Schwacha and Kleckner, 1997). During meiosis, downregulation of Rad51 is important so that it does not compete with Dmc1 for the repair of meiotic DSBs. Premature activation of Rad51 in meiosis leads to increased sister recombination and MI nondisjunction in the presence of a less efficient version of *DMC1* (Liu et al., 2014). When *DMC1* is absent, meiotic DSBs are unrepaired due to the inactivation of Rad51 (Bishop et al., 1992; Niu et al., 2009; Tsubouchi and Roeder, 2006).

Meiotic recombination occurs in the context of a meiosis-specific structure formed between homologs called the synaptonemal complex

During meiosis, homologous chromosomes condense and become physically associated by formation of a structure called the synaptonemal complex (SC). The SC is a tripartite structure that consists of a central region and two lateral elements (Page and Hawley, 2004) (**Figure 1-3**). The first step in SC formation is the condensation of sister chromatids along protein cores to form axial elements (AEs) which later become known as lateral elements when chromosomes synapse to form the SC. Condensation occurs by the formation of chromatin loops that are tethered to the chromosome axes which contain the meiosis-specific proteins, Red1, Hop1 and Rec8 (Bailis and Roeder, 1998; Hollingsworth et al., 1990; Panizza et al., 2011; Smith and Roeder, 1997; Thompson and Roeder, 1989). Rec8 is the meiosis-specific kleisin component of the multisubunit cohesin complex that hold sister chromatids together (Klein et al., 1999). Meiosis-specific cohesin complexes containing Rec8 are loaded onto chromosomes during premeiotic S phase, after which they are removed in two steps: from chromosome arms at MI and centromeres at MII (Buonomo et al., 2000). Recombination between homologs brings AEs together, which are then connected by the polymerization of the meiosis-specific transverse filament protein, Zip1 (Sym and Roeder, 1995; Tung and Roeder, 1998).

In contrast to mitotic recombination which occurs preferentially between sister chromatids, homologs are the preferred partner for DSB repair in meiosis. Only 13%-35% of joint molecules (JMs) formed in meiosis are between sister chromatids

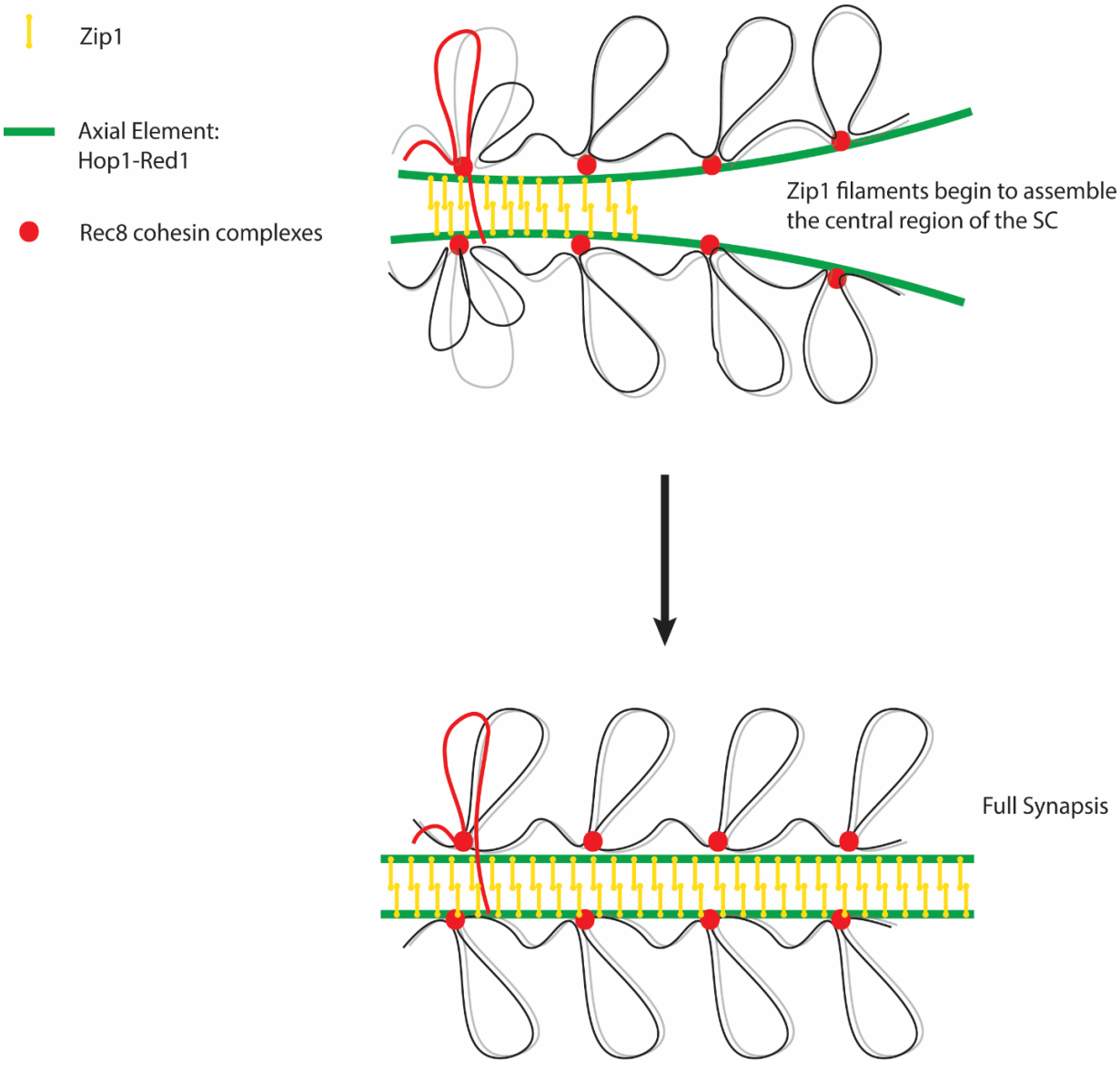

Figure 1-3: **SC assembly in meiotic prophase I.** The transverse filament, Zip1 shown in yellow, physically connects the axial elements, shown in green, to form the tripartite structure of the synaptonemal complex. Homologs are brought together by recombination, indicated in red, between homologs. Zip1 proteins form homo-oligormers to make up the transverse filament of the SC. Pachytene is the stage of meiotic prophase in which are of the chromosomes have formed SC (i.e., are fully synapsed).

(Bzymek et al., 2010; Jessop and Lichten, 2008; Kadyk and Hartwell, 1992; Kim et al., 2010; Oh et al., 2007; Schwacha and Kleckner, 1994).

This preference for interhomolog over intersister recombination is referred to as interhomolog (IH) bias. The AE components, *RED1*, *HOP1*, and the meiosis-specific kinase *MEK1* are required for interhomolog bias in meiosis (Bishop et al., 1999; Hollingsworth and Byers, 1989; Kim et al., 2010; Niu et al., 2005; Thompson and Stahl, 1999; Wan et al., 2004; Xu et al., 1997). Hop1 contains a HORMA (Hop1, Rev1, Mad2 homology) domain and other HORMA domain containing proteins have been found in humans, mice, plants, and nematodes (Aravind and Koonin, 1998; Armstrong et al., 2002; Couteau et al., 2004; Kim et al., 2014; Pangas et al., 2004). Studies of mutants in one of the orthologs of *HOP1* in nematodes, mice and plants indicate that Hop1 orthologs inhibit the use of sister chromatids as repair templates, suggesting that the mechanism for interhomolog bias is evolutionarily conserved (Caryl et al., 2000; Couteau et al., 2004; Wojtasz et al., 2009).

Meiotic cells deliberately introduce DSBs into their genomes which, if not properly repaired, would be lethal to cells. Therefore formation of DSBs is tightly regulated to occur only after premeiotic S-phase is complete (Borde et al., 2000). This timing is accomplished by phosphorylation of the axis associated protein Mer2 by Cdc7-Dbf4 kinase (called DDK for Dbf4-dependent kinase) after priming by phosphorylation the S-phase cyclin dependent kinase (Henderson et al., 2006; Sasanuma et al., 2008; Wan et al., 2008). DDK phosphorylates Mer2 as it travels with the replication fork such that only replicated DNA contains phosphorylated Mer2 (Murakami and Keeney, 2014). Phosphorylated Mer2 then recruits Rec114, Mei3 and Mer2, which bring Spo11 to the

axis (Henderson et al., 2006; Panizza et al., 2011; Sasanuma et al., 2008) (**Fig 1-4**). Hotspot sequences tend to be localized in the nucleosome free regions of promoters (Pan and Keeney, 2007; Wu and Lichten, 1994). Nucleosomes flanking hotspot sequences are trimethylated on Histone H3 by the SET1/COMPASS complex (Borde et al., 2009). A component of this complex, Spp1, binds to Mer2 and trimethylated H3K4, forming a bridge that brings the hotspot sequences to the chromosome axes where Spo11 cleavage can occur (Acquaviva et al., 2013; Sommermeyer et al., 2013) (**Fig 1-4**).

DSB formation triggers the meiotic recombination checkpoint, which is active during normal meiosis, and is spearheaded by Mec1 and Tel1, homologs of the mammalian ATR and ATM kinases, respectively (Carballo et al., 2008; Gobbini et al., 2013; Ho and Burgess, 2011; Subramanian and Hochwagen, 2014). Unresected DSBs activate a checkpoint pathway that is dependent on *TEL1*, while resected DSBs activate a checkpoint pathway dependent on *MEC1* (Ho and Burgess, 2011; Lydall et al., 1996; Usui et al., 2001). Mec1/Tel1 phosphorylates a broad set of overlapping substrates on serine-glutamine (SQ) or threonine-glutamine (TQ) residues (Traven and Heierhorst, 2005). One substrate of Mec1 is Hop1 (Carballo et al., 2008). Mek1 contains a forkhead associated (FHA) domain in its N-terminus, which is a conserved phospho-threonine binding domain (Carballo et al., 2008; Chuang et al., 2012; Durocher et al., 2000).

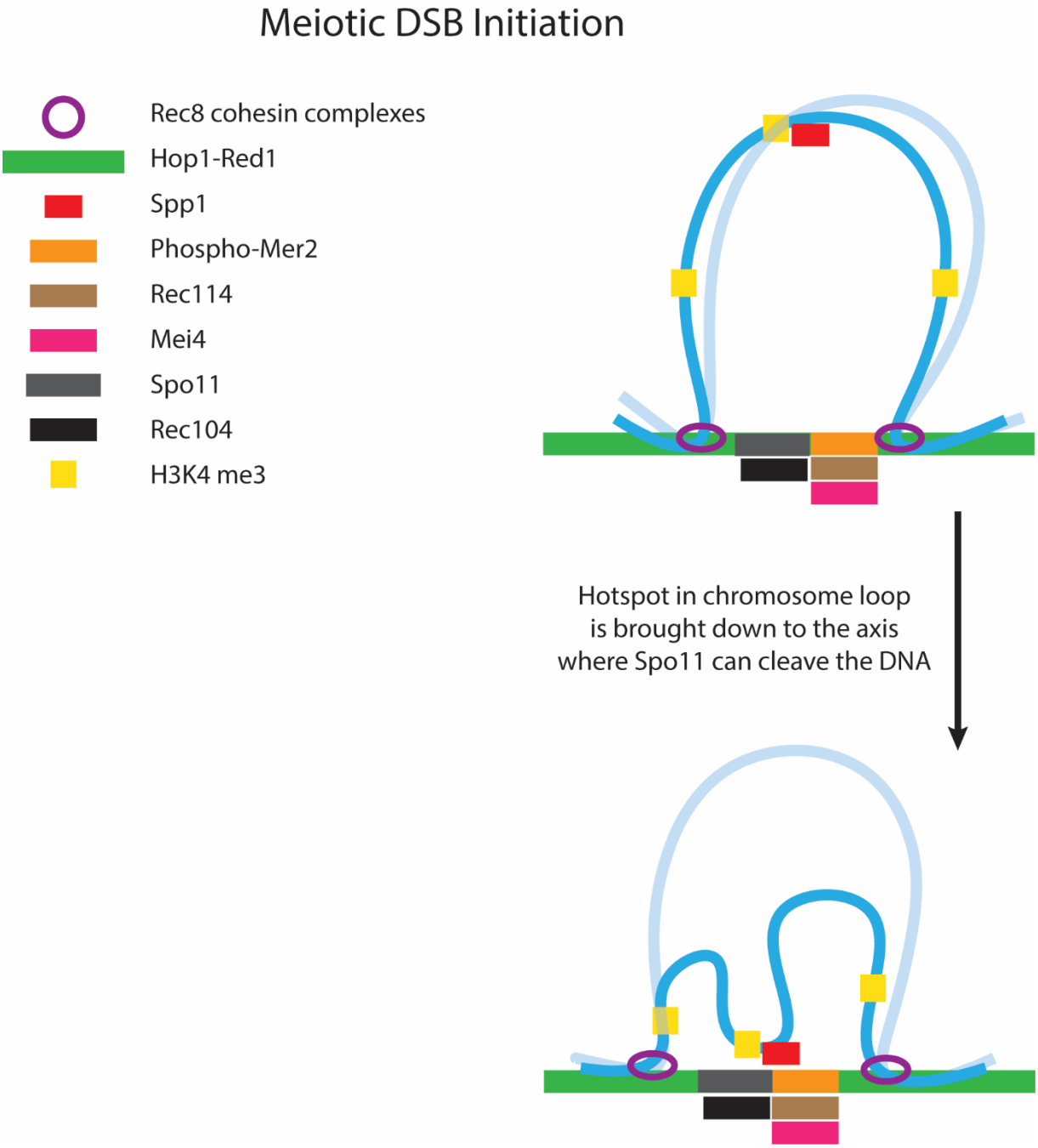

Figure 1-4: **Initiation of meiotic DSBs.** Following DNA replication, indicated by the two blue lines of DNA, the Spo11 endonuclease is recruited to the chromosome axis via its interaction with Rec114-Mei4-Rec104 that is bound to phosphorylated Mer2. The nucleosomes adjacent to hotspots are tri-methylated, indicated by yellow box, and are brought down to the chromosome axis, where Spo11 is located, via the Spp1 protein. This is accomplished through Spp1's Mer2 interaction domain as well as Spp1's PHD domain that binds tri-methylated H3K4.

Mec1/Tel1-phosphorylated Hop1 recruits Mek1 to chromosome axes via the FHA domain where the kinase becomes activated by autophosphorylation *in trans* (Carballo et al., 2008; Niu et al., 2007; Niu et al., 2005). Locally activated Mek1 is then able to regulate both the meiotic recombination checkpoint, which monitors the progression of DNA repair, interhomolog bias, and interhomolog recombination pathway choice (Chen et al., 2015; Niu et al., 2007; Niu et al., 2005; Wan et al., 2004).

Regulation of meiotic DSB repair by Mek1

In budding yeast, the purpose of the meiotic recombination checkpoint is to monitor recombination and insure that meiotic progression does not proceed into MI prior to the repair of the DSBs (Subramanian and Hochwagen, 2014). Mutants that initiate, but fail to complete, DSB repair trigger a meiotic prophase arrest (Lydall et al., 1996). For example, *dmc1*Δ generates resected DSBs that are unable to undergo strand invasion resulting in an MI prophase arrest (Bishop et al., 1992; Dresser et al., 1997; Hunter and Kleckner, 2001). This arrest was shown to be a checkpoint response in that the mitotic DNA damage checkpoint genes, *MEC1, RAD17,* and *RAD24,* are not required for DSB formation, resolution of DSBs, or for 5' resection of DSBs, but are required for the meiotic checkpoint arrest of a *dmc1*Δ strain (Lydall et al., 1996). Rad17 is part of the 9-1-1 complex (Rad17-Mec3-Ddc1) that is loaded onto the sites of DNA damage by the Rad24-RFC clamp loader via Replication Protein A (RPA) coated ssDNA (Majka and Burgers, 2003; Majka et al., 2006) (**Fig 1-5**). This leads to the recruitment of the Mec1 kinase that to the sites of DNA damage through its interaction with the Ddc2 subunit of the 9-1-1 complex and its subsequent activation (Majka et al., 2006).

Mek1 is a meiosis specific ortholog of the mitotic Rad53 checkpoint kinase in *S cerevisiae* (Usui et al., 2001). Deletion of *MEK1* results in loss of spore viability due to Meiosis I non-disjunction (Leem and Ogawa, 1992; Rockmill and Roeder, 1991). Non-disjunction is due to a loss of interhomolog bias, leading to the sister chromatid being used as the template for repair of the programmed DSBs and the random segregation of chromosomes at meiosis I (Kim et al., 2010; Niu et al., 2005). A specific point mutation in Mek1, *Q241G*, creates a conditional allele, *mek1-as,* which can be specifically inhibited by the small molecule, 1-NA-PP1 (4-amino-1-tert-butyl-3-(1'naphthyl)pyrazolo[3,4-d] pyrimidine) (Wan et al., 2004). Inhibition of *mek1-as* results in a decrease in interhomolog joint molecules, and inhibiting Mek1 in an otherwise wild-type strain results in dead spores due to non-disjunction, as interhomolog bias is lost (Kim et al., 2010; Niu et al., 2005; Wan et al., 2004).

Several *in vivo* targets of Mek1 have been identified: Mek1 itself (T327), Rad54 T132, Histone H3 T11, and Hed1 T40, (Callender et al., in press; Govin et al., 2010; Niu et al., 2007; Niu et al., 2009). While there is currently no known function for H3-T11 phosphorylation, Mek1 T327 phosphorylation is required for kinase activation (Niu et al., 2007). The meiosis specific protein, Hed1, binds Rad51 during meiotic recombination, thus preventing Rad51's interaction with its accessory factor, Rad54 (Busygina et al., 2008; Tsubouchi and Roeder, 2006). Phosphorylation of both Hed1-T40 and Rad54-T132 independently contribute to the inhibition of Rad51 activity in the absence of *DMC1* and suppression of inter-sister recombination (Callender et al., in press; Niu et al., 2009). The fact that individual non-phosphorylatable mutants of *RAD54*, *HED1* and *HHT1/2* (the genes encoding H3) do not produce a *mek1*Δ deletion phenotype suggests

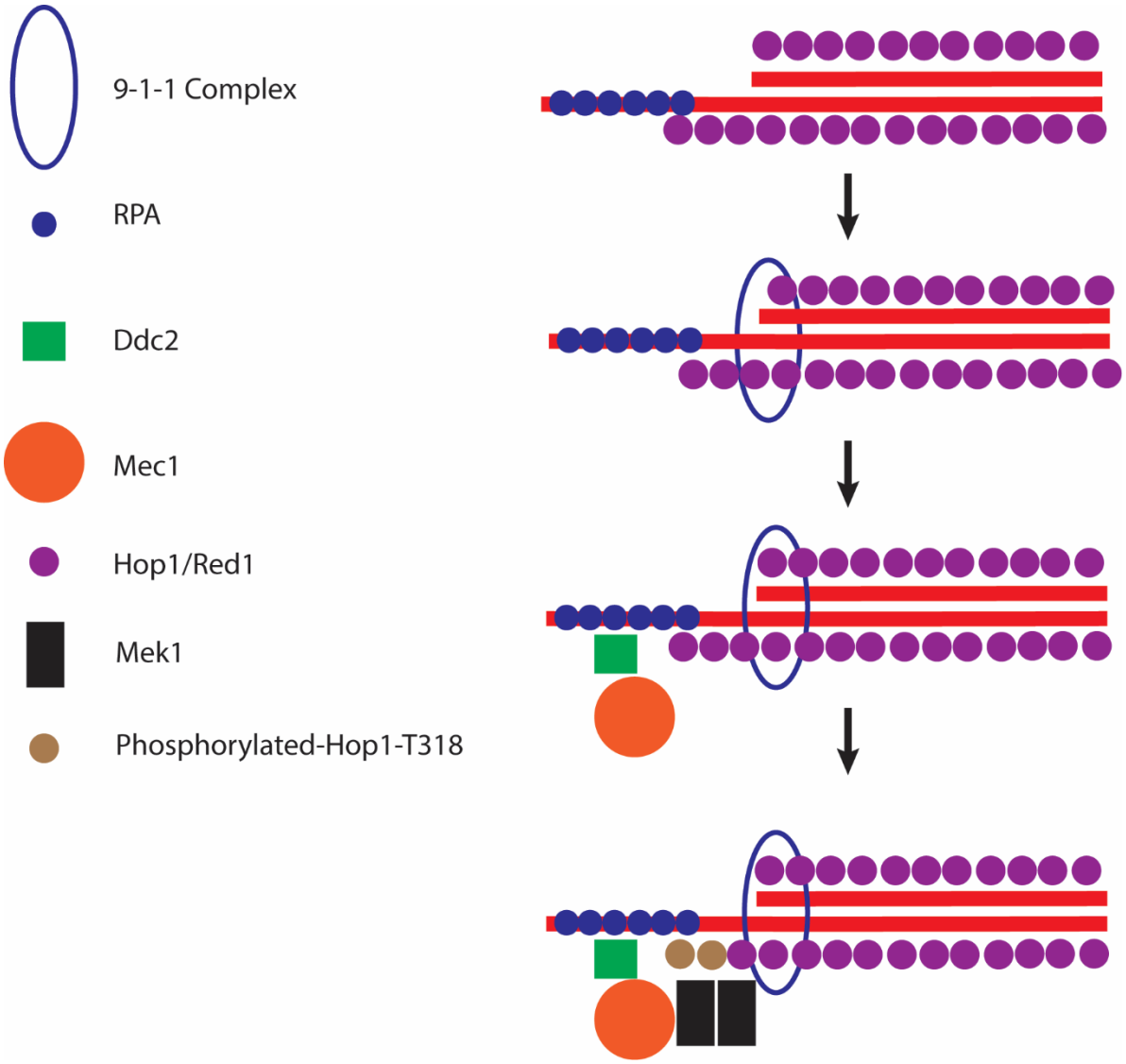

Figure 1-5: Activation of the meiotic recombination checkpoint. Following DSB formation and DNA resection, RPA coated ssDNA recruits the 9-1-1 complex (Rad17-Mec3-Ddc1) to the site of the break. This in turns recruits Ddc2 where it then recruits Mec1. Mec1 phosphrorylates Hop1-T318, thereby bringing Mek1 to the break. Mek1 is activated through *trans*-autophosphorylation on the axis.

that there remain unknown substrates of Mek1 (Callender et al., in press; Govin et al., 2010; Niu et al., 2009; Wan et al., 2004). My thesis project was to develop and execute an unbiased phosphoproteomic approach to identify additional Mek1 substrates in meiosis.

Quantitative SILAC proteomics and the synthetic sporulation problem

Quantitative proteomics has been widely used to elucidate many biological questions over the last decade (MacCoss and Matthews, 2005). Stable Isotope Labeling by Amino acids in Cell culture (SILAC) coupled with mass spectrometry (MS) has been a simple and powerful tool to improve the quality of data generated from quantitative high throughput proteomic studies (Mann, 2006). SILAC, unlike post-digestion labeling techniques such as isotope-coded affinity tags, uses cells' natural metabolic pathways to strategically label the proteome with stable heavy isotope labeled amino acids (Ong et al., 2002). The nature of this labeling procedure allows for consistent labeling efficiency of a cell's proteome, and has been extensively used in the last decade to obtain robust high-throughput data in various proteomic studies (Everley et al., 2004; Schulze et al., 2005; Schulze and Mann, 2004). SILAC is versatile and has been successfully applied to a variety of model organisms including yeast, fruit flies, plants and mice (Chen et al., 2010; Gruhler et al., 2005a; Gruhler et al., 2005b; Kruger et al., 2008; Sury et al., 2010). However, it has not been possible to use SILAC to quantitatively study the proteome of meiotic yeast cells. This is because *S. cerevisiae* sporulates inefficiently after growth in standard synthetic medium, and growth in synthetic medium is essential for the incorporation of heavy isotope labeled amino acids

into the proteome. Therefore my first challenge was to develop a synthetic pre-sporulation medium that allowed high levels of sporulation (See Chapter 2).

Using phosphoproteomics to identify kinase substrates

Phosphoproteomics is the approach in which liquid chromatography-tandem mass spectrometry (LC-MS/MS) is used to identify phosphorylation sites on proteins on a proteome wide scale. Stable isotope labeling by amino acids in cell culture (SILAC) has been coupled with phosphoproteomics to identify kinase substrates of ATM/ATR as well as Cdk1 (Holt et al., 2009; Matsuoka et al., 2007). The Cdk1 study utilized an analog sensitive allele of *CDC28, cdc28-as1,* to inhibit the kinase in the heavy culture. This was performed in both asynchronous and mitotically arrested cells. Following kinase inactivation, immobilized metal affinity chromatography (IMAC) was performed to enrich for phosphopeptides (Li and Dass, 1999). Proteins phosphorylated by Cdk1 should be under-represented in the heavy culture and this ratio was determined by quantitative MS.

IMAC has been widely used in conjunction with MS for the enrichment and identification of phosphopeptides. In the IMAC method, positively charged metal ions (i.e. Fe^{3+}, Ga^{3+}) interact with negatively charged phosphates on a peptide, allowing for the specific enrichment of phosphopeptides (Posewitz and Tempst, 1999; Thingholm and Jensen, 2009). However, IMAC purifications from whole cell extracts produce highly complex peptide mixtures, making in-depth analysis difficult due to the sampling limitations of liquid chromatography-tandem mass spectrometry (LC-MS/MS) system. Because all known Mek1 substrates are associated with chromatin, I sought to reduce some of this complexity by utilizing crude chromatin preparations, as opposed to whole

cell extracts. Another way to address reduce the peptide complexity is the application of hydrophilic liquid interaction chromatography (HILIC) to fractionate phosphopeptides prior to MS analysis (Albuquerque et al., 2008). Phosphopeptide HILIC fractionation depends on the interaction of charged amino acid side chains and negatively charged phosphate groups with the HILIC resin which is typically made from silica-based amide bonded phases (Amide-80) (Albuquerque et al., 2008; Longworth et al., 2012). When coupled with traditional LC-MS/MS, HILIC provides better fractionation compared to strong cation exchange fractionation methods (Longworth et al., 2012). Taken together, coupling SILAC, IMAC, HILIC, and LC-MS/MS allows for in-depth quantitative analysis of the phosphoproteome.

My thesis involved development of a SILAC protocol for meiotic yeast cells, then generation and analysis of a phosphoproteome dataset from *dmc1*Δ *mek1-as* cells which has led to the identification of two new candidate Mek1 substrates, Rad17 and Spp1, and the generation and analysis of a phosphproteome data set from *ndt80*Δ *mek1-as* cells which led to the discovery that phosphorylation of specific amino acids on the C-terminus of Zip1 is regulated by Mek1.

CHAPTER TWO

A method for sporulating budding yeast cells that allows for unbiased identification of kinase substrates using stable isotope labeling by amino acids in cell culture

[The text of this chapter is taken directly from a manuscript published in *G3* 4(11): 2125-35 doi: 10.1534/g3.114.013888 (Suhandynata et al. 2015). I carried out all of the experiments in the manuscript with the exception of the HILIC fractionation and mass spectrometry runs which were performed in collaboration with J. Liang, C.P. Albuquerque and H. Zhou at the University of California, San Diego].

Abstract

Quantitative proteomics has been widely used to elucidate many cellular processes. In particular, Stable Isotope Labeling by Amino acids in Cell culture (SILAC) has been instrumental in improving the quality of data generated from quantitative high throughput proteomic studies. SILAC uses the cell's natural metabolic pathways to label proteins with isotopically heavy amino acids. Incorporation of these heavy amino acids effectively labels a cell's proteome, allowing the comparison of cell cultures treated under different conditions. SILAC has been successfully applied to a variety of model organisms including yeast, fruit flies, plants and mice to look for kinase substrates as well as protein-protein interactions. In budding yeast, several kinases are known to play critical roles in different aspects of meiosis. Therefore the use of SILAC to identify potential kinase substrates would be helpful in the understanding the specific mechanisms by which these kinases act. It has previously not been possible to use SILAC to quantitatively study the phosphoproteome of meiotic *Saccharomyces cerevisiae* cells, because yeast cells sporulate inefficiently after pregrowth in standard synthetic medium. In this study we report the development of a synthetic, SILAC compatible, pre-sporulation medium (RPS) that allows for efficient sporulation of *S. cerevisiae* SK1 diploids. Pre-growth in RPS supplemented with heavy amino acids efficiently labels the proteome, after which cells proceed relatively synchronously through meiosis, producing highly viable spores. As proof of principle, SILAC experiments were able to identify known targets of the meiosis-specific kinase Mek1.

Introduction

Protein phosphorylation is critical for many different aspects of meiotic chromosome behavior in *Saccharomyces cerevisiae*. Recent studies have shown that conserved kinases such as cyclin-dependent kinase 1, Cdc7-Dbf4, casein kinase 1 (Hrr25) and the polo-like kinase, Cdc5, are involved in a variety of meiosis-specific processes, including the initiation of meiotic recombination, resolution of recombination intermediates, synaptonemal complex disassembly, mono-orientation of homologous pairs of sister chromatids at Meiosis I and/or cleavage of cohesion at the onset of Anaphase I (Henderson et al., 2006; Katis et al., 2010; Lo et al., 2012; Lo et al., 2008; Matos et al., 2008; Sourirajan and Lichten, 2008; Wan et al., 2008). In addition, during meiosis, the conserved checkpoint kinases, Mec1 and Tel1, promote recombination between homologs as well as control the meiotic recombination checkpoint (Carballo et al., 2008; Grushcow et al., 1999). Finally, the meiosis-specific kinase, Mek1, is required both for promoting recombination between homologous chromosomes instead of sister chromatids, as well as the meiotic recombination checkpoint (Kim et al., 2010; Niu et al., 2005; Wan et al., 2004; Xu et al., 1997). Understanding the mechanisms by which these kinases control various meiotic processes requires the identification of their substrates, coupled with functional analyses of mutants that are unable to be phosphorylated.

In vegetative yeast cells, combining Stable Isotope Labeling by Amino acids in Cell culture (SILAC) with phosphopeptide purification and mass spectrometry (MS) has been successful in identifying putative kinase substrates (for a review see (Zhou et al., 2010) . This approach relies on cells' natural metabolism to incorporate heavy isotopes

of specific amino acids into the proteome. The increased mass of the proteins generated using these “heavy” amino acids makes them isotopically distinct by MS from proteins from control cells (Ong et al., 2002). A requirement for SILAC, therefore, is the ability to grow in synthetic medium so that the presence of either heavy or light amino acids can be controlled. The inefficiency with which *S. cerevisiae* cells sporulate after pre-growth in standard synthetic medium has precluded the application of SILAC to meiotic cells. We have now developed a synthetic pre-sporulation medium that supports efficient sporulation of S*. cerevisiae* SK1 diploids, thereby making SILAC experiments in meiotic cells possible. Importantly, analysis of various meiotic landmarks indicates that pre-growth in this synthetic medium results in delayed, but otherwise normal, meiosis.

As proof of principle, our SILAC protocol tested to see if it could identify amino acids on proteins known to be phosphorylated by Mek1, modeled on an approach previously developed for identification of CDK substrates in vegetative cells (Holt et al., 2009). This strategy involves growing a strain containing an analog-sensitive version of the kinase (*mek1-as*) in the presence of either light or heavy arginine and lysine, arresting the cells, and then adding inhibitor for a short time to the heavy culture to inactivate the kinase. Proteins from each culture are then isolated, combined together and digested with trypsin to generate peptides. Using immobilized metal affinity chromatography (IMAC), phosphopeptides are purified and the light to heavy ratio of specific peptides is determined (Chen et al., 2010; Ficarro et al., 2002). When phosphates added to proteins by the kinase of interest are removed by phosphatases during the period of kinase inactivation, they cannot be replaced, and therefore these phosphopeptides should be under-represented in the heavy culture, resulting in a ratio

of light to heavy phosphopeptides greater than one. Mek1 is an excellent kinase to use as a test case because (1) its activity is constitutively required to maintain the meiotic prophase arrest conferred by deletion of the meiosis-specific recombinase, *DMC1*, (Niu et al., 2005; Wan et al., 2004), (2) there is a well characterized analog-sensitive allele of *MEK1*, *mek1-as*, and (3) *in vivo* targets of Mek1 are already known, Mek1 T327, Rad54-T132 and Histone H3 T11, thereby allowing validation of the approach (Govin et al., 2010; Niu et al., 2007; Niu et al., 2009). All three of these substrates match the consensus sequence for Mek1 phosphorylation (RXXT/S) determined by screening peptide libraries (Mok et al., 2010).

Materials and Methods

Yeast strains: All yeast strains are derived from the efficiently sporulating SK1 background and their genotypes are given in Table 2-1. The construction of the *dmc1*Δ *mek1-as lys4*Δ *arg4* diploid, NH2092, used in the SILAC experiment took several steps. First *MEK1* was deleted from DKB187, which contains *dmc1*Δ*::LEU2*, using the polymerase chain reaction (PCR)-mediated deletion approach with the *kanMX6* cassette (Longtine et al., 1998). The *LYS4* gene was then similarly deleted using *hphMX4* (Goldstein and McCusker, 1999). All knockouts were confirmed either by PCR or phenotypic analysis. To introduce the *arg4-Nsp* allele, DKB187 *mek1*Δ *lys4*Δ was crossed to S2683 (Hollingsworth et al., 1995) and *MAT***a** and *MATα* segregants containing *dmc1*Δ*::LEU2, mek1*Δ*::kanMX6, lys4*Δ*::hphMX4* and *arg4-Nsp* were selected. These haploids were transformed with the *mek1-as URA3* plasmid, pJR2 (Callender and Hollingsworth, 2010), digested with *Rsr*II to target integration of the

plasmid immediately adjacent to *mek1*Δ*::kanMX6*. The transformants were then mated to make NH2092.

Media: YPD, YPA and Spo medium are described in (Lo and Hollingsworth, 2011). To make RPS medium, a drop out powder lacking arginine and lysine is first created by combining 5.0 g each adenine-HCl (Sigma #A8751), uracil (Sigma #U0750), tryptophan (Sigma #T0254), histidine-HCl (Sigma #H8125), methionine (Sigma #M9625), 7.5 g each tyrosine (Sigma #T3754), leucine (Sigma #L8000), isoleucine (Sigma #I2752), valine (Sigma #V0500), threonine (Sigma #T8625), serine (Sigma #S4500) and 12.0 g phenylalanine (Sigma #P2126) in a blender. The nutrients are mixed together by 5 X 1 min pulses and the resulting –Arg -Lys powder is transferred to a sterile bottle. To make a 250 X solution of light lysine and arginine (3% lysine, 2% arginine), 3 g L-lysine-HCl (Sigma #L5626) and 2 g L-arginine-HCl (Sigma #A5131) are dissolved in 100 ml water and the solution is filter sterilized. The heavy arginine and lysine amino acids contain stable heavy isotopes of both ^{13}C and ^{15}N. To make a 250 X heavy lysine and arginine stock, 0.3 g L-lysine:2HCl (Cambridge Isotope #CNLM-291-H) and 0.2 g L-arginine:HCl (Cambridge isotope # CNLM-539-H) are resuspended in 10 ml water and filter sterilized. Both light and heavy amino acid stocks are stored in the dark at room temperature. The heavy amino acids are expensive and more stable in powder form and so smaller stocks are made and used within two months.

Table 2-1. *S. cerevisiae* strains

Name	Genotype	Source
NH144	*MATα leu2-K HIS4 arg4-Nsp ura3 lys2 hoΔ::LYS2* *MAT**a** leu2::hisG his4-X ARG4 ura3 lys2 hoΔ::LYS2*	(Hollingsworth et al., 1995)
NH716	*MATα leu2::hisG his4-X::LEU2(NgoMIV) hoΔ::hisG ura3(Δpst-sma)* *MAT**a** leu2::hisG HIS4::LEU2(Bam) hoΔ::hisG ura3(Δpst-sma)*	(Callender and Hollingsworth, 2010)
S2683	*MATα leu2-K arg4-Nsp ura3 lys2 hoΔ::LYS2*	HOLLINGSWORTH *et al.* 1995)
DKB187	*MAT**a** leu2::hisG his4-X ura3 lys2 ho::LYS2 dmc1Δ::LEU2*	Doug Bishop
NH2092	*MATα leu2 arg4-Nsp hoΔ::LYS2 lys2 ura3 lys4Δ::hphMX4* *MAT**a** leu2 arg4-Nsp hoΔ::LYS2 lys2 ura3 lys4Δ::hphMX4* *dmc1Δ::LEU2 mek1Δ::kanMX6::URA3::mek1-as* *dmc1Δ::LEU2 mek1Δ::kanMX6::URA3::mek1-as*	This work

RPS medium is made by dissolving 28 g yeast nitrogen base without amino acids, 20 g potassium acetate, and 8 g –Arg –Lys powder in a total volume of 1 L in a 2 L beaker on a stir plate at room temperature. After filter sterilization using a Stericup 0.22 μM filter apparatus (Millipore), 12.5 ml 40% sterile glucose is added to a final concentration of 0.5%. RPS-L or RPS-H is created by the addition of 1.6 ml 250 X light or heavy Lysine/Arginine solution, respectively, to 400 ml RPS medium. RPS medium should be stored in the dark at room temperature. Fresh RPS medium exhibits a light greenish color. After three days, the color begins to get darker and this correlates with less efficient sporulation. Therefore RPS medium should be used within three days.

Sporulation conditions: Sporulation of cells after YPA pregrowth is described in (Lo and Hollingsworth, 2011). The following protocol describes sporulation of cells after pregrowth in either RPS-L or RPS-H. On the first day, a single colony is used to inoculate 2 ml YPD which is then grown at 30°C on roller between 14 to 24 hours. Part of the colony is patched onto YP glycerol plates to ensure that the colony is not petite (Lo and Hollingsworth, 2011). The maximum volume of Spo medium for which efficient sporulation has been observed is 200 ml. To ultimately obtain this volume of sporulating culture, overnight cultures are diluted the next day 1:2000 in RPS-L or RPS-H medium in a 2 L flask (200 µl into 400 ml RPS-L or H). Aeration is important for both pre-growth in RPS and sporulation, so there should always be a flask volume:culture ratio of at least 5:1. The culture is incubated at 30°C in a shaker at 250 rpm until it reaches an optical density (OD_{660}) of 1.4-1.8. Depending upon the strain, this can take from 24-48 hours. The cells are pelleted by centrifugation and washed once with sterile water. The cells are then resuspended at a cell density of 3 X 10^7 cells/ml in a 2 L flask (for a conversion chart of OD to cell density, see (Lo and Hollingsworth, 2011). The culture is then incubated in a 30°C shaker to allow sporulation. Sporulation efficiency can be monitored by phase contrast microscopy to determine the fraction of cells that form spores. Sporulation efficiency for wild-type strains after pregrowth in either RPS-L or RPS-H should be ~80%.

Timecourse analysis: The method for using flow cytometry to monitor premeiotic DNA replication is described in (Wan et al., 2006). DSB repair and crossover formation were analyzed using the *HIS4/LEU2* hotspot as described in (Hunter and Kleckner, 2001). This hotspot contains a double strand break (DSB) site flanked by XhoI restriction sites.

Diagnostic parental and recombinant XhoI restriction fragments are visualized by Southern blot analysis. DNA was isolated using the Epicentre Yeast DNA extraction kit from Illumina. DNA was digested with XhoI and probed with the 0.6 kb AgeI/BglII fragment from pNH90 (from Neil Hunter, University of California, Davis). DSBs and crossovers were quantitated using MultiGauge software with a Fujifilm FLA-7000 phosphoimager. To monitor meiotic progression, nuclei were stained with 4',6-diamindino-2-phenylindole (DAPI) and examined by fluorescence microscopy.

SILAC labeling of proteins from a *dmc1*Δ *mek1-as* diploid in meiosis: The *dmc1*Δ *mek1-as* diploid, NH2092, was pre-grown in either RPS-L or RPS-H (hereafter referred to as the "light" and "heavy" cultures, respectively) and transferred to Spo medium. Two hundred ml cells were incubated in a 2 L flask in a 30°C shaker for 10 hours to allow the cells to arrest with unrepaired DSBs. At this time, 21 µl of dimethyl sulfoxide (DMSO) was added to the light culture and 21 µl 10 mM 1-NA-PP1 (4-amino-1-*tert*-butyl-3-(1'napthyl)pyrazolo[3,4-*d*]pyrimidine) (Tocris Bioscience) dissolved in DMSO was added to the heavy culture (1 µM final concentration). After 20 min, 7 ml cells from each culture were transferred to a 25 ml flask and returned to the 30°C shaker until the next day. Inhibition of Mek1-as allows DSB repair by Rad51, thereby eliminating the signal to the checkpoint and allowing the cells to sporulate (Wan et al., 2004). Therefore the effectiveness of both the *dmc1*Δ arrest and the Mek1-as inhibition can be determined by analyzing the percent sporulation of the light and heavy cultures. The remaining 193 ml of cells from light and heavy sporulating cultures were then collected by centrifugation and washed once with 40 ml cold sterile water. After the cells were resuspended in cold sterile water, they were transferred to 50 ml conical tubes and the

cells collected again by centrifugation. After pouring off the supernatants, the cell pellets were stored at -80°C.

Preparation of crude chromatin and trypsin digestion: All the quantities described in this protocol are meant for 1 ml yeast pellet volume, unless otherwise specified. To enrich for chromosome associated proteins, crude chromatin is prepared. The heavy and light cell frozen pellets are thawed by adding 10 mL of 30°C reducing buffer [100 mM Tris, pH 9.4 and 10 mM dithiothreitol (DTT) (DTT is added fresh from a 1 M freezer stock)] and incubating at 30°C for 15 min. The cells are pelleted by centrifugation at 3,700 X *g* for 5 minutes at room temperature. The temperature of the centrifuge is then lowered to 4˚C so that it is ready for the next spin. Measure the volume of the cell pellet and, for every ml of cell pellet, 10 ml of 30°C spheroplasting solution (50 mM KPO_4, pH7.5, 1.0 M Sorbitol and 10 mM DTT) are added. The cell walls are removed to create spheroplasts by adding 100 µl of 25 U/µL Lyticase (Sigma) and then incubating at 30°C for 45 minutes with rotation. To determine the efficiency of spheroplasting, 20 µL of cells are added to 1 mL of 0.1% sodium-dodecyl-sulfate (SDS) and the cells are examined by phase contrast microscopy for lysis. Lysed cells look gray while unlysed cells remain bright and refractile. After >80% spheroplasting is achieved (usually ~ 45 min), the spheroplasts are pelleted at 1,500 X *g* for 5 minutes at 4°C and washed with 10 mL of ice-cold washing buffer (0.1 M KCl, 50 mM HEPES, pH 7.5, 1.0 M Sorbitol). There is no need to resuspend the pellet during this wash, instead dislodge the pellet from the bottom of the tube by lightly blowing the edges of the pellet with the wash buffer using a P1000 pipette. After harvesting the cells as before, re-suspend the pellet in 1 mL of EB buffer [0.1 M KCl, 50 mM HEPES, pH 7.5, 5 mM EDTA, 50 mM NaF, 5

mM β-glycerol phosphate, 1mM PMSF and 2X complete, Mini EDTA-free protease inhibitor cocktail (Roche, made fresh every time)] gently with a 1 ml pipette. To lyse the cells, 50 µl 10% Triton X-100 is added (0.5% final concentration) and the spheroplasts are incubated at 4°C with gentle rotation for 15 minutes. This step can be done without rotation if the suspension is too thick and mixed periodically with a pipette instead. The lysate is then gently placed on top of a one sample volume of a 30% sucrose cushion in an ultracentrifuge tube (Beckman #326819) and centrifuged at 30,000 X *g* (SW50 or SW55Ti, Beckman Ultracentrifuge) for 15 minutes at 4°C. While loading the sample, make sure that the boundary between the sample and the sucrose cushion is completely planar. Any unevenness can lead to the sample breaking through the cushion leading to failure of fractionation. After centrifugation, the supernatant is checked for yellowish tinge. An absence of yellow tinge suggests a failure to fractionate and the sample should be discarded. The supernatant is removed and the chromatin pellet is thoroughly resuspended in 2 mL Urea Extraction Buffer (8 M Urea, 100 mM Tris pH8.0, 300 mM KCl and 10 mM DTT) and incubated at 37°C for 30 min with rotation. The resuspended pellet is then centrifuged as before but for 15 minutes at 20°C. The supernatant is transferred to a new 50 ml conical tube. The pellet is extracted once more with 1 mL of Urea Extraction Buffer and the supernatants combined. At this point, the pellet should appear almost white due to all proteins being extracted from it. The protein concentration of each chromatin preparation is measured using the BioRad Protein Assay reagent. Equal amounts (ideally 10 mg) of light and heavy crude chromatin preparations are combined in a 50 conical tube. 500 mM Iodoacetamide is added to the crude chromatin to a final concentration of 30 mM and incubated for 10

minutes at room temperature in the dark. Iodoacetamide alkylates the reduced cysteine residues thereby preventing the reformation of disulfide bonds. The chromatin preparations are then diluted fivefold with TBS (50 mM Tris-HCl, pH8.0, 150 mM NaCl) so that the concentration of urea is less than 2 M. To digest the proteins into peptides, trypsin [30 mg TPCK-treated trypsin (Worthington, 31P13122) in 0.1% acetic acid] is added so that the amount of trypsin is equal to 1/100 the amount of chromatin protein. The chromatin is incubated with the trypsin with rotation for 15 hours at 37°C. The resulting peptides are acidified by addition of 10% tri-fluoroacetic acid (TFA) to a final concentration of 0.2% and then centrifuged at 3,700 x *g* to remove insoluble material. During this time, C18 columns are prepared by washing sequentially with 1 column volume (column volume is indicated on the side-wall of the column) of methanol, 80% acetonitrile / 0.1% Acetic Acid, 0/1% Acetic acid, and finally 0.1%TFA. The peptides are de-salted by loading the supernatant onto a 500 mg Sep-Pak C_{18} column (Waters) at a ratio of 10 mg total protein per 1 g of C18 resin, washed with 1 column volume of 0.1% TFA using gravity flow, followed by two column volumes of 0.1% acetic acid. Peptides are eluted using 3 ml 80% acetonitrile, 0.1% acetic acid. To maximize the yield, collect any liquid remaining in the column by placing a rubber bulb on top of the column and pushing the liquid out. The peptide solution is aliquoted into glass cuvettes (National Scientific, C4015-843) and dried under vacuum until the volume is reduced sufficiently to fit into one cuvette (approximately an hour). The walls of the cuvettes are washed with 80% acetonitrile, 0.1% acetic acid and then everything is pooled into one cuvette. This cuvette is then placed back into the speedvac overnight to completely dry the peptides. To measure the efficiency of heavy amino acid labeling, 1 mg of heavy crude

chromatin alone is treated with iodoacetamide and trypsin as described above and analyzed using the mass spectrometer.

Preparation of columns for immobilized metal affinity chromatography (IMAC): Gel loading tips (Fisher #02-707-138) are used to make IMAC columns. A small bunch of glass fibers (Fisher #11-388) is carefully placed inside the top half of the tip, and are then carefully maneuvered with a piece of thin wire into the narrow part of the tip. Glass fibers are continuously pushed through the tip until they will not move any further. At this point, excess fibers protruding from the tip are cut off with scissors flush with the end of the tip. The end of the tip containing the frit is bent and flattened with the back of a forceps to decrease the flow rate. The top part of the tip is trimmed until the diameter is small enough so that a 1 ml syringe can fit snugly, creating an airtight seal. To test the column, 10 µl water is loaded into the tip from the top, and the syringe is attached to the tip with the plunger drawn up all the way. If water flows out when pushed with the syringe, the column tip is ready to use.

Resin from three silica-nitrilotriacetic acid spin columns (Qiagen, Valencia, CA) is pooled in 50 ml of stripping buffer (5 mM EDTA, pH 8.0, 1 M NaCl) in a 50 ml conical tube and incubated for 1 hour at room temperature with rotation. To collect the resin from the columns, each column is turned upside-down over the 50 ml tube and the frit and dry resin are carefully pushed out using a blunt needle. Gently tap the column to collect resin that is stuck to the column wall. The resin is pelleted by centrifugation at 1,500 x *g* and washed with 50 ml water, followed by a 50 mL wash of 0.6% acetic acid. The resin is then incubated with 100 mM $FeCl_3$ in 0.3% acetic acid overnight at room temperature with rotation. The resin is washed once with 50 ml 0.6% acetic acid, then

twice with 50 ml 0.1% acetic acid. The amount of resin is estimated by comparing to the volume of water in a comparable tube so that the resin can be suspended in 0.1% acetic acid as a 50% (volume/volume) slurry and stored at 4°C. The final product should have a yellowish tinge.

The appropriate amount of packed resin required for IMAC is calculated (40 µl packed resin/5 mg peptides), and the same amount of water is loaded into the top of the column tip. A 1 ml syringe is attached to the tip and water pushed very slowly until its lower level touches the glass frit. The syringe is removed immediately to prevent the water from flowing through. The upper level of the water is marked, and then it is forced out with the syringe. The 50% resin slurry is loaded into the tip and slowly pushed with the syringe to pack the resin till the water meniscus touches the resin bed. Once the packed resin reaches the mark for the correct volume, the column is ready. Push out all the excess liquid, but do not allow the resin to dry.

Purification of phosphopeptides using IMAC: The method for purifying phosphopeptides using IMAC resin is adapted from Albuquerque et al. (2008). The dried peptides are resuspended in 100 µl 0.1% acetic acid (10 µg/µl peptide concentration) and spun for 5 min at 2,300 x *g* in a microcentrifuge. The supernatant is loaded using a micropipette onto a gel loading tip column with fiber glass as a frit containing the appropriate amount of fresh immobilized metal affinity chromatography (IMAC) resin (usually around 60 µl) (see above). After loading, the IMAC resin is washed twice with 60 µL of wash buffer containing 25% acetonitrile, 100 mM NaCl, and 0.1% acetic acid, once with 60 µL 0.1% acetic acid, and finally with 30 µl water. Loading and washes are performed by slowly pushing the buffer through the column

using a syringe at a flow rate of 1 to 2 µl/min. The syringe is attached to the tip with the plunger fully drawn and then the plunger is pushed from the 1 ml to the 0.9 ml marking. This causes the sample to slowly ooze out of the tip. The flow through is collected in a glass cuvette that can be freeze dried and used later in case the first round of IMAC fails to purify any phosphopeptides. The column is allowed to run with close monitoring to make sure that the meniscus of the liquid does not drop below the bed level. Once the meniscus reaches the bed, the syringe is removed and next wash solution is added to the top of the column. The plunger is drawn to 1 ml and the syringe is reattached and used as before. The resin should not be allowed to dry at any point (the meniscus of each loading or wash should be right at the resin surface). Phosphopeptides are eluted into a new glass cuvette using 180 µl 6% NH_4OH and then dried under vacuum. The dried phosphopeptides can be stored at -20^{o}C until ready for MS.

HILIC (Hydrophilic Interaction Liquid Chromatography) fractionation and mass spectrometry: Phosphopeptides eluted from IMAC were subjected to an offline HILIC fractionation method as previously described (Albuquerque et al., 2008). Fractionated samples were run on an LTQ Orbitrap XL using a 1100 Quad PUMP HPLC system (Agilent, Santa Clara, CA) with Ultimate 3000 autosampler (Dionex, Sunnyvale, CA).

Data Analysis using SEQUEST: To search tandem mass spectra, a composite database is used containing both the yeast protein database and its decoy database. The use of a reverse protein database allows for the estimation of the false discovery rate (Elias and Gygi, 2007). The data are analyzed using the Sorcerer system (SageN, San Jose, CA; SEQUEST), and a semi tryptic restriction is applied to the search. The parameters used for the search are a parent mass tolerance of 20 ppm, +80.0 Da

variable modification of STY (serine, threonine and tyrosine) due to phosphorylation, and a maximum of two modifications per peptide. After searching, the raw results of SEQEST are then filtered using their provided *p* value to a 1% false discovery rate (# of decoy database hits/total hits).

Results

Pregrowth in RPS-L medium allows for normal meiosis and sporulation

Synthetic dextrose (SD) medium for growth of budding yeast cells is usually comprised of 0.67% yeast nitrogen base without amino acids and 2% glucose, which can then be supplemented with appropriate amino acids and nucleotides to final concentrations of between 20-400 mg/L (Rose et al., 1990). Cells pregrown in SD medium plus nutrients do not sporulate efficiently when transferred to Spo medium (data not shown). Sporulation in SK1 strains is enhanced by pregrowth in a rich acetate medium called YPA (Padmore et al., 1991). To create a synthetic sporulation medium (RPS) that supports efficient sporulation, the major carbon source in SD was changed from glucose to 2% acetate, similar to YPA. A small amount of glucose (0.5%) is included and is necessary for cells to grow well. In addition, four times the amount of dropout powder is used compared to conventional SD dropout medium (see Materials and Methods for recipes). "Heavy" versions of lysine and arginine contain stable heavy isotopes of ^{13}C and ^{15}N. RPS supplemented with "light" or "heavy" arginine/lysine is indicated as RPS-L and RPS-H, respectively.

Although a slight reduction in sporulation (84% from 95%) was observed in two different wild-type strains pregrown in RPS-L compared to YPA, spore viability was wild type (Table 2-2). Timecourse analyses were used to monitor various meiotic

parameters. Cells pregrown in RPS-L exhibit a two hour delay in the onset of premeiotic DNA synthesis compared to YPA pregrowth (Figure 2-1A). Once the cells enter meiosis, however, meiotic parameters such as DSB and crossover formation, as well as meiotic progression, occur with normal timing (taking into account the initial delay) (Figure 2-1B, C and D). These results indicate that the transition from vegetative growth to meiosis takes longer after pregrowth in RPS medium, but having once entered meiosis, cells proceed normally and relatively synchronously to form highly viable spores.

Pregrowth in RPS-H efficiently labels proteins both in vegetative cells and after the induction of meiosis

For SILAC experiments to work, the labeling of proteins with heavy amino acids must be highly efficient. Peptides from RPS-H grown vegetative cultures were analyzed by MS and 3900 out of 4064 total identified peptides (96%) contained heavy amino acids. One question is whether the fraction of heavy labeled proteins remains high after hours in Spo medium. Meiosis and sporulation are induced by transferring cells into a medium that lacks nitrogen and contains a non-fermentable carbon source such as acetate. The absence of nitrogen means that no new amino acid synthesis can occur. Instead amino acids used for new protein synthesis are recycled from existing proteins by autophagy, as evidenced by the fact that protease activity is essential for sporulation (Onodera and Ohsumi, 2005; Zubenko et al., 1979). This recycling is an advantage for meiotic SILAC experiments, given that proteins produced during meiosis must be made using heavy amino acids that were present during the pregrowth period.

Table 2-2. Sporulation and spore viability under various conditions after pregrowth in either YPA, RPS-L or RPS-H.

Strain	Relevant genotype	Pregrowth medium	% sporulation[a]	% spore viability[b]
NH144	WT	YPA	94.5 ± 1.4	96.3 ± 1.8
		RPS-L	83.4 ± 4.6	95.6 ± 0.9
NH716	WT	YPA	95.5 ± 0.7	95.0 ± 1.8
		RPS-L	84.3 ± 1.1	95.0 ± 3.5
NH2092	*mek1-as dmc1Δ* - I	YPA	0.0 ± 0.0	ND
	mek1-as dmc1Δ - I	RPS-L	0.0 ± 0.0	ND
	mek1-as dmc1Δ - I	RPS-H	0.0 ± 0.0	ND
	mek1-as dmc1Δ +I[c]	YPA	91.0 ± 2.1	ND
	mek1-as dmc1Δ +I	RPS-L	80.1 ± 1.8	ND
	mek1-as dmc1Δ +I	RPS-H	84.0 ± 2.8	ND

[a]Numbers represent the average and standard deviation from two independent experiments.

[b]Spore viability was determined by dissection of 20 tetrads for each experiment.

[c]"I" indicates addition of 1-NA-PP1 to a final concentration of 1 μM. Inhibitor was added to the YPA and RPS pregrown strains 5 and 10 hours after transfer to Spo medium, respectively.

Consistent with this idea, 5443 out of 5611 (97%) of the identified peptides analyzed 10 hours after transfer to Spo medium from RPS-H pregrown cells still contained heavy amino acids.

Another possible problem is that catabolism of heavy arginine could produce proline and glutamic acid residues with heavy atoms that could skew the quantification of heavy peptides (Middelhoven, 1964).To determine how frequently this happens, the

raw data were analyzed for the presence of heavy proline or glutamate and low levels (<1.0%) of these amino acids were observed. Analysis of the most abundant proline and glutamate-containing peptides exhibited L/H ratios not significantly different than one. Therefore catabolism of arginine during meiosis is unlikely to significantly affect the quantification of proline/glutamate containing peptides.

SILAC, combined with phosphopeptide purification, identifies known substrates of Mek1

To validate the method, a meiotic SILAC experiment was performed to see if it could identify known substrates of Mek1. The experimental strategy used for the *dmc1*Δ *mek1-as* SILAC experiments is shown in Figure 2-2A. In the absence of *DMC1*, cells arrest in prophase with resected double strand breaks (Bishop et al., 1992) (Figure 2-2B). Rad51 is loaded onto the breaks but its activity is indirectly inhibited by Mek1 (Bishop, 1994; Niu et al., 2009). Inactivation of Mek1-as in *dmc1*Δ *mek1-as* arrested cells allows repair of the breaks using sister chromatids as templates, thereby removing the signal to the meiotic recombination checkpoint and allowing meiotic progression (Niu et al., 2005) (Figure 2-2B). An overnight culture of a *dmc1*Δ *mek1-as* diploid was diluted into either RPS-L or RPS-H, the cells were grown to an OD_{660} of ~1.7 and then transferred to Spo medium for 10 hours to allow cells to arrest in meiotic prophase with unrepaired DSBs. The effectiveness of both the arrest and Mek1 inhibition were assessed by removing small aliquots of cells before and after addition of the Mek1-as inhibitor, 1-NA-PP1, and incubating them at 30°C overnight. While no asci were observed in the absence of inhibitor, indicating a robust arrest, inactivation of Mek1 resulted in high levels of sporulation as expected (Table 2-2).

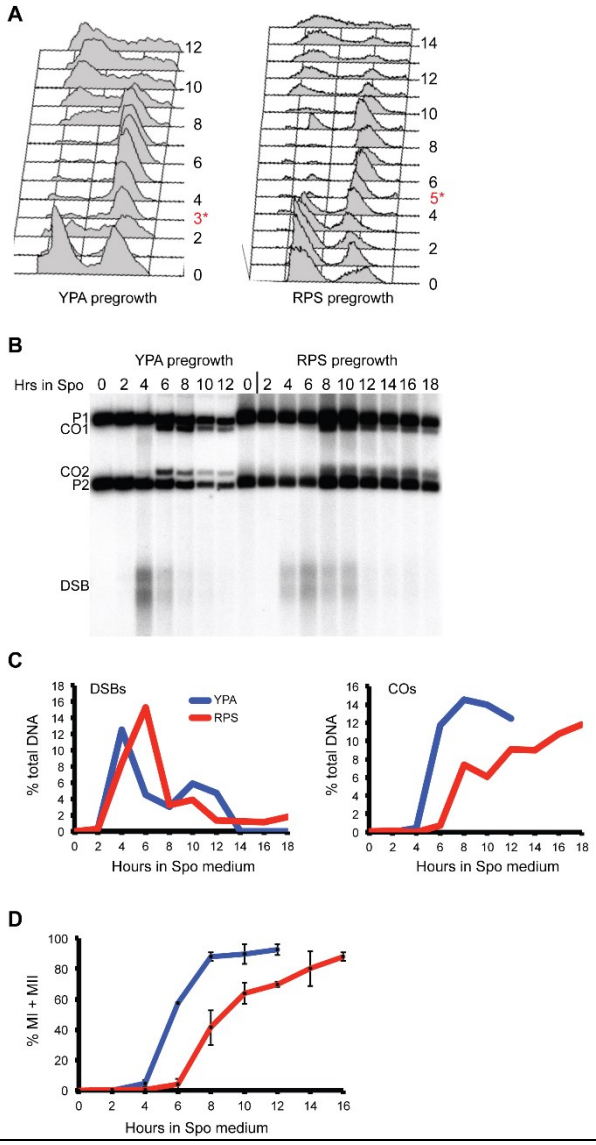

Figure 2-1. Comparison of various meiotic parameters in cultures grown in either YPA or RPS-L prior to sporulation. The wild-type SK1 strain, NH716, was pre-grown in either YPA or RPS-L, transferred to Spo medium at 30°C and samples were taken at two hour intervals. A. Flow cytometry analysis of premeiotic DNA synthesis. Numbers indicate hours after transfer to Spo medium. Red numbers with asterisks indicate the timepoints at which DNA synthesis is complete. B. DSB and crossover analysis was performed using the *HIS4/LEU2* hotspot (Hunter and Kleckner, 2001). P1 and P2 indicate parental fragments, CO1 and CO2 indicate crossover fragments and DSB indicates DSB fragments. This analysis was performed for two different timecourses with similar results. C. Quantitation of the DSBs and COs shown in Panel B. D. Meiotic progression was measured by staining cells with DAPI and counting the number of nuclei in each cell (binucleates indicate completion of Meiosis I and tetranucleates indicate completion of Meiosis II). For each timepoint, 200 cells were examined by fluorescent microscopy. Error bars represent the standard deviation observed for the two independent experiments.

For the SILAC experiment, cells were harvested 20 min after addition of inhibitor. Since all of Mek1's known substrates are associated with DNA, crude chromatin was isolated to enrich for proteins that are potential targets of the kinase. The chromatin preparations from the heavy and light cultures were combined and treated with trypsin. Trypsin cuts after arginine or lysine to generate peptides. Analysis of a fraction of the total peptides by MS showed that 96% of the total peptides exhibited an L/H ratio around 1, indicating that most proteins were present in equal abundance in the two chromatin preparations (Figure 2-3A). Phosphopeptides were then enriched using IMAC. The peptides were subjected to HILIC fractionation prior to MS analysis, which allows for in-depth mapping of protein phosphorylation sites in a complex sample. HILIC is largely orthogonal to reverse phase high pressure liquid chromatography for phosphopeptide separation, but does not require a de-salting step before LC-MS/MS analysis, preventing sample loss after fractionation (Albuquerque et al., 2008). In two different experiments, 16,036 and 16,555 total peptides were identified, of which 15,241 (95%) and 13,959 (84%) were phosphorylated, respectively. The peptides from these two experiments represent 1,985 and 2,058 unique phosphorylated proteins. As the purpose of this paper is meant to report the method for doing SILAC in meiosis, the entire dataset of identified phosphopeptides will be made available elsewhere. A plot of the L/H ratios of the phosphorylated peptides shows that approximately 80% of these peptides are equally abundant in the light and heavy cultures (Figure 3B). Peptides that exhibit a L/H ratio > 2 (indicated by the red box) are potential substrates of Mek1. The data were examined for phosphopeptides from the three known *in vivo* targets of Mek1: Mek1 threonine 327, Rad54 threonine 132 and histone H3 threonine 11.

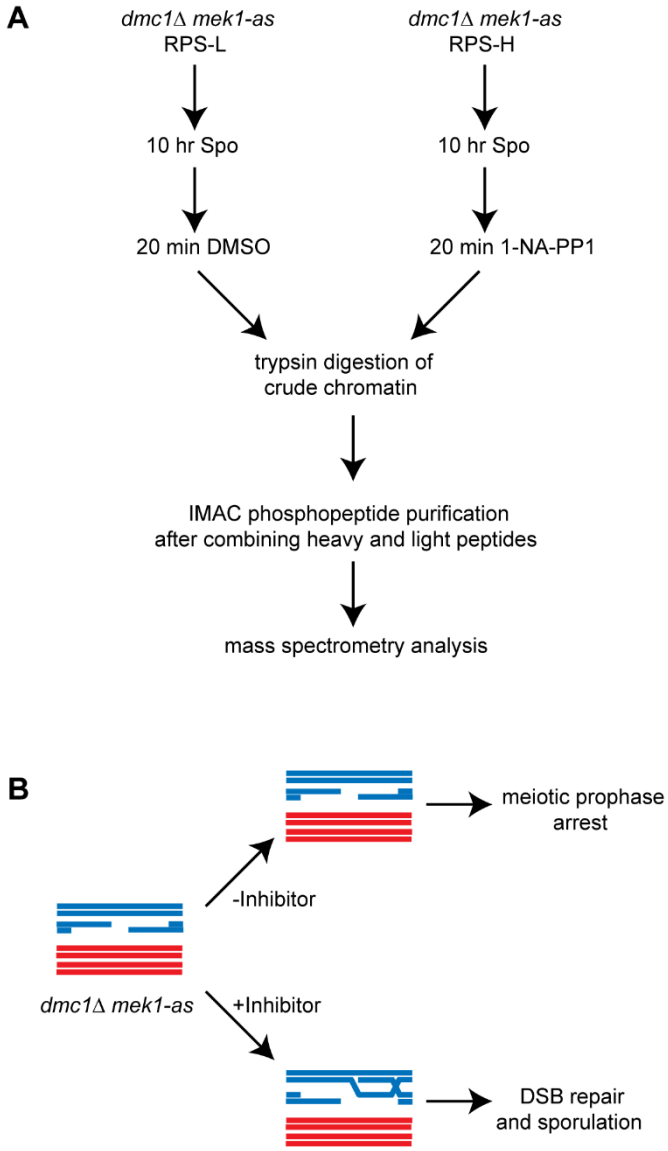

Figure 2-2. Fate of meiotic DSBs in *dmc1*Δ *mek1-as* diploids with or without inhibitor. A. Experimental flow chart for a SILAC experiment using *dmc1*Δ *mek1-as*. B. Inactivation of Mek1-as allows DSB repair in a *dmc1*Δ mutant. Two homologs (one red and one blue) are shown after DNA replication to make sister chromatids. Each chromatid is represented as a duplex of DNA. DSBs formed on one of the four chromatids remain unrepaired in the absence of the 1-NA-PP1 inhibitor, thereby triggering the meiotic recombination checkpoint and arresting the cells in meiotic prophase (Bishop et al., 1992; Lydall et al., 1996). Addition of 1-NA-PP1 inactivates Mek1, thereby allowing Rad51 to repair the DSBs using sister chromatids as templates. This repair eliminates the signal to the checkpoint, thereby allowing meiosis to proceed and asci to form (Niu et al., 2005; Wan et al., 2004).

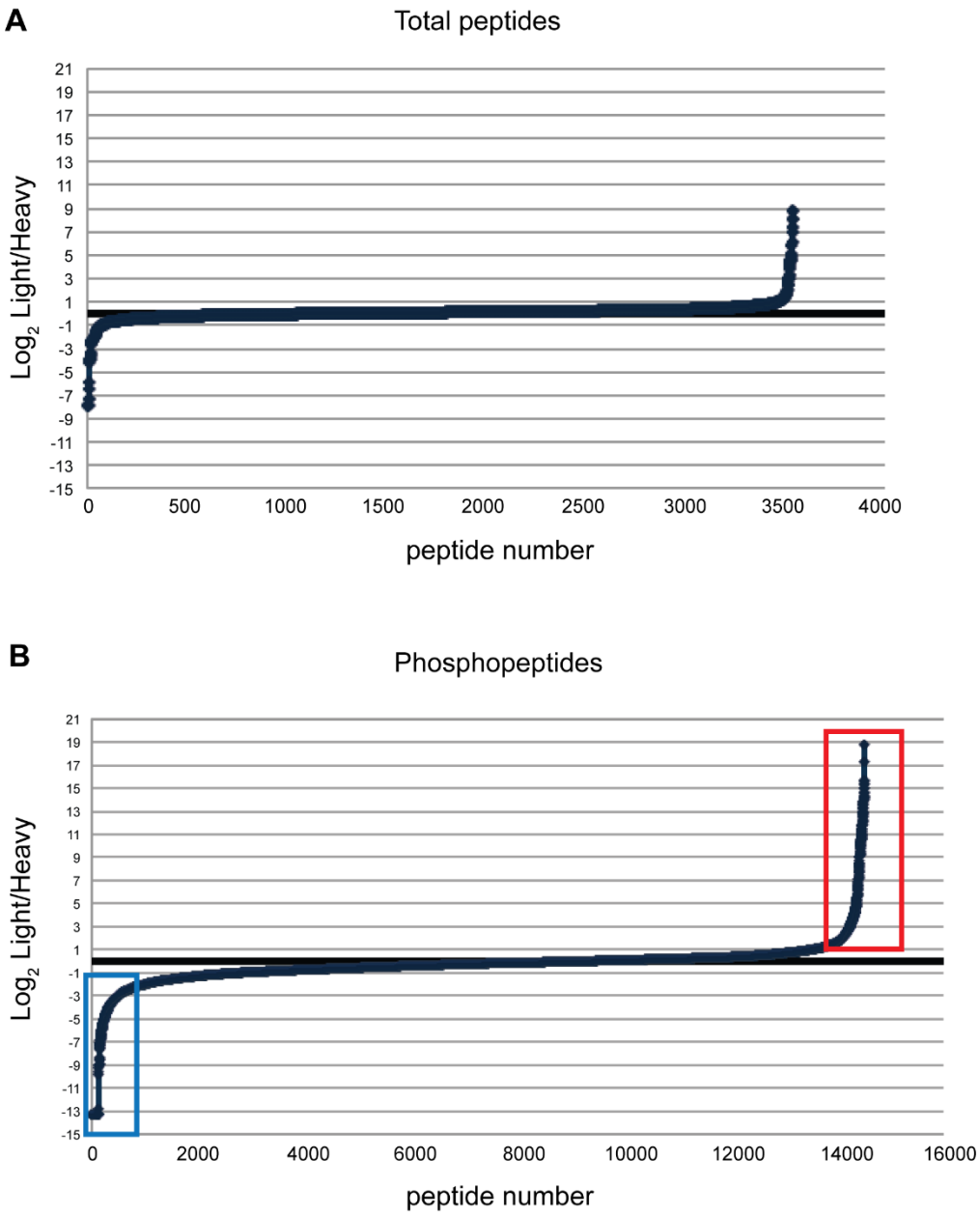

Figure 2-3. Relative abundance of total and phosphorylated peptides from a *dmc1*Δ *mek1-as* SILAC experiment. Representative distributions of $\log_2$ L/H ratios for total peptides are plotted on the Y-axis, while an arbitrary peptide identification number is assigned to each individual peptide, shown on the X-axis. Peptides with L/H ratios greater than 2-fold are indicated by the red box, while peptides with L/H ratios <1 are indicated by the blue box.

No peptides for H3 were observed, perhaps because the abundance of arginine and lysine residues in this histone produces very small peptides that are not efficiently detected by MS. In contrast, several phosphopeptides were found for both Mek1 and Rad54 (Figure 2-4). Mek1 activates itself by autophosphorylation of T327 (Niu et al., 2007). The Mek1 T327 site was twice identified by LC-MS/MS and exhibited an average L/H ratio of 12.4 (Figure 2-5A). In addition, seven peptides were observed that contain phosphorylated T331, which is also located in the Mek1 activation loop and whose phosphorylation is required for wild-type levels of Mek1 activity, exhibiting an average L/H ratio of 4.2 (Niu et al., 2007). High L/H ratios could occur simply because there is less Mek1 protein in the heavy culture. This potential artifact is ruled out in the case of Mek1 because other phosphopeptides (presumably phosphorylated by other kinases) are present that have L/H ratios less than or equal to one. For example, peptides containing phosphorylated serine 143 are present with an average L/H ratio = 0.72 (Figure 2-4 and 2-5A), supporting the idea that the large L/H ratios for T327 and T331 are Mek1-dependent. Another *in vivo* target of Mek1 is threonine 132 of Rad54 (Niu et al., 2009). Rad54 is an accessory factor for Rad51 and the negative charge conferred by phosphorylation makes Rad51-Rad54 complex formation more difficult. A high L/H ratio for a peptide containing phosphorylated T132 of Rad54 was observed, consistent with being a Mek1 target (Figure 2-5B). This ratio is not due to differential amounts of Rad54 in the two cultures as other phosphopeptides from Rad54 exhibited L/H ratios ranging from 0.06 to 1.35 (Figure 2-4 and 2-5B).

Mek1

MRPLYSCNLA TKDDIEMAGG VAPAHLEVNV GGYNTEQTIP IVKHQLVKVG RNDKECQLVL TNPSISSVHC
VFWCVFFDED SIPMFYVKDC SLNGTYLNGL LLKRDKTYLL KHCDVIELSQ GSEENDIKKT RLVFMINDDL
QSSLDPKLLD QMGFLREVDQ WEITNRIVGN GTFGHVLITH NSKERDEDVC YHPENYAVKI IKLKPNKFDK
EARILLRLDH PNIIKVYHTF CDRNNHLYIF QDLIPGGDLF SYLAKGDCLT SMSETESLLI VFQILQALNY
LHDQDIVHRD LKLDNILLCT PEPCTRIVLA DFGIAKDLNS NKERMHTVVG TPEYCAPEVG FRANRKAYQS
FSRAATLEQR GYDSKCDLWS LGVITHIMLT GISPFYGDGS ERSIIQNAKI GKLNFKLKQW DIVSDNAKSF
VKDLLQTDVV KRLNSKQGLK HIWIAKHLSQ LERLYYKKIL CNNEGPKLES INSDWKRKLP KSVIISQAIP
KKKKVLE

Rad54*

MARRRLPDRP PNGIGAGERP RLVPRPINVQ DSVNRLTKPF RVPYKNTHIP PAAGRIATGS DNIVGGRSLR
KRSATVCYSG LDINADEAEY NSQDISFSQL TKRRKDALSA QRLAKDPTRL SHIQYTLRRS FTVPIKGYVQ
RHSLPLTLGM KKKITPEPRP LHDPTDEFAI VLYDPSVDGE MIVHDTSMDN KEEESKKMIK STQEKDNINK
EKNSQEERPT QRIGRHPALM TNGVRNKPLR ELLGDSENSA ENKKKFASVP VVIDPKLAKI LRPHQVEGVR
FLYRCVTGLV MKDYLEAEAF NTSSEDPLKS DEKALTESQK TEQNNRGAYG CIMADEMGLG KTLQCIALMW
TLLRQGPQGK RLIDKCIIVC PSSLVNNWAN ELIKWLGPNT LTPLAVDGKK SSMGGGNTTV SQAIHAWAQA
QGRNIVKPVL IISYETLRRN VDQLKNCNVG LMLADEGHRL KNGDSLTFTA LDSISCPRRV ILSGTPIQND
LSEYFALLSF SNPGLLGSRA EFRKNFENPI LRGRDADATD KEITKGEAQL QKLSTIVSKF IIRRTNDILA
KYLPCKYEHV IFVNLKPLQN ELYNKLIKSR EVKKVVKGVG GSQPLRAIGI LKKLCNHPNL LNFEDEFDDE
DDLELPDDYN MPGSKARDVQ TKYSAKFSIL ERFLHKIKTE SDDKIVLISN YTQTLDLIEK MCRYKHYSAV
RLDGTMSINK RQKLVDRFND PEGQEFIFLL SSKAGGCGIN LIGANRLILM DPDWNPAADQ QALARVWRDG
QKKDCFIYRF ISTGTIEEKI FQRQSMKMSL SSCVVDAKED VERLFSSDNL RQLFQKNENT ICETHETYHC
KRCNAQGKQL KRAPAMLYGD ATTWNHLNHD ALEKTNDHLL KNEHHYNDIS FAFQYISH

Rec8*

MAPLSLNFKD DKKYKGLTTV WLLSALGNSI VKESNNYYSN KSNSTGNISS STVKKKDIVN ISIPKTCDEI
QNFENDFSLR YISNLLYGVT ICYNKKTEYV LNDLNHLLVQ LQKNDVYAFK AKNKSTRING LNSNNSIIGN
KNNNYTWEEC VFFDDDPLYD ITKVPALEFL NTTLQDNVSF IEEAKSIRRQ DYINELSNSN RFELHGDMTN
SDAQSNLGSN VRNSFPLDEI PVDVDFNLDL DDIVSHQGTP LGSHSSSQKD GNDFKFNYQG DELVLNFEND
NENNSNGGED TSVENEGPVA NLKDYELGLE AQASEEENDL QQKLNTRMQR GHRADVGGQF SKVQFDAKTS
YPNEVLKFNH GNYSHLMEKN RIRKLTGQNF LTSNISSLVR SCGEEEFFST NWLSIFNDFS NIKTSEWDLY
PQGFSSVERG RKRAHSLVST QSSSSTRSHE YGRKSFRNNK NDNYSSDMEN DNLLLNLEQI NEDLEDGHYI
EENSQGNILD FNLNLPPSSF GRSHTRNSTR SSGFNEDIVG ALRRRVGPSE QNFAEEDDSS NSCFSDGSQQ
NLQQDKTNFQ DVILDYQTKK FYDYIKERSI VVGRTTRSNP PFKRKMLLVD IIPSRMGEAQ TGANFDDVER
GVSRQIAASA FLSLLNLATK GMVKLNEYPV ADAVTKDLKL RREDEIIVYA

Figure 2-4. Location of phosphopeptides on Mek1, Rad54 and Rec8. Sequences in red indicate peptides that were detected by mass spectrometry. In some cases, two peptides overlap. Amino acids indicated in bold with blue color are phosphorylated. Phosphorylated sites that have previously been identified in the literature are bold and green.

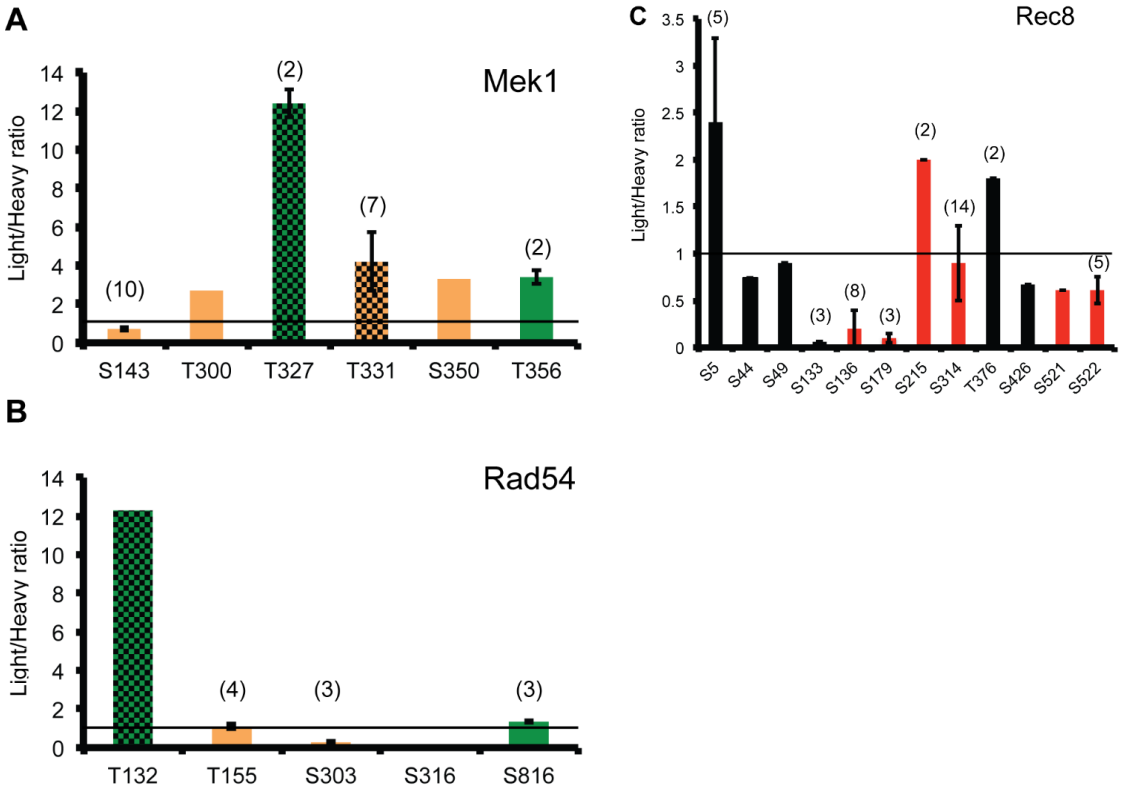

Figure 2-5. Distribution of phosphorylated peptides and their light:heavy (L/H) ratios for Mek1, Rad54 and Rec8. The average L/H ratios are plotted for peptides from *dmc1*Δ *mek1-as* SILAC experiments containing the phosphorylated amino acid indicated on the X-axis. Error bars indicate the standard deviations. A complete list of the each peptide sequence and its ratio for the proteins shown here can be found in Supplementary Table 1. For those phosphosites identified by more than one peptide, the number of peptides is indicated in parentheses. Green indicates phosphosites that match the Mek1 consensus of arginine in the -3 position. Hatch marks indicate *in vivo* Mek1 targets important either for Mek1 auto-activation (T327, T331) or for inhibiting Rad51-Rad54 interaction (T132). For Rec8, red indicates phosphosites previously identified by (Brar et al., 2006) and/or (Katis et al., 2010). Phosphorylation of these sites promotes separase cleavage (Katis et al., 2010). Lines across each graph indicate a ratio of 1.0.

In addition to peptides exhibiting L/H ratios greater than 1, there is also a class of peptides in which the L/H ratio is less than one (represented by the blue box in Figure 2-3B). These are phosphopeptides that are over-represented in the heavy culture, suggesting that phosphorylation occurs in response to Mek1 inhibition. In fact, inactivation of Mek1 in *dmc1*Δ-arrested cells changes the cellular physiology, as DSB repair can now occur, thereby relieving the signal to the checkpoint and allowing meiotic progression (Niu et al., 2005; Wan et al., 2004) (Figure 2-2B). Although the inhibitor was present for only 20 min, the presence of phosphopeptides with ratios <1 suggests that this is enough time for at least some proteins that are phosphorylated only after strand invasion to be modified. An excellent example of this type of regulation was observed with Rec8. Rec8 is a meiosis-specific subunit of cohesin, the multisubunit complex that holds sister chromatids together (Klein et al., 1999). The spindle checkpoint monitors the attachment of homologous pairs of sister chromatids to opposite poles of this spindle at Meiosis I (Shonn et al., 2000). Once all homologous pairs are properly oriented, separase is activated to cleave Rec8 specifically along chromosome arms, thereby allowing reductional segregation (Buonomo et al., 2000). This cleavage requires phosphorylation of Rec8 by several kinases, including Cdc7-Dbf4 and Hrr25 (Katis et al., 2010). Our SILAC experiments identified eight phosphosites on Rec8 that are present on peptides that exhibit ratios less than 1 (Figure 2-5C). Five of these have been previously identified by MS studies of Rec8 enriched from meiotic cells and phosphorylation of these amino acids helps promote separase cleavage (Figure 2-4) (Brar et al., 2006; Katis et al., 2010). Our MS data suggest, therefore, that phosphorylation of these sites on Rec8 does not occur until after strand invasion.

Discussion

SILAC requires that cells be grown in medium containing either light or heavy amino acids so that proteins coming from different cultures can be distinguished by the differences in their mass. Controlling the source of amino acids requires the use of synthetic medium. A problem for using SILAC for studying meiosis is that cells pre-grown in standard synthetic medium do not sporulate well. Our development of a synthetic medium that allows efficient sporulation has enabled the application of SILAC to meiotic yeast cells for the first time. In comparison to YPA pre-growth medium, there is approximately a two-hour delay in the onset of premeiotic DNA synthesis after pre-growth in RPS-L. This delay may be due to the need to deplete particular nutrients such as glucose before entry into meiosis. Importantly, after pre-growth in RPS-L, meiotic recombination and progression occur relatively synchronously and with high efficiency to produce viable spores.

One way to identify kinase substrates using SILAC is to arrest cells containing an analog-sensitive allele of the kinase, and then to inhibit the kinase in either the heavy or light culture (Holt et al., 2009). For meiotic studies, a number of different arrest points are available. In addition to the *dmc1*Δ arrest used in this work, *ndt80*Δ can be used to arrest cells in pachytene when homologous chromosomes are completely synapsed and double Holliday junction intermediates have formed and *pCLB2-CDC20* can be used to arrest cells in Metaphase I, after synaptonemal complex disassembly and crossover formation are complete (Allers and Lichten, 2001; Lee and Amon, 2003; Xu et al., 1995). In addition, analog-sensitive kinases have been developed for several kinases known to play key roles in meiosis, including *CDC7*, *CDC28*, *IME2*, and *HRR25*

(Benjamin et al., 2003; Katis et al., 2010; Wan et al., 2008). An alternative approach to using analog-sensitive kinase mutants is to induce transcription of a gene encoding a wild-type kinase during an arrest. For example, induction of *CDC5*, the polo-like kinase in budding yeast, in *ndt80*Δ arrested cells is sufficient for Holliday junction resolution and synaptonemal complex disassembly (Sourirajan and Lichten, 2008). Therefore by inducing *CDC5* in *ndt80*Δ cells specifically in the light culture, a high L:H phosphopeptide ratio would be expected for Cdc5 substrates. SILAC can now be used to look at the function of these kinases (and others) at various times during meiosis.

Our method was validated by showing that known targets of Mek1 can be detected with high L:H ratios from *dmc1*Δ arrested cells. One of these peptides contained Mek1 T327, which is present in the Mek1 activation loop and is autophosphorylated *in trans* to activate the kinase (Niu et al., 2007). In addition, peptides with L:H ratios >2 were observed for Mek1 T331. These ratios suggest that Mek1 may be the kinase that phosphorylates T331, even though this threonine is not contained within a Mek1 consensus site (Mok et al., 2010). It should be noted that the experimental approach of inhibiting the kinase for a brief time during an arrest may underestimate the number of kinase substrates. This is because high L:H ratios are predicted for peptides containing phosphorylation sites based on the assumption that phosphatases can remove phosphates from substrates during the time that the kinase is inactivated, which may not always be true. In addition, the data can also be analyzed to determine proteins with L/H ratios <1 which may represent phosphorylation that is happening as a result of kinase inhibition, as was seen for Rec8.

Although our goal is to define kinase substrates in meiosis, SILAC has other applications as well. For example, SILAC can also be used to look at protein-protein interactions (Blagoev et al., 2003). By allowing meiotic proteins to be labeled with heavy amino acids, our protocol opens the door for many different SILAC applications to meiosis.

ACKNOWLEDGEMENTS

We thank Aaron Neiman and Nikhil Bhagwat for comments on the manuscript and Xiangyu Chen for helpful discussions. We are grateful to Doug Bishop and Neil Hunter for a strain and plasmid, respectively. This work was supported by National Institutes of Health grants R01 GM050717 to N. M. H. and T32 GM008468 to R. S.

CHAPTER THREE

Identifying novel substrates of Mek1 at the *dmc1*Δ arrest using quantitative phosphoproteomics

[This chapter contains text and figures from *PLoS One. 2016 May 23;11(5):e0155931. doi: 10.1371/journal.pone.0155931. eCollection 2016*)(Suhandynata et al., 2016). I carried out all of the experiments in the manuscript with the exception of the *rad17* mutant characterization which was performed by L. Wan at Stonybrook University, Stonybrook NY]

Introduction

SILAC experiments using meiotically arrested *dmc1*Δ *mek1-as* cells detected two known *in vivo* Mek1 phosphorylation sites: Mek1 T327 and Rad54 T132 (Suhandynata et al., 2014). The question then is whether the datasets from these experiments can be used to identify unknown Mek1 substrates. Two *dmc1*Δ *mek1-as* SILAC datasets were merged into one non-redundant set of 6,609 peptides for analysis and then divided into three classes based on their light/heavy (L/H) ratios (Table 3-1). Class 1 is comprised of 329 peptides (containing 379 phosphosites due to multiple phosphorylation events) in which the L/H ratio is greater than two (indicated by the red box in Figure 3-1). These phosphosites are candidates for regulation by Mek1 since inhibition of Mek1-as in the heavy culture should lead to underrepresentation of Mek1 phosphopeptides relative to the light culture (Suhandynata et al., 2014). Class 2 contains 5,318 peptides (containing 5,317 sites due to mis-cleaved peptides with identical phosphorylation sites) with L/H ratios < 2 but > 0.5. Phosphorylation of the peptides in this class are apparently unaffected by the presence of the Mek1-as inhibitor. Finally, Class 3 contains 963 phosphorylated peptides (1050 sites) with L/H ratios < 0.5 (indicated by black box) (Figure 3-1). This ratio is indicative of phosphorylation occurring in response to Mek1 inactivation, which allows DSB repair and meiotic progression (Niu et al., 2007; Niu et al., 2009; Suhandynata et al., 2014)(Table 3-1).

Results

Although an L/H ratio >2 is suggestive of Mek1 regulation, there may be other reasons for this ratio that do not involve the proteins being substrates of Mek1.

Table 3-1. Number of phospho-peptides containing consensus motifs in *dmc1*Δ *mek1-as* phosphopeptides with different L/H ratios

Number of peptides = 8563							Potential Kinases based on (Mok et al., 2010)
	Number of unique phosphopeptides= 6609						
	Class 1 379 sites		Class 2 5317 sites		Class 3 1050 sites		
Motif	p-Thr	p-Ser	p-Thr	p-Ser	p-Thr	p-Ser	
Total	96	270	977	4275	226	794	
TP	25	-	470	-	95	-	CDK, Fus3, Hog1, Pho85
SP	-	47	-	749	-	139	CDK, Hog1, Pho85
SQ	-	29	-	197	-	29	Mec1/Tel1 (Traven and Heierhorst, 2005)
RXXT	18	-	140	-	30	-	Mek1, Gin4, Hsl1, Ksp1, Psk2, Snf1, Yak1
RXXS	-	22	-	732	-	98	Gin4, Hsl1,Ksp1, Psk2, Rck2, Snf1, Yak1
SXXD	-	29	-	457	-	70	?
SXXXL	-	17	-	356	-	64	?
SXXE	-	34	-	544	-	85	?
SXXSp	-	34	-	554	-	119	?
EXS	-	21	-	278	-	76	Cdc5?
SA	-	14	-	241	-	75	?
DXS	-	19	-	282	-	68	Cdc5

*Red text indicates motifs that are enriched in either Class 1, 2, or 3

? indicates motifs unassociated with a particular kinase

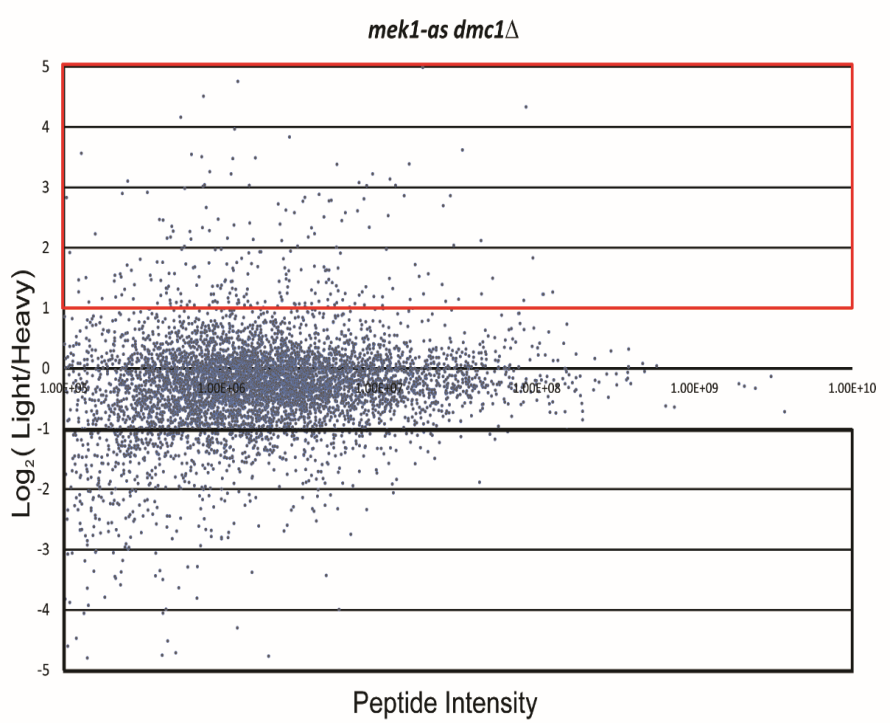

Figure 3-1. Integrated light/heavy (L/H) ratios of phosphopeptides obtained from the merged non-redundant phosphopeptide datasets from two SILAC experiments using *dmc1*Δ *mek1-as* diploids. L/H ratios of phosphorylated peptides are plotted on a $\log_2$ scale (Y-axis) as a function of peptide intensity (X-axis). The red box indicates Class 1 peptides with L/H ratios > than 2.0, while the black box indicates Class 3 peptides with L/H ratios < 0.5. Peptide intensity is a measure of how well each peptide is ionized and subsequently detected by the MS and is correlated to the quantity of each peptide in the sample. Highly abundant peptides will display peptide intensities with large signal to noise ratios and therefore have more accurate L/H ratios when compared to lower abundance peptides with signal to noise ratios closer to 1. L/H ratios were calculated by dividing the integrated peptide intensities of light and heavy peptides. Integrated peptide intensities are defined as the area under the curve of the peptide elution peak.

For example, if a protein that is phosphorylated at the *dmc1*Δ arrest is dephosphorylated in response to meiotic progression, then an L/H ratio >2 would be obtained due to the loss of phosphorylation in the heavy sample. Alternatively, if a protein is degraded in response to meiotic progression, then a L/H ratio >2 would be observed due to the loss of protein in the heavy sample. Therefore further analysis was

performed to determine which of the 379 phosphorylation sites are most likely to be Mek1 substrates.

One way to identify potential kinase substrates in large phosphoproteomic screens is to ask whether amino acids surrounding the phosphorylated amino acid match a known consensus sequence for a kinase of interest, as has been done for CDK and Mec1/Tel1 (Chen et al., 2010; Holt et al., 2009). I employed an alternative approach that asked, in an unbiased way, what motifs are enriched in the *dmc1*Δ *mek1-as* dataset. These motifs were then compared to previously identified consensus sequences to identify the potential kinases involved. The Motif-X algorithm was developed in 2005 by the Gygi group and works by extracting statistically significant motifs from large data sets of naturally occurring phosphorylation sites (Schwartz and Gygi, 2005). The algorithm works by taking the six residues upstream and downstream of a specified phosphorylated amino acid and determining whether the observed number of occurrences for a particular amino acid at one of these positions is statistically enriched over background. The background probability is calculated using the distribution of amino acids surrounding either serine or threonine in the yeast proteome.

Motif-X can only analyze one type of phosphorylated amino acid at a time. Therefore enrichment analysis around phospho-threonine must be performed independently from phospho-serine and phospho-tyrosine. The 379 Class I phosphorylation sites were therefore divided into three query sets: 96 phosphothreonine sites, 270 phosphoserine sites, and 13 phosphotyrosine (Table 3-1). To be detected as a motif, the sequence must be present at a frequency of at least 3.96% with a *p*-value of

0.01 (Fig 3-2A). Three consensus sites were detected for the Class 1 peptides: T/SP, SQ, and RXXT. No motifs containing phopsho-tyrosine were detected, perhaps due to the small number of peptides, therefore phospho-tyrosine was excluded from further analyses. The T/SP consensus could be indicative of CDK phosphorylation (Holt et al., 2009), while the SQ motif suggests Mec1/Tel1 phosphorylation (Chen et al., 2010)

The remaining motif, RXXT, was present in 18 of 96 Class I peptides containing phosphothreonine and is the same as the Mek1 consensus site determined both *in vitro* and *in vivo*. *In vitro*, incubation of peptide libraries with ATP and partially purified GST-Mek1 produced a consensus of RXXT/S (Mok et al., 2010). Mek1 phosphorylation sites that occur *in vivo* are all phosphorylated on threonine (Rad54 T132, Mek1 T327, H3 T11 and Hed1 T40) (Govin et al., 2010; Niu et al., 2007; Niu et al., 2009; Suhandynata et al., 2014) (Nancy Hollingsworth, personal communication), consistent with the Motif-X analysis that detected enrichment of RXXT, but not RXXS, in the Class I sites. To test whether enrichment of the RXXT motif is specific to Class 1 peptides as would be predicted for Mek1 targets, Motif-X analysis was performed on the Class 2 and Class 3 phosphosites. Seven motifs were revealed using the 5,317 Class 2 sites: TP/SP, RXXS, SXXE, SXXXL, SXXD, and SXXSp (p indicates the phosphorylated residue in cases where multiple serines/theronines are present in the motif) (Fig 3-2B), while six motifs were identified from the 1,050 Class 3 phosphosites: T/SP, DXS, RXXS, KXXS, SA, SXXSp, EXS, and SSp (Fig 3-2C). Interestingly the RXXT motif was enriched only in Class 1 peptides, consistent with the phosphates being added by Mek1.

Of the 175 RXXT sites in the dataset, only 18 are Class I. The Class 2 and Class 3 RXXT peptides are likely due to other arginine-directed kinases such as Gin4, Hsl1,

Ksp1, Psk2, Rck2, Snf1, and Yak1 (Mok et al., 2010) (Table 3-1). To illustrate the distribution of the RXXT motif across the entire dataset, the 175 RXXT sites were plotted by their L/H ratios as a function of their peptide intensity. As seen in Figure 3-3, there are more than twice as many phosphosites with L/H ratios greater than 4 as there are phosphosites with L/H ratios less than 0.25, indicating that the RXXT sites are enriched in the light culture where Mek1 is still active. This suggests RXXT sites that have SILAC ratios that are unchanged or less than 0.25 are due to other arginine directed kinases. Together with the Motif-X analysis, the conclusion is that the RXXT motif is specifically enriched in the Mek1 active culture. The 18 RXXT phospho-peptides identify 16 proteins, due to the presence of two RXXT phospho-sites on Mek1 and Rfx1 (Table 3-2). Two of these sites are confirmed *in vivo* targets of Mek1: Mek1 T327 and Rad54 T132 (Niu et al., 2007; Niu et al., 2009). Two known substrates were not detected: H3 T11 and Hed1 T40. H3 T11 was likely not identified as the expected tryptic peptide containing the T11 residue is too small to be detected in the mass window used by the MS method. Phosphorylation of Hed1 T40 *in vivo* was originally

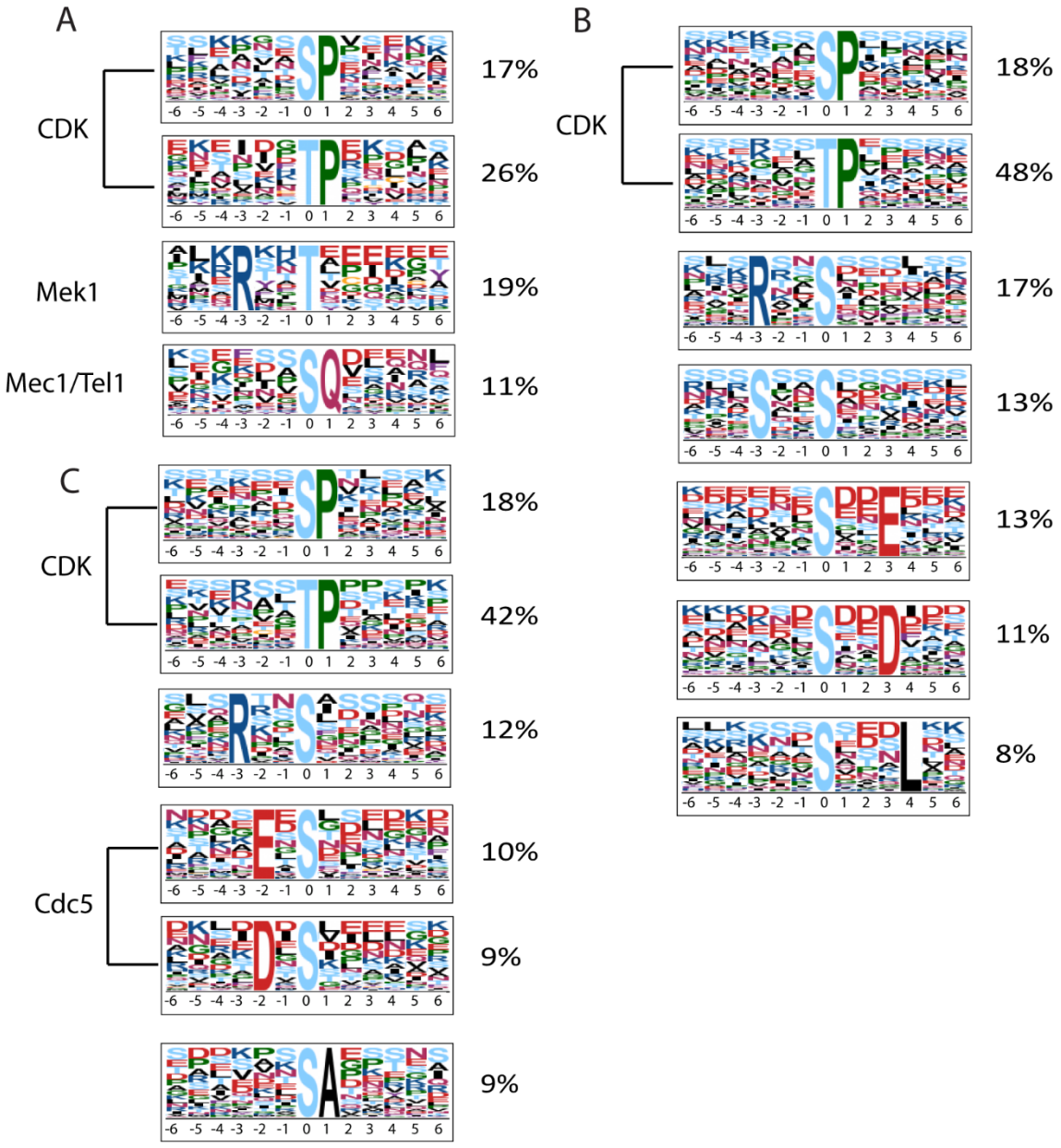

Figure 3-2. Motif analysis of the *dmc1*Δ *mek1-as* SILAC phosphopeptides. A. Consensus sites detected by the Motif-X algorithm using the 379 Class I phosphosites with L/H ratios > 2. The size of each amino acid shows how enriched it is relative to the phosphorylated amino acid, and the color indicates physical and chemical properties of the indicated amino acid (Red: acidic; Dark blue: basic; Black: hydrophobic; Yellow: cysteine; Green: proline/Glycine). The numbers indicate the frequency of sites containing the motif. All of the indicated motifs exhibited significant enrichment with a *p*-value of 0.01. B. Same as in A except Motif-X analysis was performed on the 5,317 Class 2 sites with L/H ratios between 0.5-2.0. C. Same as in A except Motif-X analysis was performed on the 1,050 Class 3 sites with L/H ratios < 0.5.

discovered by LC-MS using whole cell lysates (Aaron Neiman, personal communication). In contrast, the *dmc1*Δ *mek1-as* datasets were generated using crude chromatin. One possible explanation for the failure to detect Hed1 T40 phosphorylation is that Hed1 interacts transiently with chromatin and was lost in the cytosolic fraction during the chromatin enrichment step.

The fact that this analysis detected known Mek1 substrates raises the possibility that one or more of the remaining 16 proteins is also phosphorylated or regulated by Mek1 (Table 3-1). To determine which proteins are most likely to be *bona fide* substrates of Mek1, a number of additional criteria were applied. First, since Mek1 is a nuclear protein (Bailis and Roeder, 1998) and all of its known targets are present on chromatin, a reasonable assumption is that additional substrates will also be present in the nucleus. Therefore proteins with cytosolic functions such as Akr1 and Ydj1 are considered low priority. A second assumption is that Mek1 substrates will be associated with DNA processes, ruling out proteins involved in splicing and ribosome assembly/function such as Cus1, Utp14, Set7 and Nop14. Third, Mek1 is involved in DSB repair, making proteins involved in DNA replication, transcription, and chromatin modification of lower priority than proteins known to have a role in DSB formation or repair such as Spp1 and Rad17 (Table 3-2). In Table 3-2, the proteins are listed from top to bottom in descending order of likelihood for being Mek1 substrates involved in meiotic recombination.

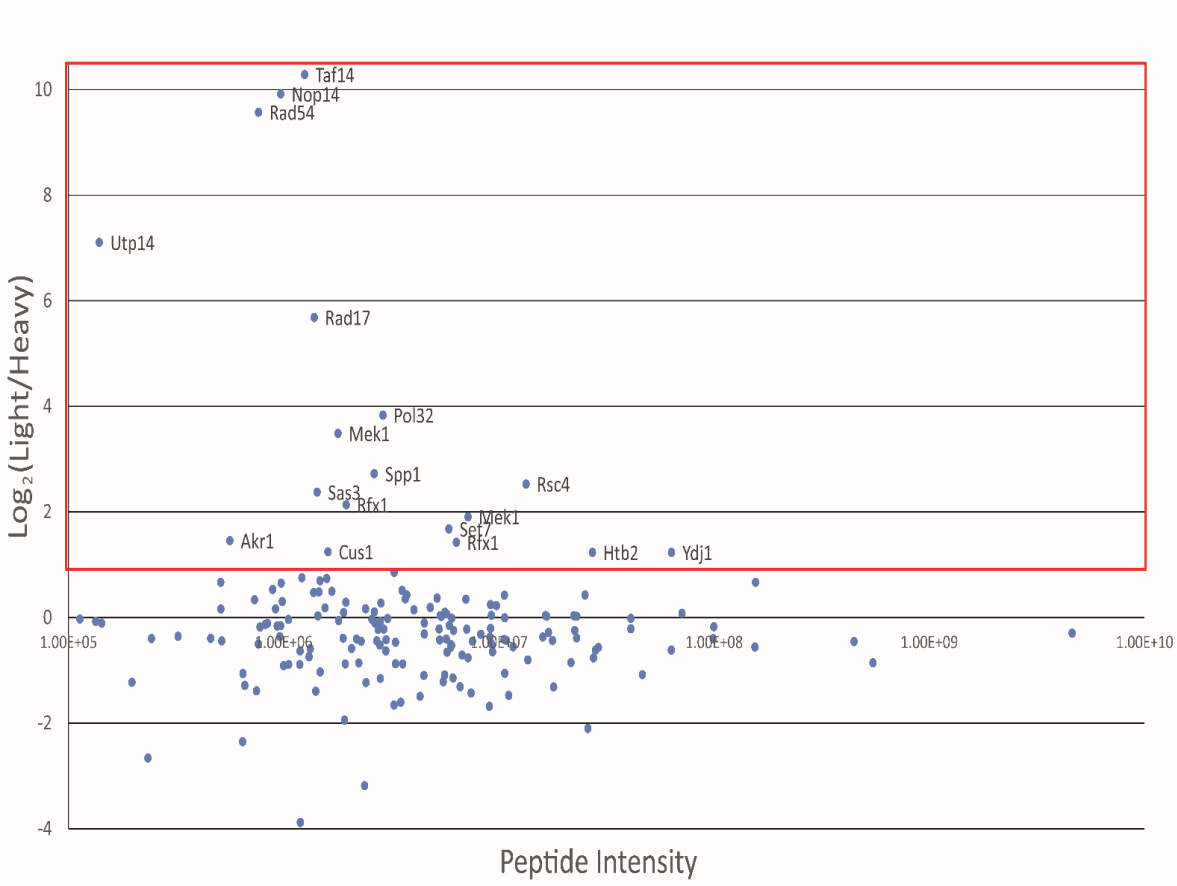

Figure 3-3. Graphical representation of RXXT phosphorylation sites identified in *dmc1*Δ *mek1-as cells.* The L/H ratios of 175 RXXT phosphopeptides were plotted on a $\log_2$ scale (Y-axis) as a function of peptide intensity (X-axis). The red box indicates peptides that are >2-fold enriched in the Light (Mek1 active) culture. The name indicates the protein from which the phosphopeptide was derived.

Table 3-2. Proteins containing RXXT motifs from the subset of *dmc1*Δ *mek1-as* phosphopeptides with L/H ratios >2.

RXXT Protein[a]	Phosphopeptide Sequence[b]	Site
Mek1	R.MHT#VVGTPEYCAPEVGFR.A	T327
	R.AAT#LEQR.G	T356
Rad54	R.SFT#VPIK.G	T132
Spp1	R.NPT#TGEDVYCICK.R	T18
Rad17	R.YGT#DKGNETS#NDNLLQLNGK.K	T350
Rsc4	R.STT#SDIEK.T	T405
Pol32	R.SKT#TPEETTGR.K	T146
Rfx1	R.TNT#FPSIPSSTK.K	T199
	R.RNT#QEIIAK.Q	T226
Htb2	R.KET#YSSYIYK.V	T39
Taf14	R.RTTT#NTTAEPK.A	T154
Sas3	R.KIT#LIEDDEE.-	T824
Nop14	R.TKT#EEEKNAEAEEK.K	T291
Set7	R.KLT#EEEK.S	T480
Utp14	K.RLDT#YGSGEANEYVLPSANAASGASGK.L	T218

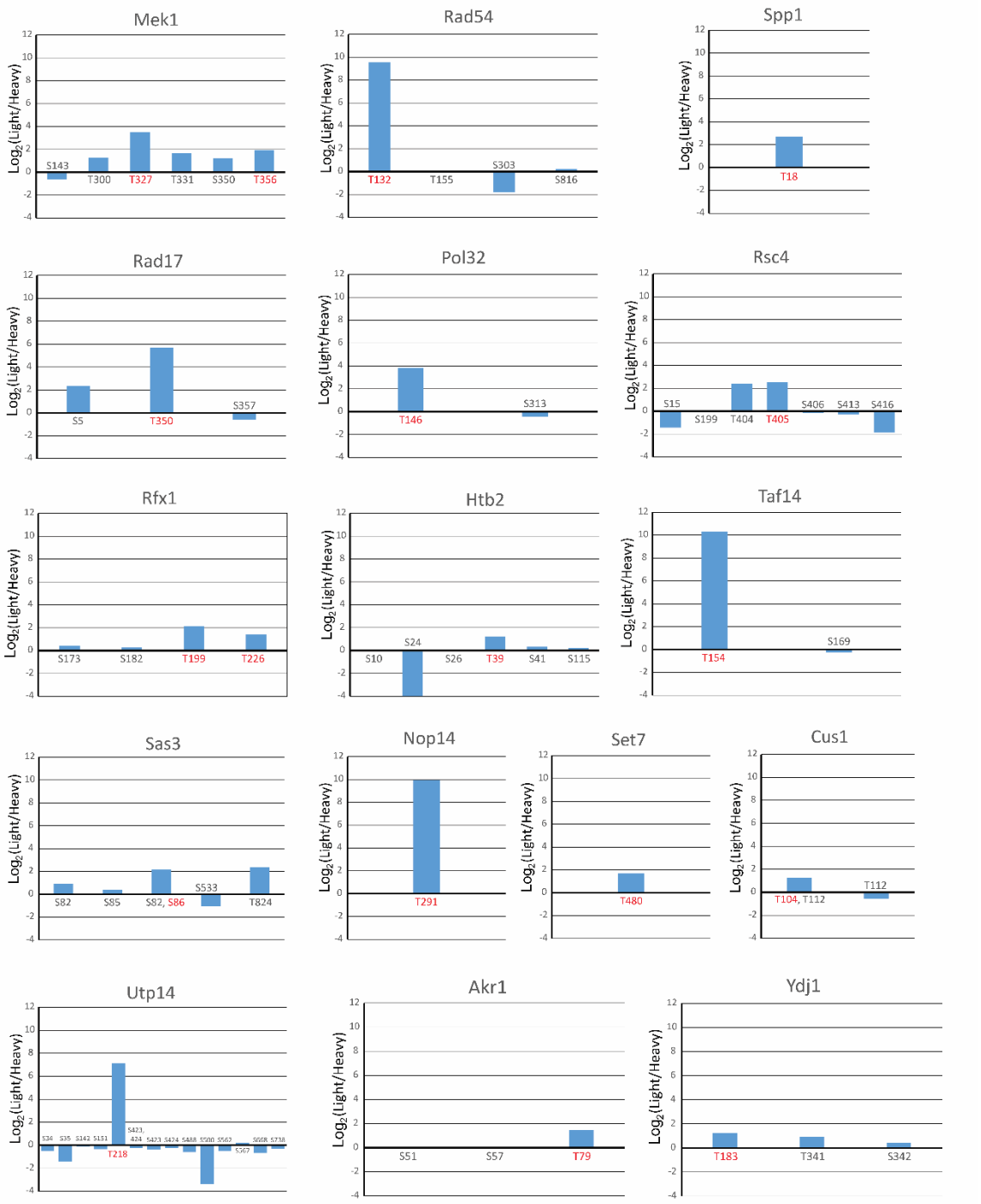

Figure 3-4. Distribution of phosphosites on Class 1 proteins containing at least one RXXT motif. L/H ratios for individual phosphosites identified on Class I RXXT proteins (X-axis) were plotted on the Y-axis. RXXT sites are colored in red.

A summary of the molecular processes each Class I protein is involved in is listed below.

Ydj1: Ydj1 is a non-essential Hsp40 molecular chaperone that regulates Hsp70 proteins, specifically Ssa1 and Ssa2, to promote polypeptide folding (Cyr and Douglas, 1994; Cyr et al., 1992). Outside of polypeptide folding, Ydj1 is involved in the cellular processes of stress response, mitochondrial and endoplasmic reticulum protein translocation, and ubiquitin dependent degradation (Caplan et al., 1992; Lee et al., 1996; Lu and Cyr, 1998). Loss of *YDJ1* results in cells that are slow growing at 25˚C, inviable at 37˚C, and exhibit improper folding of Cdc28 as well as other nascent kinases (Fan et al., 2005; Mandal et al., 2008). As seen in Figure 3-4 three unique phosphorylation sites were identified on Ydj1, T183, T341 and S342, with T183 fitting the RXXT consensus motif. T183 has a Log_2 (L/H) of 1.2, which is just over the arbitrary fold enrichment cutoff of 1. Given its cytosolic function and marginal L/H ratio, it is questionable whether Ydj1 is truly a Mek1 substrate.

Akr1: Akr1 is an Ankyrin repeat containing protein that is the palmitoyl transferase for Yck2p, a budding yeast isoform of casein kinase I, and is localized on Golgi membranes (Babu et al., 2004). Palmitoylation of Yck2p is required for efficient targeting of the casein kinase isoform to plasma membranes. Deletion of *AKR1* results in cells with abnormal cell morphology, inviability at 37˚C and reduced sporulation (Enyenihi and Saunders, 2003; Kao et al., 1996). Three unique phosphorylation sites were identified on Akr1 with T79 fitting the RXXT motif (Figure 3-4). The other two phosphorylation sites are S51 and S57 which both have Log_2 (L/H) of nearly 0. This suggests that the enrichment of T79 in the light culture is due to a reduction in phosphorylation of the T79

site in the heavy culture, and not due to a change in the protein abundance of Akr1. However, like Ydj1, its cytosolic function suggests it is unlikely to be a target for Mek1. The RXXT phosphorylation site identified on Akr1 has not been previously reported according to PhosphoGRID, and therefore could potentially be meiosis specific (PhoshoGRID, 2015).

Cus1: Cus1 is an essential nuclear protein that is required for the assembly of U2 snRNP into the spliceosome and has been identified as a suppressor of U2 snRNP mutants, such as *prp11 and prp5,* in budding yeast (Pauling et al., 2000; Wells et al., 1996). The essential region of Cus1 shares homology with human splicing protein SAP145, and is also required for Cus1 binding to yeast splicing factor Hsh49 (Pauling et al., 2000). As seen in Figure 3-4, two sites were identified on Cus1, T104 and T112, with T104 fitting the RXXT motif. The Log_2 (L/H) of T104 was 1.2, which just makes the arbitrary cutoff for being a potential candidate. Although Cus1 does function in the nucleus, its function in splicing and marginal L/H ratio makes it less likely to be a Mek1 substrate involved in recombination.

Utp14: Utp14 is a component of the small subunit processome which is a large ribonucleoprotein complex that is involved in rRNA processing and assembly of the 40s ribosomal subunit (Fromont-Racine et al., 2003). Utp14 associates with an rRNA methyltransferase known as Bud23 that is involved in the processing of rRNA, and mutations in *UTP14* suppress the *bud23* rRNA processing defect (Sardana et al., 2014). As seen in Figure 3-4, 13 unique sites were identified on Utp14, with T218 being the site that fits the RXXT motif. The RXXT phosphorylation site identified on Utp14 has not been previously reported according to PhosphoGRID, and therefore could potentially be

meiosis specific (PhoshoGRID, 2015). Although T218 has a Log_2 (L/H) 7.1, and is the only site identified on Utp14 that is enriched in the light culture, the role of Utp14 in rRNA processing lowers the likelihood that Utp14 is a substrate of Mek1.

Set7: Set7/Rkm4 is a ribosomal lysine methyltransferase that is required for Lys-55 monomethylation of the ribosomal 60s subunit proteins Rpl42ap and Rpl42bp (Webb et al., 2008). Loss of Set7 results in a slow growth phenotype that has not been characterized (Webb et al., 2008). As seen in Figure 3-4 only one site, T480 (Log_2 (L/H): 1.68), was identified on Set7. The RXXT phosphorylation site identified on Set7 has not been previously reported according to PhosphoGRID, and therefore could potentially be meiosis specific (PhoshoGRID, 2015). Set7's function in methylating ribosomes makes it less likely to be a target Mek1.

Nop14: Nop14 is functionally conserved in eukaryotes, and is encoded by a stress-responsive gene that is required for 18S rRNA maturation and 40S ribosome production. Yeast cells deleted for *NOP14* have reduced levels of mature 18S rRNA and reduced levels of the 40S ribosome subunit (Liu and Thiele, 2001). A recent study in in HeLa cells suggests that Nop14 is an RNA binding protein that controls RNA fate from synthesis to degradation (Castello et al., 2012). As seen in Figure 3-4, only one phosphorylation site, T291 (Log_2(L/H): 9.9), was identified on Nop14. The extremely large Log_2 (L/H) suggests that Nop14 is phosphorylated in the light culture and that it is either dephosphorylated or degraded after Mek1 inactivation. The RXXT phosphorylation site identified on Nop14 has not been previously reported according to PhosphoGRID, and therefore could potentially be meiosis specific (PhoshoGRID, 2015).

Nop14 is a low priority candidate because its role in 40S ribosome production decreases the probability that it is a Mek1 substrate.

Sas3: Sas3 is the catalytic subunit of the NuA3 histone acetyl transferase (HAT) complex that acetylates H3K9 and H3K14 (Vicente-Munoz et al., 2014). Recruitment of NuA3 to nucleosomes *in vivo* requires methylation of H3K4 and H3K36, which is catalyzed by the Set1 and Set2 histone methytransferases, respectively (Martin et al., 2006; Vicente-Munoz et al., 2014). *sas3*Δ does not exhibit any obvious phenotypes. However, deleting both *SAS3 and GCN5,* another HAT, results in cell death, suggesting that *SAS3* and *GCN5* have overlapping roles (Vicente-Munoz et al., 2014). As seen in Figure 3-4, five unique sites were identified on Sas3 with T824 (Log_2 (L/H): 2.3) fitting the RXXT motif. The RXXT phosphorylation site identified on Sas3 has not been previously reported according to PhosphoGRID, and therefore could potentially be meiosis specific (PhoshoGRID, 2015). Sas3 is known to associate with chromatin, and thus makes it a more likely Mek1 target then the previously mentioned candidates, however it is not known to associate with DSBs, which is where activated Mek1 is localized.

Taf14: Taf14 physically associates with the general transcription factors TFIID and TFIIF, the chromatin remodeling complexes SWI/SNF, INO80 and RSC, and the histone modification enzyme NuA3 (Schulze et al., 2010). Cells lacking *TAF14* are viable but are thermo/osmo sensitive and display morphological defects (Welch and Drubin, 1994). Taf14 contains a conserved YEATS domain (Yaf9, ENL, AF9, Taf14, Sas5 containing domain) that has been suggested to play a negative role in cell growth (Schulze et al., 2010). Cells lacking this domain grow better under stress conditions

such as in the presence of the microtubule destabilizing drug benomyl (Schulze et al., 2010). As seen in Figure 3-4, the potential Mek1 phosphorylation site, T154 (Log_2(L/H): 10.2), is located in the YEATS domain, however since most of the work involving Taf14 has been done in vegetative cells, characterization of T154 in mitotic cells should be done before characterization in meiotic cells. T154 is enriched in the light culture while S169 has a Log_2 (L/H) of close to 0, suggesting that T154 phosphorylation is rapidly lost after addition of inhibitor to the heavy culture. The RXXT phosphorylation site identified on Taf14 has not been previously reported according to PhosphoGRID, and therefore could potentially be meiosis specific (PhoshoGRID, 2015). Taf14 T154 is therefore considered a potential Mek1 phosphosite.

Rfx1/Crt1: Rfx1, also known as Crt1, is a transcriptional repressor responsible for repressing the DNA damage inducible ribonucleotide reductase (*RNR*) genes (Zhang and Reese, 2005). It is a DNA binding protein with a unique winged-helix binding domain, and loss of *RFX1* disrupts nucleosome arrays and gene activation (Li and Reese, 2001; Zhang and Reese, 2005). As seen in Figure 3-4, four unique sites were identified on Rfx1, with two of the sites, T199 and T226, fitting the RXXT motif. Both T199 and T226 have modest Log_2 (L/H) of 2.1 and 1.4 respectively. The T226 phosphorylation site identified on Rfx1/Crt1 has not been previously reported according to PhosphoGRID, and therefore could potentially be meiosis specific, whil e the T199 has been identified in vegetative cells (PhoshoGRID, 2015). Rfx1/Crt1 T199 is therefore considered a potential Mek1 phosphosite.

Pol32: Pol32 is the non-essential subunit of Polδ and is required for the initiation of Rad51-dependent break induced replication (BIR) (Lydeard et al., 2007). BIR is an

efficient homologous recombination pathway that is used in mitotic, but not meiotic, cells when homology is present on only one end of the DSB (Lydeard et al., 2007). Deletion of *POL32* leads to cells being deficient for damage induced mutagenesis as well as being unable to grow at cold temperatures (13˚C) (Gerik et al., 1998). This result suggests that *POL32* functions in error-prone DNA repair and could explain why deletion of *POL32* results in an anti-mutagenic effect (Gerik et al., 1998). Two sites were identified on Pol32, T146 and S313, with T146 fitting the RXXT motif (Figure 3-4). T146's Log_2 (L/H) is 3.8 and the fact that S313 has a Log_2 (L/H) of close to 0 indicates that equal amounts of Pol32 were present in the light and heavy chromatin preparations, ruling out a trivial explanation for the increased L/H ratio. The RXXT phosphorylation site identified on Pol32 has not been previously reported according to PhosphoGRID, and therefore could potentially be meiosis specific (PhoshoGRID, 2015). Pol32 T146 is therefore considered a potential Mek1 phosphosite.

Rsc4: Rsc4 is a subunit of the essential RSC multi-subunit chromatin remodeling complex (Laurent et al., 1992). Rsc4 contains Bromodomains that allow it to interact with acetylated histones, specifically H3K14 (Kasten et al., 2004). The RSC complex is involved in the repair of DSBs, specifically by facilitating dissociation of the invading DNA strand before ligation, in the homologous recombination pathway (Chai et al., 2005; Chambers and Downs, 2012). Seven unique phosphorylation sites were identified on Rsc4 (Figure 3-4), with only T405 (Log_2 (L/H):2.5) fitting the RXXT motif. Interestingly the only other light enriched site identified on Rsc4 is T404 (Log_2 (L/H): 2.4), which has a Log_2 (L/H) very similar to T405, suggesting that active Mek1 could promote phosphorylation of both T404 and T405 (Figure 3-4). The fact that Rsc4 is part of a

complex known to be recruited to DNA DSBs and is also thought to be implicated in the homologous recombination pathway makes it a very interesting target for Mek1 phosphorylation.

H2B: The (H2B) protein (encoded by the *HTB1* and *HTB2* genes) is one of four histone subunits that make up the histone octamer around which DNA wraps to form a nucleosome (Briggs et al., 2002). Previous studies have shown that ubiquitylation of H2B promotes the formation of meiotic DSBs (Yamashita et al., 2004), suggesting that H2B might be involved in the processes occurring near meiotic DSBs. *In vitro* kinase assays with partially purified Mek1 and histones purified from yeast demonstrated that H2B is phosphorylated on T39 by Mek1 *in vitro* ((Niu, 2007) and N. M. Hollingsworth, personal communication). Mutation of the phosphorylation site from both copies of *HTB1/2* genes had no obvious defects in spore viability (N. M. Hollingsworth, personal communication). Six unique phosphorylation sites were identified on H2B with T39 (Log_2 (L/H): 2.36) being the only one to fit the RXXT motif (Figure 3-4). T39 is the only site identified on H2B that is enriched in the light culture after the inactivation of Mek1 suggesting that the phosphorylation is independent of protein abundance and is specific to the activity of Mek1 (Figure 3-4). The discovery that the T39 is phosphorylated *in vivo* and is potentially regulated by Mek1, suggests that more in-depth analysis of this mutant would be worthwhile.

Rad17: Rad17 is part of the “9-1-1” complex (Ddc1-Rad17-Mec3) in budding yeast which is involved in the mitotic DNA damage response, as well as the meiotic recombination checkpoint (Lydall et al., 1996; Majka and Burgers, 2003). The 9-1-1 complex has a ring-like structure and is a clamp loaded onto the ssDNA-dsDNA junction

by the Rad24-replication factor complex (RFC) (Majka and Burgers, 2003; Shiomi et al., 2002). After being loaded, the clamp has the ability to slide across double stranded DNA much like the DNA replication clamp PCNA and is able to promote downstream events such as the activation of Mec1 (Majka and Burgers, 2003; Majka et al., 2006). The 9-1-1 complex promotes end resection by recruiting the nuclease/helicase pair Dna2-Sgs1 and the nuclease Exo1 (Ngo et al., 2014). Deletion of *RAD17* results in increased sensitivity to DNA damage such as UV, MMS, and HU in mitotic cells (Kobayashi et al., 2004) and delayed meiotic progression and loss of the meiotic recombination checkpoint in *dmc1*Δ cells (Lydall et al., 1996). Rad17 is implicated in one of the two known pathways for Mek1 activation in meiosis, Mec1 via Rad17 and Tel1 via Pch2 (Ho and Burgess, 2011). Deletion of *RAD17* lowers spore viability to 37.1% due to a decrease in interhomolog recombination, (Ho and Burgess, 2011). A recent study showed that the 9-1-1 complex promotes the assembly of a functionally diverse set of proteins called the ZMM proteins at DSBs (Shinohara et al., 2015). *MEK1* is required for phosphorylation of the C terminus of Zip1, one of the ZMM proteins. In the absence of phosphorylation, the Zip1 mutant protein forms foci which have been proposed to be Zip1 bound to DSBs (Chen et al., 2015). One possible model is that phosphorylation of Rad17 by Mek1 helps recruit Zip1 proteins to DSBs thereby promoting COs through the ZMM pathway. As seen in Figure 3-4, the Rad17 T350 exhibits a L/H ratio of 5.6, which is significantly more affected by the inhibition of the Mek1 kinase compared to other phosphorylation sites on Rad17, supporting the idea that the phosphorylation is Mek1 specific. Furthermore, the T350 phosphorylation site identified on Rad17 has not been previously reported according to PhosphoGRID, and

therefore could potentially be meiosis specific (PhoshoGRID, 2015). To test if the Rad17 T350 phosphorylation is functional *in vivo,* the site should be mutated to alanine (to prevent phosphorylation) or aspartic/glutamic acid (to act as phosphomimics). Comparison of mitotic DNA damage sensitivity to the a *rad17*Δ strain would determine if the site is functional in vegetative cells, while spore viability, meiotic progression assays and the ability to bypass the *dmc1*Δ, could determine whether phosphorylation of T350 functions specifically in meiosis, as would be expected for a Mek1 site. *In vitro* kinase assays using an analog-sensitive version of Mek1 (GST-Mek1-as) with recombinant Rad17 protein can determine whether phosphorylation is direct (Niu et al., 2009). The fact that Rad17 is implicated in the meiotic recombination checkpoint and is also localized to DSBs, makes it a very promising target of Mek1.

Spp1: Spp1 is a subunit of the Set1/COMPASS (complex of proteins associated with Set1) complex (Miller et al., 2001). The complex is composed of seven subunits in addition to Set1, which are Bre2, Swd1, Spp1, Swd2, Swd3, Sdc1, and Shg1 (Miller et al., 2001). In vegetative cells, Set1/COMPASS catalyzes H3K4 methylation, which then recruits chromatin remodelers and promotes gene activation (Flanagan et al., 2005; Lauberth et al., 2013; Shilatifard, 2012). Spp1 has recently been shown to be a bridge that brings hotspot sequences in the loop regions of meiotic chromosomes to the chromosome axes where Spo11 then catalyzes DSBs (Acquaviva et al., 2013; Sommermeyer et al., 2013). Spp1 contains a PHD finger domain that allows it to bind to H3 proteins trimethylated on lysine 4 (Shi et al., 2007). It also contains a Mer2 binding domain which is the proposed mechanism by which Spp1 brings the DSB hotspots in the loop regions down to the axes where Mer2 is located (Panizza et al., 2011). While

deletion of *SPP1* has no effect on spore viability, *spp1*Δ mutants alter the pattern of DSB formation, with breaks at some hotspots becoming reduced, while at the same time novel hotspots arise in previously cold regions of meiotic chromosomes (Acquaviva et al., 2013; Sommermeyer et al., 2013). Only one phosphorylation site was detected Spp1 (Figure 3-4). However, it is a high confidence site that was identified multiple times. Moreover, the Spp1 T18 phosphorylation has not been previously reported according to PhosphoGRID, and therefore could potentially be meiosis specific (PhoshoGRID, 2015). Since Spp1 has been suggested to bring down the chromosome loops down to the axis, we speculate that phosphorylation of Spp1 by Mek1 promotes the release of one end of the DSB, possibly facilitating DSB repair by enabling the end of the break to find the homolog. Phenotypic analysis of the effects of *spp1-T18A* and *T18D* mutants on DSB patterns and meiotic progression could indicate whether phosphorylation of this site is important in meiosis.

In addition to the RXXT motif, the SQ motif is also enriched within Class 1 phosphosites. The S/TQ sequence is a well-established Mec1/Tel1 consensus motif (Traven and Heierhorst, 2005). Mec1/Tel1, yeast homologs of mammalian ATM and ATR respectively, are responsible for controlling the signal transduction cascade of the DNA damage checkpoint (Harrison and Haber, 2006). In vegetative cells, Mec1 has a more prominent role in the activation of downstream checkpoint kinases such as Rad53 (Sanchez et al., 1996; Sun et al., 1996), while Tel1 has a prominent role in regulating telomere length (Greenwell et al., 1995). Mec1/Tel1 are integral for a functional meiotic checkpoint network (Subramanian and Hochwagen, 2014). While Mec1 is activated by RPA coated ssDNA that results from DSB processing, Tel1 is activated primarily by

blunt and protein conjugated DSB ends (Subramanian and Hochwagen, 2014). Mec1/Tel1 promote interhomolog bias by phosphorylating the meiosis specific protein Hop1 in response to DSBs, thereby recruiting and activating Mek1 (Carballo et al., 2008; Chuang et al., 2012). Moreover, Mec1 and Tel1 activate Mek1 via two distinct pathways, Mec1 through the 9-1-1 (Rad17-Mec3-Ddc1) complex and Tel1 through Pch2's interaction with the Mre11-Rad50-Xrs2 (MRX) complex (Carballo et al., 2008)

The Class 1 sites with SQ motifs may identify Mec1/Tel1 substrates important for the activation and maintenance of the meiotic recombination checkpoint. Because addition of 1-NA-PP1 results in repair of DSBs using sister chromatids, the checkpoint is no longer activated, thereby allowing the removal of Mec1/Tel1-mediated phosphorylation. These sites should therefore be under-represented in the heavy culture, resulting in L/H ratios >2. There are 29 unique SQ sites, representing 28 proteins, present in the Class 1 phosphosite dataset (Table 3-3).

Table 3-3. Class 1 proteins containing the SQ Mec1/Tel1 motif.

SQ Protein	SQ Peptide	SQ Site
Atp3	GLCGSIHS#QLAK	S122
Brn1	DSLVDDENEPS#QSLISTR	S254
Hos1	IDYNPS#QDLQR	S110
Ies4	SES#QEQLANNPK	S11
Ioc2	EGSSS#QVSQTpLNIPIK	S262
Ioc3	DQSVSVS#QSSDNLR	S46
Leu4	EIEVSFPSAS#QTDFDFTR	S107
Loc1	EVAPEVFQDS#QAR	S24
Mec1	VPTDPSSS#QEYAK	S38
Ngg1	SEFVVS#QTLPR	S231
Nop58	VSS#QLEK	S70
Pex25	DDGS#QSPIR	S302
Red1	LTNFKPIIDVPS#QDKR	S597
Rfa2	GYGS#QVAQQFEIGGYVK	S122
Rnq1	SGGSDAS#QDR	S64
Rpl1b	ITS#S#QVR	S7
Rpl35b	FEAS#QVTEK	S98
Rts2	S#QQEEQEVIAAELLK	S160
Rtt107	IDSpEEISLS#QDVER	S806
Sas3	LAS#ENSS#QNIVNR	S86
Sgd1	DYS#QDER	S23
Sir3	IEPSADDDVNNGNIPS#QR	S263
Tat1	NSELES#QEKNNLTK	S84
Twf1	LVS#QDSASPLSLTFR	S167
Ume6	ANNS#QESNNATSSTSQGTR	S751
Vps8	IIEDSS#QDLVQQYRK	S1176
Yra1	EFFAS#QVGGVQR	S100
Zip1	STLSS#QK	S515
Zip1	ISS#QNEIVK	S593

Phosphorylated residues containing the SQ motif are followed by "#" while other phosphorylation sites are marked by p following the phosphorylated residue

Further prioritization of the SQ proteins was performed based on their biological functions. The criteria used to separate the SQ proteins was: 1) Proteins that are involved in the mitotic and/or meiotic recombination checkpoint 2) Proteins that exhibit sensitivity to DNA damage when their genes are mutated and 3) proteins previously identified as Mec1/Tel1 targets. The nine proteins, Red1, Mec1, Zip1, Ies4, Rtt107, Ioc2, Rfa2, Spt7, and Rfx1 all satisfy at least one of the three criteria mentioned above, while Mec1, Ies4, Rtt107, Ioc2 and Rfa2 also are sensitive to DNA damage and are also previously identified Mec1/Tel substrates (Chen et al., 2010; Kapitzky et al., 2010). Zip1 and Red1 are meiosis-specific proteins required for crossover interference and IH bias/meiotic recombination checkpoint, respectively (Shinohara et al., 2008; Xu et al., 1997). Zip1is a known target of Mec1 and is phosphorylated by Mec1 on S75, persistence of this phosphorylation was shown to block centromere pairing during meiotic prophase (Falk et al., 2010). Phenotypic analysis of mutants in these putative Mec1/Tel1 phosphosites could determine whether phosphorylation of these proteins is important for activation or maintenance of the meiotic recombination checkpoint.

Class 3 phosphosites may reveal substrates of the polo-like kinase Cdc5

One way that the low L/H ratios observed for Class 3 phosphosites could occur is if the proteins were phosphorylated in response to Mek1 inactivation. Because inactivation of *mek1-as* in the *dmc1*Δ background results in DSB repair using sister chromatids, the cells in the heavy culture were no longer arrested by the meiotic recombination checkpoint and were able to progress through meiosis. Meiotic progression requires induction of *NDT80*, a meiosis-specific transcription factor that is responsible for the expression of >200 genes, including the gene including the polo-like

kinase, *CDC5*, and the cyclin-dependent kinase, *CLB1* (Chu and Herskowitz, 1998). Therefore substrates of both Cdc5 and Cdc28-Clb1 would be predicted to occur in the heavy but not the light culture in the *dmc1*Δ *mek1-as* SILAC experiment. In fact, Cdk consensus T/SP is enriched in the Class 3 phosphosites, as well as the DXS motif, which closely matches the D/EXS/Tψ (where ψ represents a hydrophobic residue) consensus of Polo-like Kinase (PLK) (Nakajima et al., 2003). Furthermore, Polo-like Kinase is known to have conserved Polo-box domains that target the kinase to its substrates (Lee et al., 2005). The human homolog of Cdc5, Plk1, preferentially binds phosphopeptides sequences of Ser-pThr/pSer-Pro/X (Elia et al., 2003a; Elia et al., 2003b). *CDC5* is required for many cell division processes, including CDK activation, spindle formation, cohesin removal from chromosome arms, and cytokinesis (Barr et al., 2004). In budding yeast, PLK is known as Cdc5, and has been shown to play essential roles in mitotic exit and cytokinesis (Lee et al., 2005). In meiotic cells, ectopic expression of Cdc5 at the *ndt80*Δ arrest is sufficient for JM resolution and SC disassembly (Sourirajan and Lichten, 2008). Cdc5 is also necessary for cleavage and removal of cohesion from chromosome arms and mono-orientation of sister kinetochores during meiosis I (Lee and Amon, 2003).

Thus candidate Cdc5 substrates will meet the following criteria: 1) Phosphosites with L/H ratio < 0.5; (2) phosphosites with the D/EXS/Tψ PLK consensus motif and (3) phosphosites on the same protein containing the Ser-pThr/pSer-Pro/X Polo-box binding motif. Prioritization using known biological functions of the candidate proteins can then be used to further refine the list for future characterization of the candidate substrates and their phosphorylation sites. Out of the 1,050 class 3 sites, 13 sites (representing 10

proteins) contained the PLK phosphorylation motif of D/EXS/Tψ consensus motif and the Polo-box binding domain of Ser-pThr/pSer-Pro/X (Table 3-4). The most interesting protein on the list is the meiosis specific protein Zip3.

Zip3 is a member of the ZMM proteins, which are necessary for the formation of 85% of all crossovers in budding yeast (Börner et al., 2004; Lynn et al., 2007). During yeast meiosis, the ZMM proteins stabilize single end invasion (SEI) intermediates, which are then processed into double Holliday junctions (dHJs) that are preferentially resolved into crossovers (CO) (Börner et al., 2004; Hunter and Kleckner, 2001). Deletion of *ZIP3* results in a delay in meiotic progression, a reduction in the formation of cross-overs and spore viability, (12% in the SK1 background) (Agarwal and Roeder, 2000). Interestingly, Zip3 is a reported meiosis specific SUMO (small ubiquitin-related modifier)-E3 ligase and its SUMO-E3 ligase activity has been suggested to play a role in SC assembly (Cheng et al., 2006; Hooker and Roeder, 2006).

The above global phospho-proteomic analysis of *dmc1*Δ *mek1-as* strains has provided insight into not only potential Mek1 substrates but also potential Mec1 and PLK substrates as well. These data have provided new directions for the functional analysis of these potential substrates and how they might be implicated in the meiotic recombination checkpoint, IH bias and perhaps even JM resolution. Additional effort is needed to address the function of these identified sites *in vivo*, and in this perspective the tools of molecular genetics and cytology could be used to elucidate the finer molecular mechanisms of budding yeast meiosis.

Table 3-4. Proteins containing D/EXS/Tψ motif and the Polo Box binding motif from the subset of *dmc1*△ *mek1-as* phosphopeptides with L/H ratios <0.5.

D/EXS/Tψ Protein	D/EXS/Tψ Peptide	D/EXS/Tψ Site
Abp1	DSEFNSFLGTTKPPSMTESS#LK	S296
Cst9/Zip3	SSDIS#IINLVESK	S97
Isw1	IREEFADQT#ANEKENVDGVESK	T1089
Lsb3	SFAGEES#GDLPFR	S408
Net1	DIS#LHSpLK	S744
Nop4	ITGQNNEDEDDADGEDS#MLK	S141
Nup60	ISSMPGGYFHSEIS#PDSTVNR	S81
Nup60	SAEGNNIDQS#LILK	S171
Nup60	SNVVVAETS#PEKK	S382
Rif1	LEDS#GTCELNK	S1694
Rif1	DIS#VLPEIR	S1755
Sef1	LNLHPTPTPGTIIPNPDSS#PSSpGSPTSSAAQR	S160
Shp1	NTFAGGETS#GLEVTDPSDPNSLLK	S155

Phosphorylated residues containing the D/EXS/Tψ motif are followed by "#" while other phosphorylated residues are indicated by a p after the phosphorylated residue.

CHAPTER FOUR

Identifying the synaptonemal complex protein, Zip1, as a Mek1-dependent substrate using SILAC

[Figure 4-3 and Table 4-2 were published in *PLOS Biology (*Chen X., Suhandynata R.T., Sandhu R., Rockmill B., Mohibullah N., Niu H., Liang J., Lo H.C., Miller D.E., Zhou H., Borner G.V., Hollingsworth N.M. (2015) Phosphorylation of the synaptonemal complex protein Zip1 regulates the crossover/noncrossover decision during yeast meiosis. PLoS Biol 13(12): e1002329. doi:10.1371/journal.pbio.1002329*).*]
I am an author on this manuscript and here I describe my contributions to the study.

Introduction

In addition to looking for Mek1 substrates at the *dmc1*Δ arrest, I also performed an experiment to identify Mek1 targets at the *ndt80*Δ arrest. Ndt80 is a meiosis-specific transcription factor that controls the expression of many middle and late sporulation genes (Shin et al., 2010). In particular Ndt80 controls the expression of *CDC5*, the only polo-like kinase in yeast, which is necessary and sufficient for JM resolution and disassembly of the SC (Sourirajan and Lichten, 2008). In addition, Ndt80 induces transcription of *CLB1*, the cyclin required for entry into Meiosis I division (Chu and Herskowitz, 1998; Grandin and Reed, 1993). Due to the absence of *CDC5* and *CLB1*, an *ndt80*Δ mutant arrests in the pachytene stage of meiosis with unresolved dHJs and fully synapsed chromosomes (Allers and Lichten, 2001; Xu et al., 1995). The *ndt80*Δ arrest is distinct from the *dmc1*Δ arrest as there are no unrepaired DSBs to induce the meiotic recombination checkpoint checkpoint (Zakharyevich et al., 2012). It appears as though IH bias is still active at the *ndt80*Δ arrest, as new IH joint molecules continue to be formed (Allers and Lichten, 2001; Kaur et al., 2015). This result is consistent with the fact that Mek1 remains active, as indicated by the presence of phosphorylated Mek1 T327 (Wu et al., 2010), leading to the proposal that Mek1 is maintaining IH bias at the *ndt80*Δ arrest by phosphorylating its targets. These targets could be distinct from the Mek1 targets that are involved in activating the checkpoint, and thus this approach could potentially identify Mek1 targets that are specifically involved in maintaining IH bias apart from targets that are involved in activating/maintaining the checkpoint.

I performed the SILAC experiment using *mek1-as dmc1*Δ once while at Stony Brook, but had technical difficulties sporulating the cells when I moved to UC San

Diego. I have therefore been unable to do the type of analysis carried out for the *dmc1*Δ *mek1-as* SILAC experiments. However the *mek1-as ndt80*Δ experiment described below was successful in identifying Zip1, the meiosis-specific transverse filament protein of yeast synaptonemal complexes, as a potential Mek1 target. Subsequent work by Xiangyu Chen in the Hollingsworth lab showed that this phosphorylation is indeed dependent on *MEK1*, but is mediated directly by Cdc7-Dbf4 and is important for generating IH COs that are distributed throughout the genome by interference (Chen et al., 2015). This paper therefore describes a previously unknown role for Mek1 in the IH CO/NCO decision.

Methods

Yeast Strain Construction: The *mek1-as ndt80*Δ *arg4-NSP lys4*Δ*::hphMX4* SILAC strain, NH2221, was derived from the efficiently sporulating SK1 background. The construction of NH2221 took several steps. First the *URA3* gene was popped out of the *MAT**a*** and *MATα* haploid strains, NH2091-8-2::pJR2 and NH2091-2-4::pJR2, described in chapter two by plating on 5-FOA plates. The genotypes of these strains are *MAT**a*** *mek1-as::URA3 dmc1*Δ*::LEU2 lys4*Δ*::hphMX4 arg4-NSP* and *MATα mek1-as::URA3 dmc1*Δ*::LEU2 lys4*Δ*::hphMX4 arg4-NSP,* the *URA3* gene marking the *mek1-as* allele was popped out (Boeke et al., 1987). This allowed the integration of the *DMC1* allele 600 bp upstream of the deleted *DMC1* ORF by transformation using the HindIII digested linearized plasmid, pNH301 (Liu et al., 2014). *NDT80* was then deleted from the *DMC1* haploids using the polymerase chain reaction (PCR)-mediated deletion approach with the *natMX4* cassette (Goldstein and McCusker, 1999). The resulting haploids, NH2091-8-2::pJR2 *DMC1::URA ndt80*Δ*::natmx4* and NH2091-2-4::pJR2 *DMC1::URA*

*ndt80*Δ*::natmx4*, were then mated to form NH2221. All knockouts were confirmed either by PCR or phenotypic analysis.

Media: YPD, YPA, Spo and RPS media were made as described in Suhandynata et al., 2014.

Sporulation conditions: Sporulation of cells after YPA pregrowth was performed as described in Suhandynata et al., 2014.

SILAC labeling of proteins from a *mek1-as ndt80*Δ diploid in meiosis: The *mek1-as ndt80*Δ diploid, NH2221, was pre-grown in either RPS-L or RPS-H (hereafter referred to as the “light” and “heavy” cultures, respectively) and transferred to Spo medium. Two hundred ml cells were incubated in a 2 L flask in a 30°C shaker for 14 hours to allow the cells to arrest in pachytene. At this time, 2 mL of heavy and light cells were set aside for chromosome spreads by pelleting the cells and then resuspending them in 1 mL 50% glycerol. Following centrifugation and removal of 950 µl glycerol, the cell pellets were frozen at -80°C. Twenty µl of dimethyl sulfoxide (DMSO) was added to the remainder of the light culture and 20 µl 10 mM 1-NA-PP1 (4-amino-1-*tert*-butyl-3-(1’napthyl)pyrazolo[3,4-*d*]pyrimidine) (Tocris Bioscience) dissolved in DMSO was added to the rest of the heavy culture (1 µM final concentration). After 20 min, the remaining 198 ml of cells from the two sporulating cultures were pelleted by centrifugation and washed once with 40 ml of cold sterile water. The cells were transferred to 50 ml conical tubes and pelleted again by centrifugation. After pouring off the supernatants, the cell pellets were stored at -80°C.

Chromosome Spreads: The 2 ml sporulating cultures were thawed on ice, and the cells pelleted by centrifugation at 2200 rpm for 2 min and resuspended in 500 µl of 200

mM Tris pH 7.5. Ten µL of 1M DTT (di-thio-threitol) was added and the cells incubated for 2 min at RT. Then the cells were pelleted and resuspended in 500 µL of 2% potassium acetate in1M sorbitol. After the addition of 6.5 of 10mg/ml Zymolase 100T to spheroplast the cells, the cells were incubated on a rotator at 30º C for 20 min. After spheroplasting was complete, the cells were pelleted at 2400 rpm for 3 min and washed with 2 mL of ice cold MES-Sorbitol (0.1M MES-NaOH pH6.4,1mM EDTA, 0.5mM $MgCl_2$,1M Sorbitol). Resuspension of the cells was done by gently tapping the tube. The cells were then pelleted again at 2400 rpm and resuspended in 55 µL MES-Sorbitol. Twenty µL of the spheroplasted cells were placed on ethanol cleaned glass microscope slides and 40 µL of fixative (3% paraformaldehyde, 3.4% Sucrose) was added, followed immediately by 80 µL of 1% Lipsol. After 1 minute, 80 µL of fixative was added again to the slide, and a glass rod was used to roll the liquid without touching the slide. The slides were allowed to dry for approximately 1 hour and then washed for 2 min with 0.4% photoflo by soaking them in the photoflo filled coplin jars. The slides were then allowed to dry overnight in the hood, after which they were ready for antibody staining.

Zip1 antibody staining: Prior to primary antibody incubation, spreads were rinsed with PBS (Phosphate Buffered Saline pH 7.5) for 10 min in a coplin jar at room temperature (RT) with gentle rotation. Spreads were then blocked with 100 µL of blocking buffer [1X PBS pH 7.5, 0.2% gelatin, 0.5% BSA (Bovine Serum Albumin)] for 2 hr in a sealed container lined with moist paper towels. The blocking solution was drained off using a paper towel as a sponge. An anti-Zip1 antibody from Santa Cruz Biotechnology (Cat # sc-33733) was diluted 1:100 in blocking buffer and 100 □L of the diluted primary antibody was added and the spreads incubated overnight without rotation at 4º C. The

slides were washed three times for three minutes each with PBS with gentle shaking in a coplin jar. The secondary antibody, Goat Anti-Rabbit-Alexa Fluor 488 (Thermo Fisher Scientific Cat# Z-25302) was diluted 1:100 in blocking buffer and 100 µL were added and the spreads incubated for 4 hr at RT in a moist chamber. After incubation, the slides were washed three times for three minutes each with PBS with gentle shaking, and rinsed once with filtered distilled water. One drop of Vectashield with DAPI (Vector Laboratories Cat# H-1200) was placed on the spreads and a coverslip (24mm x 60mm) was put on top of the spreads. Excess liquid was drained with a paper towel and the edges between the cover slips and the slides were sealed with nail polish. The slides were then either viewed immediately by fluorescence microscopy using a Zeiss Axioplan 2 imaging microscope with an HBO 100 fluorescent bulb or stored at -80ºC until ready for viewing.

Phosphopeptide preparation and analysis

Preparation of crude chromatin and trypsin digestion, purification of phosphopeptides using IMAC and HILIC fractionation were all performed as described in Suhandynata et al., 2014.

Data Analysis using SEQUEST was performed as described in Chapter 3.

Results

To look for phosphorylation sites potentially regulated by Mek1 at the *ndt80*Δ arrest, a SILAC experiment was performed using a *mek1-as ndt80*Δ diploid. A *mek1-as ndt80*Δ *arg4 lys4* diploid was grown in 200 mL of RPS medium containing either “heavy” or “light” versions of arginine and lysine was transferred to Spo medium for 14 hours to allow the cells to arrest in pachytene. The Mek1-as kinase was inhibited in the heavy

culture by addition of 1-NA-PP1 to a final concentration of 1 μM for 20 minutes and cells were harvested. To ensure that a majority of the cell population was in the pachytene stage of meiosis, chromosome spreads were stained with anti-Zip1 antibody. Chromosome spreads were scored for full-synapsis, partial synapsis, or no synapsis (foci). Of 50 nuclei scored both the light and heavy cultures exhibited at least 70% fully synapsed Zip1 staining (Figure 4-1 and Table 4-1). Furthermore, both cultures exhibited similar frequencies of the three staining patterns, indicating they were behaving similarly. Chromatin from both heavy and light cells were prepared as described in Suhandynata et al., 2014, and 5 mg of heavy and light protein were mixed together and digested with trypsin.

Table 4-1. Scoring of *mek1-as ndt80*Δ chromosome spreads for Zip1 staining

Culture-Strain	Full SC	Partial SC	Dispersed Zip1 Staining
Light-*mek1-as ndt80*Δ	37	5	8
Heavy-*mek1-as ndt80*Δ	35	8	7

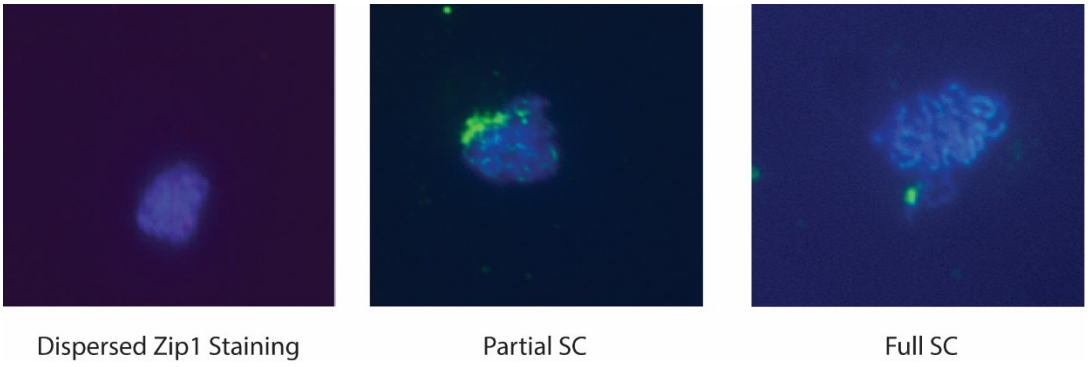

Figure 4-1. **Zip1 staining can be broken down into three distinct patterns.** Meiotic chromosome spreads were stained with anti-Zip1 antibody from Santa Cruz Biotechnology (Cat # sc-33733) and Goat Anti-Rabbit-Alexa Fluor 488 secondary antibody. Chromosome spreads were scored by fitting individual spreads into one of the three Zip1 staining patterns to determine what stage of meiosis cells were in.

Phosphopeptides were enriched by IMAC and analyzed by MS as performed in Suhandynata et al., 2014. This resulted in the identification of 4,008 unique phosphorylated peptides. The data were analyzed using the Sorcerer system as described in Suhandynata et al., 2014. Most of the phosphopeptides were present at approximately equal abundance in both the light and heavy cultures (Figure 4-2). This indicates that an equal amount of proteins from the light and heavy cultures were combined so that any significant changes in the L/H ratios are not due to differences in protein amounts. Non-*MEK1*-dependent phosphopeptides should be present in equal amounts in both cultures giving L/H ratios around 1. However, *MEK1*-dependent phosphopeptides are predicted to be under-represented in the heavy culture and therefore should exhibit L/H ratios > 1. Manual inspection of the dataset revealed Zip1 as a potential Mek1 substrate, as nearly all Zip1 phosphopeptides were enriched in the

light culture in which Mek1 was active (Fig 4-2-red triangles). Zip1, belongs to the ZMM class of proteins, and is known to stabilize/protect IH JMs from disassembly by the Sgs1-Tope-Rmi1 complex, resulting in the biased resolution of dHJs into COs which are distributed by interference (Fig 4-3A) (De Muyt et al., 2012; Kaur et al., 2015; Tang et al., 2015). MS analysis revealed 18 phosphorylation sites on Zip1 distributed throughout the protein (Figure 4-3B) (Table 4-2).

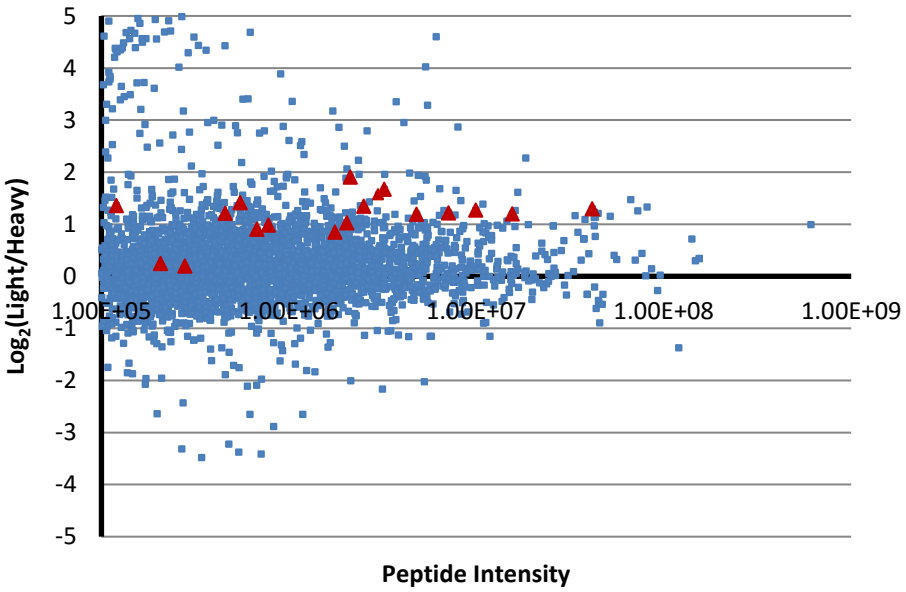

Figure 4-2. Integrated light/heavy (L/H) ratios of phosphopeptides obtained from the merged non-redundant phosphopeptide datasets from two SILAC experiments using *mek1-as ndt80*Δ. L/H ratios of phosphorylated peptides are plotted on a $\log_2$ scale (Y-axis) as a function of peptide intensity (X-axis). Peptide intensity is a measure of how well each peptide is ionized and subsequently detected by the MS and is correlated to the quantity of each peptide in the sample. Highly abundant peptides will display peptide intensities with large signal to noise ratios and therefore have more accurate L/H ratios when compared to lower abundance peptides with signal to noise ratios closer to 1. L/H ratios were calculated by dividing the integrated peptide intensities of light and heavy peptides with the highest peak intensities. Integrated peptide intensities are defined as the area under the curve of the peptide elution peak. The 18 unique Zip1 phosphopeptides, representing 18 unique phosphorylation sites, are plotted in red triangles.

In particular, three out of four adjacent serine residues in the C-terminus (S815-S818, from here on referred to as Zip1-4S) exhibited L/H ratios >3, suggesting potential regulation by Mek1 (Figure 4-3C and 4-3D). Zip1-4S is located within a 25 amino acid region required for chromosome synapsis and wild-type recombination, suggesting that phosphorylation of these residues may be implicated in these processes (Tung and Roeder, 1998). Although transverse filament (TF) proteins have similar tertiary structures, their primary structure is not well conserved (Page and Hawley, 2004). It is interesting that the Zip1-4S region is conserved among yeast, human, mouse, rat, and zebrafish TF proteins (Figure 4-3E-the alignment was generated by Danny Miller at the Stowers Institute). This region contains several negatively charged amino acids, and NetPhos analysis predicts that at least two of the residues in the conserved Zip1-4S region are phosphorylated in all five species (Blom et al., 1999) (NetPhos analysis performed by Miller). The functional significance of phosphorylation at these sites was tested using *ZIP1* alleles in which all four serines were mutated either to alanine (*zip1-4A*) to prevent phosphorylation or to aspartic acid (*zip1-4D*) to mimic phosphorylation.

Characterization of *zip1-4A* and *zip1-4D* is fully described in Chen et al., 2015. Since this characterization was carried out by other members of the Hollingsworth as well as collaborators, I have not included the entire paper as a chapter in my thesis. The following is a brief summary of the characterization of the Zip1 4S region. Briefly, Zip1-4S phosphorylation promotes interactions between homologous chromosomes that result in the negative feedback regulation of Spo11 (Thacker et al., 2014). This was shown by the fact that DSBs in *zip1-4A* and *zip1*Δ mutants occur at the same time as in wild-type cells and *ZIP1-4D* mutants but at later timepoints, DSBs accumulate.

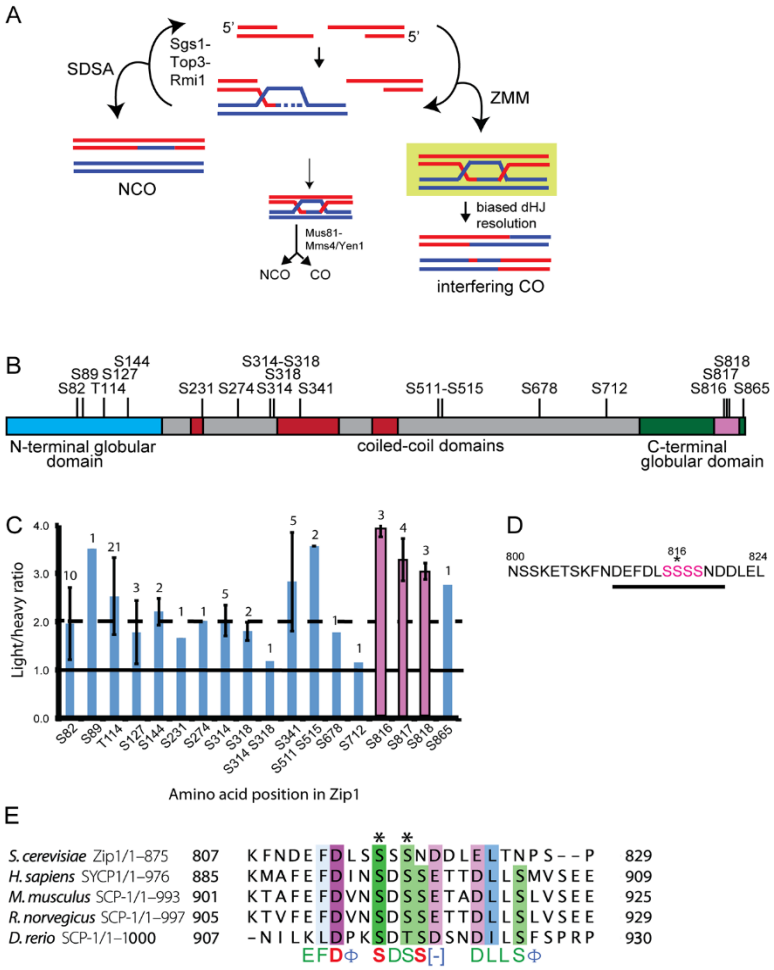

Figure 4-3. Identification of putative Mek1-regulated phosphosites on Zip1. A. Different pathways of meiotic DSB repair in yeast (adapted from (De Muyt et al., 2012). Red and blue represent a pair of homologous chromosomes. B. Schematic showing the positions of the phosphates on Zip1 detected by SILAC analysis of proteins isolated from *mek1-as ndt80*Δ arrested cells (NH2221). Gray boxes indicate predicted coiled coil domains (Tung and Roeder, 1998). The yellow box represents the region from 800 to 824 defined by Tung and Roeder (1998) to be required for synapsis. C. Average Light/heavy ratios of the Zip1 phosphopeptides detected in the SILAC experiment. Ratios above the dashed line indicate possible regulation by Mek1. Numbers above each bar indicate the number of peptides. Error bars indicate the standard deviation. D. Sequence of the region indicated by the yellow box in A. Pink color indicates the serines mutated in the *zip1-4A* and *ZIP1-4D* alleles. Antibodies against phosphorylated S816 (indicated by an asterisk) were generated using the peptide shown by the black line. E. ClustalO alignment of *S. cerevisiae*, *H. sapiens, M. musculus, R. norvegicus*, and *D. rerio* TF proteins in the 4S region. Identical amino acids are noted and amino acids with at least 50% conservation are colored. Hash marks (-#-) denote removed sequence for ease of viewing the conserved regions and dashes (–) indicate gaps in alignment. Asterisks (*) represent residues predicted to be phosphorylated by NetPhos analysis in all five species. **Figure taken from Chen et al (2015).**

Table 4-2 Zip1 phosphopeptides and their Light/Heavy (L/H) ratios from a *mek1-as ndt80*Δ SILAC experiment

Peptide[a]	L/H	amino acid
R.NHGYS[167.00]DDMEIGSPK.K	2.65	S82
R.NHGYS[167.00]DDMEIGSPK[136.11].K	2.65	S82
R.NHGYS[167.00]DDMEIGSPK[136.11].K	2.32	S82
R.NHGYS[167.00]DDMEIGSPK.K	2.29	S82
R.NHGYS[167.00]DDMEIGS[167.00]PK.K	2.21	S82
R.NHGYS[167.00]DDMEIGSPK.K	2.17	S82
R.NHGYS[167.00]DDMEIGSPK[136.11].K	2.17	S82
R.NHGYS[167.00]DDMEIGS[167.00]PK[136.11].K	1.93	S82
R.NHGYS[167.00]DDMEIGSPK.K	0.93	S82
R.NHGYS[167.00]DDMEIGSPK.K	0.32	S82
R.NHGYSDDMEIGS[167.00]PK.K	3.51	S89
K.NDVAAIENDT[181.01]DEDFEITEVR.E	4.37	T114
K.NDVAAIENDT[181.01]DEDFEITEVR[166.11].E	4.37	T114
K.NDVAAIENDT[181.01]DEDFEITEVR.E	3.76	T114
K.NDVAAIENDT[181.01]DEDFEITEVR.E	2.60	T114
K.NDVAAIENDT[181.01]DEDFEITEVR.E	2.58	T114
K.NDVAAIENDT[181.01]DEDFEITEVR.E	2.51	T114
K.NDVAAIENDT[181.01]DEDFEITEVR.E	2.47	T114
K.NDVAAIENDT[181.01]DEDFEITEVR[166.11].E	2.46	T114
K.NDVAAIENDT[181.01]DEDFEITEVR.E	2.46	T114
K.NDVAAIENDT[181.01]DEDFEITEVR[166.11].E	2.46	T114
K.NDVAAIENDT[181.01]DEDFEITEVR.E	2.46	T114
K.NDVAAIENDT[181.01]DEDFEITEVR[166.11].E	2.45	T114
K.NDVAAIENDT[181.01]DEDFEITEVR.E	2.44	T114
K.NDVAAIENDT[181.01]DEDFEITEVR.E	2.39	T114
K.NDVAAIENDT[181.01]DEDFEITEVR.E	2.38	T114
K.NDVAAIENDT[181.01]DEDFEITEVR.E	2.37	T114
K.NDVAAIENDT[181.01]DEDFEITEVR[166.11].E	2.37	T114
K.NDVAAIENDT[181.01]DEDFEITEVR.E	2.20	T114
K.NDVAAIENDT[181.01]DEDFEITEVR.E	1.49	T114
K.NDVAAIENDT[181.01]DEDFEITEVR[166.11].E	1.45	T114
K.NDVAAIENDT[181.01]DEDFEITEVR.E	1.05	T114
R.EVS[167.00]EGVAKET.K	2.30	S127
R.EVS[167.00]EGVAK.E	2.01	S127
R.EVS[167.00]EGVAK[136.11]ET.K	1.04	S127
K.ESHGDPNDS[167.00]ETTLK.D	2.40	S144
K.ESHGDPNDS[167.00]ETTLK[136.11].D	2.01	S144
K.S[167.00]C[160.03]LETLQER.I	1.66	S231
K.TS[167.00]IENLNK.T	2.01	S274
R.ELDDC[160.03]S[167.00]GQLSEEK.I	2.30	S314
R.ELDDC[160.03]S[167.00]GQLSEEK[136.11].I	2.29	S314
R.ELDDC[160.03]S[167.00]GQLSEEK[136.11].I	2.17	S314
R.ELDDC[160.03]S[167.00]GQLSEEK.I	1.74	S314
R.ELDDC[160.03]S[167.00]GQLSEEK.I	1.62	S314
R.ELDDC[160.03]S[167.00]GQLS[167.00]EEKIK.N	1.19	S314, S318
R.ELDDC[160.03]SGQLS[167.00]EEK.I	1.93	S318

R.ELDDC[160.03]SGQLS[167.00]EEK[136.11]IK[136.11].N	1.66	S318
K.S[167.00]IENFFSEDK.A	4.66	S341
K.S[167.00]IENFFSEDK[136.11].A	2.50	S341
K.S[167.00]IENFFSEDK.A	2.50	S341
K.S[167.00]IENFFSEDK[136.11].A	2.28	S341
K.S[167.00]IENFFSEDK[136.11].A	2.23	S341
R.S[167.00]TLSS[167.00]QKNQIISSLGTK.E	3.57	S511, S515
R.S[167.00]TLSS[167.00]QK[136.11]NQIISSLGTK[136.11].E	3.57	S511, S515
K.ETGVEES[167.00]LSDVK[136.11].T	1.78	S678
K.LELQDNLES[167.00]LEEVTK.N	1.15	S712
K.FNDEFDLSS[167.00]SSNDDLELTNPSPIQIKPV.R	4.16	S816
K.FNDEFDLSS[167.00]SSNDDLELTNPSPIQIKPVR.G	3.90	S816
K.FNDEFDLSS[167.00]SSNDDLELTNPSPIQIKPVR.G	3.78	S816
K.FNDEFDLSSS[167.00]SNDDLELTNPSPIQIK[136.11]PVR[166.11].G	3.88	S817
K.FNDEFDLSSS[167.00]SNDDLELTNPSPIQIK.P	3.32	S817
K.FNDEFDLSSS[167.00]SNDDLELTNPSPIQIKPVR.G	3.14	S817
K.FNDEFDLSSS[167.00]SNDDLELTNPSPIQIK[136.11]PVR[166.11].G	2.83	S817
K.FNDEFDLSSSS[167.00]NDDLELTNPSPIQIKPVR.G	3.21	S818
K.FNDEFDLSSSS[167.00]NDDLELTNPSPIQIKPVR.G	3.08	S818
K.FNDEFDLSSSS[167.00]NDDLELTNPSPIQIKPVR.G	2.87	S818
K.LLLVEDEDQS[167.00]LK.I	2.76	S865

[a]"." represents a trypsin cleavage site. "[167.00]" follows phosphorylated serine, "[181.01]" follows phosphorylated threonine, "[136.11]" and "[166.11]" indicate heavy lysine and arginine respectively. Only fully digested peptides are shown.

A possible explanation is that new DSBs continue to be created due to a failure to trigger the negative feedback regulation of Spo11 that is mediated by *ZMM*-dependent interhomolog engagement (Thacker et al., 2014). Zip1-4S was further shown to be involved in the promotion of COs by physical analysis of the *HIS4-LEU2* hotspot. As for both *zip1-4A* and *zip1*Δ, COs were reduced to the same extent, while NCOs were increased, with significantly more NCOs observed for *zip1-4A* compared to *zip1*Δ. It is important to note that the increased NCOs in the *zip1-4A* were dependent upon *SGS1,* suggesting that the Sgs1 helicase can remove *zip1-4A* from the DNA and suggesting that DSBs in *zip1-4A* are channeled down the Sgs1 pathway to generate NCOs. Furthermore, phosphorylation of the Zip1-4S region is required for the generation of

COs that are distributed by interference as well as efficient chromosome synapsis. Phosphorylation of Zip1-S816 was further characterized using a phospho-specific antibody. Phosphorylation of Zip1-S816 is dependent on *SPO11* but not on *SAE2/COM1,* which suggests that phosphorylation of Zip1-4S requires formation, but not processing of DSBs.

Phosphorylation of Zip1-S816 is promoted by *MEK1*, *MEC1, HOP1* and *RED1*. Mek1 kinase activity is specifically required for Zip1-S816 phosphorylation as the catalytically inactive *mek1-K199R* mutant also greatly reduced Zip1-S816 phosphorylation. Although Zip1-S816 phosphorylation is dependent upon Mek1 kinase activity, the S816 site does not match the Mek1 consensus motif (RXXT). This suggests that Mek1's regulation of the S816 site is indirect, and that phosphorylation of S816 could come from a different kinase. In fact, *in vitro* kinase using an analog-sensitive version of Mek1, GST-Mek1-as, in conjunction with an analog version of ATP, furfuryl-ATPγS (Wan et al., 2004) demonstrated that Zip1 is not a direct substrate of Mek1 and instead is directly phosphorylated by Cdc7-Dbf4 (DDK).

In summary, Chen et al. (2015), showed that DDK can directly phosphorylate Zip1-S816, and that the physiological function of the Zip1-4S region is to create a negatively charged patch, created by multiple phosphates, for proper Zip1 function in the IH CO/NCO pathway. By helping to identify the phosphorylation events in the Zip1-4S region, a link between Mek1 and the IH CO/NCO pathway has been revealed. Chen et al., 2015 showed that Mek1 regulates IH CO formation by enabling DDK to phosphorylate Zip1. However, how Mek1 regulates DDK to phosphorylate Zip1 remains unknown. It is possible that Mek1 phosphorylates itself or nearby targets at DSBs, thereby recruiting DDK to DSBs. This would allow DDK to then phosphorylate Zip1 as it

would be in close proximity to Zip1. Thus, we propose that Mek1 kinase activity is the link by which IH bias and IH CO formation are coordinated to ensure proper chromosome segregation during meiosis.

CHAPTER FIVE

Discussion

My thesis was focused on identifying Mek1 kinase substrates using SILAC. My first objective was to develop a method that would allow for the application of the SILAC quantitative phosphoproteomic approach to meiotic budding yeast cells (Suhandynata et al., 2014). My second objective was to apply this technique to systematically analyze candidate Mek1 substrates from *dmc1*Δ *mek1-as* arrested cells to identify a set of putative Mek1 substrates for further studies. In addition, manual inspection of phosphopeptides from a SILAC experiment conducted in *mek1-as ndt80*Δ arrested cells led to the discovery that phosphorylation of a conserved region in the C-terminus of the synaptonemal complex protein, Zip1, is required for the production of interfering crossovers during meiosis (Chen et al., 2015). My third objective, which did not work out due to technical difficulties, was to compare the candidate Mek1 substrates at the *dmc1*Δ arrest to candidate Mek1 substrates at the *ndt80*Δ arrest.

The development of a method to implement quantitative SILAC phosphoproteomics in meiotic yeast has potentially opened the door to a meiotic yeast phosphoproteome that has not been fully analyzed to this date. Other quantitative phosphoproteomic methods that were previously available to groups studying yeast meiosis required extensive technical knowledge (e.g. ITRAQ) that may have discouraged groups from attempting such an approach (Thompson et al., 2003). However, the SILAC approach only substantially differs from standard yeast protocols with regard to the pre-sporulation of cells, thus eliminating much of the technical difficulties when compared to other quantitative proteomic methods. Moreover, other quantitative phosphoproteomic methods require post digestion labeling, which can be inconsistent, thus adding more variables to an experiment when compared to the SILAC

proteomic approach. Thus, the development of the synthetic sporulation protocol has potentially opened up the door for many groups to utilize quantitative SILAC phosphoproteomics as an approach for investigating biological phenomena in yeast meiosis.

When evaluating the Mek1 candidates identified by my quantitative phosphoproteomic approach, Rad17 and Spp1 are particularly interesting. For instance, phosphorylation of Spp1 by Mek1 could allow the release of the DNA from the axis where Spo11 initiates the cut. Deletion of Spp1 results in altered patterns of meiotic DSB formation, with breaks at some hotspots becoming reduced, while at the same time novel hotspots arise in previously cold regions of meiotic chromosomes (Acquaviva et al., 2013; Sommermeyer et al., 2013). If phosphorylation of Spp1 by Mek1 allows for the release of the cut DNA from the axis, then a non-phosphorylatable *spp1-A* mutant would be expected to have a slower meiotic progression compared to WT cells, and a phosphomimetic *spp1-D* mutant would look more like a WT strain. If the phosphorylation of Spp1 by Mek1 is promoting IH recombination then an *spp1-A* mutant might show defects in spore viability as a result of reduced IH recombination, while a *spp1-D* mutant might even be able to alleviate spore viability defects of a *mek1*Δ strain. Zip1, along with the other ZMM proteins, is recruited to DSBs via the 9-1-1 complex comprised of the Ddc1, Rad17, and Mec3 proteins (Shinohara et al., 2015). Phosphorylation of Rad17 by Mek1 might be important for the recruitment of Zip1 proteins to DSBs thereby promoting COs through the ZMM pathway. If the phosphorylation of Rad17 by Mek1 is important for Zip1 recruitment, then a *rad17-A* mutant would be expected to have lower Zip1 recruitment at meiotic DSBs. Thus, a *rad17-A* mutant might have reduced CO levels

compared to WT and a *rad17-D* mutant might even show higher levels of COs compared to WT cells. Additionally chromatin immuno-precipitation (ChIP) profiles of the Zip1 protein might show that less Zip1 is recruited to meiotic hotspot regions in a *rad17-A* mutant compared to WT cells, while more Zip1 protein is recruited to hotspot regions in *rad17-D* mutants. Another possibility for why Rad17 is being phosphorylated by Mek1 is to regulate the meiotic recombination checkpoint. The *rad17*Δ mutant bypasses the *dmc1*Δ arrest due to the loss of the meiotic recombination checkpoint, if the phosphorylation of Rad17 by Mek1 upholds this checkpoint, then a *rad17-A* mutant may be able to bypass the *dmc1*Δ checkpoint and allow for meiotic progression to occur. However, phenotypic analysis of *rad17-T350A* and *rad17-T350D* indicated that the phosphorylation of Rad17 is not required for the primary function of *RAD17* during meiosis (Suhandynata et al., 2016).

Aside from identifying candidate Mek1 substrates, my phosphoproteomic screen has the possibility of identifying potential PLK (Cdc5) targets. Although our screen did not inactivate Cdc5, it did compare two cultures in which one should not have active Cdc5 with another culture that could have active Cdc5. This, coupled with the motif analysis performed in chapter 3, identified a few potentially interesting candidate Cdc5 substrates. In particular, the Zip3 protein was identified as a potential Cdc5 substrate, and it is reported to be a meiosis specific SUMO (small ubiquitin-related modifier)-E3 ligase and its SUMO-E3 ligase activity has been suggested to play a role in SC assembly (Cheng et al., 2006; Hooker and Roeder, 2006). Therefore with its implication in SC assembly, it is possible that the phosphorylation of Zip3 by Cdc5 could be a signal to promote the disassembly of the SC. Obviously further studies would need to be

performed to validate these potential Cdc5 substrates, however our phosphoproteomic dataset allows groups already working on meiotic Cdc5 substrates to have a reference of the potential phosphorylation events that Cdc5 is performing during meiosis that was not previously available.

Although the Zip1-S816 phosphorylation is dependent upon Mek1, the direct kinase is DDK (Chen et al., 2015). This implies that DDK could be part of one of the pathways by which Mek1 modulates meiotic events downstream of IH bias and the meiotic recombination checkpoint. Therefore it would be interesting to look for DDK substrates at the *dmc1*Δ arrest by using a *cdc7-as* allele that can be specifically inhibited much like the *mek1-as* allele (Wan et al., 2006). Morever, many other analog sensitive alleles of kinases known to play roles in meiosis such as *CDC28, IME2* and *HRR25* have been developed, and thus the same approach could be utilized to identify candidate substrates of other kinases in meiosis (Abdel-Fattah et al., 2015; Benjamin et al., 2003).

The use of SILAC in meiotic yeast cells is not limited to phosphoproteomic studies. The protocol can be tailored to achieve many other goals as well. For instance, SILAC followed by IP-MS/MS (Immuno Precipitation tandem Mass Spectrometry) can be used identify protein-protein interactions, as has been done in vegetative cells (Chen et al., 2010; Miteva et al., 2013). In addition, being able to sporulate after transfer from minimal medium can be used to maintain selection of a plasmid, ensuring that the plasmid is not lost as can be the case when grown in rich medium. Furthermore, the synthetic sporulation protocol opens up the possibility for approaches that utilize dNTP labeling which was not possible when pre-growth was performed in rich medium.

The analysis of candidate Mek1 substrates identified at the *dmc1*Δ arrest provides a data rich reference for many other groups studying yeast meiosis as a number of phosphorylation sites identified in my phosphoproteomic screens have not been previously described. Second, while my analysis focused mainly on Mek1 specific phosphorylation events, there are many other kinase motifs that were not thoroughly analyzed that were identified in the screens. The identification of these phosphorylation events could be very useful to other groups that are studying these kinases in meiosis. Finally, our analysis focused on the phosphoproteome of meiotic yeast. It would be interesting to also look at other post translational modifications such as sumoylation in yeast meiosis, as the SUMO E3 ligase Mms21 and sumoylation itself has been implicated to be functionally important for proper meiotic function (Cheng et al., 2006; Hooker and Roeder, 2006; Xaver et al., 2013). The synthetic sporulation protocol has opened many experimental approaches that were previously not possible, and in the future I hope that many groups will utilize the method to further elucidate the biology of yeast meiosis.

References

Abdel-Fattah, W., Jablonowski, D., Di Santo, R., Thuring, K.L., Scheidt, V., Hammermeister, A., Ten Have, S., Helm, M., Schaffrath, R., and Stark, M.J. (2015). Phosphorylation of Elp1 by Hrr25 is required for elongator-dependent tRNA modification in yeast. PLoS genetics *11*, e1004931.

Acquaviva, L., Drogat, J., Dehe, P.M., de La Roche Saint-Andre, C., and Geli, V. (2013). Spp1 at the crossroads of H3K4me3 regulation and meiotic recombination. Epigenetics *8*, 355-360.

Agarwal, S., and Roeder, G.S. (2000). Zip3 provides a link between recombination enzymes and synaptonemal complex proteins. Cell *102*, 245-255.

Albuquerque, C.P., Smolka, M.B., Payne, S.H., Bafna, V., Eng, J., and Zhou, H. (2008). A multidimensional chromatography technology for in-depth phosphoproteome analysis. Molecular & cellular proteomics : MCP *7*, 1389-1396.

Allers, T., and Lichten, M. (2001). Differential Timing and Control of Noncrossover and Crossover Recombination during Meiosis. Cell *106*, 47-57.

Aravind, L., and Koonin, E.V. (1998). The HORMA domain: a common structural denominator in mitotic checkpoints, chromosome synapsis and DNA repair. Trends in biochemical sciences *23*, 284-286.

Argueso, J.L., Wanat, J., Gemici, Z., and Alani, E. (2004). Competing crossover pathways act during meiosis in Saccharomyces cerevisiae. Genetics *168*, 1805-1816.

Armstrong, S.J., Caryl, A.P., Jones, G.H., and Franklin, F.C. (2002). Asy1, a protein required for meiotic chromosome synapsis, localizes to axis-associated chromatin in Arabidopsis and Brassica. Journal of cell science *115*, 3645-3655.

Babu, P., Deschenes, R.J., and Robinson, L.C. (2004). Akr1p-dependent palmitoylation of Yck2p yeast casein kinase 1 is necessary and sufficient for plasma membrane targeting. The Journal of biological chemistry *279*, 27138-27147.

Bailis, J.M., and Roeder, G.S. (1998). Synaptonemal complex morphogenesis and sister-chromatid cohesion require Mek1-dependent phosphorylation of a meiotic chromosomal protein. Genes & development *12*, 3551-3563.

Barr, F.A., Sillje, H.H., and Nigg, E.A. (2004). Polo-like kinases and the orchestration of cell division. Nature reviews Molecular cell biology *5*, 429-440.

Benjamin, K.R., Zhang, C., Shokat, K.M., and Herskowitz, I. (2003). Control of landmark events in meiosis by the CDK Cdc28 and the meiosis-specific kinase Ime2. Genes & development *17*, 1524-1539.

Bishop, D.K. (1994). RecA homologs Dmc1 and Rad51 interact to form multiple nuclear complexes prior to meiotic chromosome synapsis. Cell *79*, 1081-1092.

Bishop, D.K., Nikolski, Y., Oshiro, J., Chon, J., Shinohara, M., and Chen, X. (1999). High copy number suppression of the meiotic arrest caused by a dmc1 mutation: REC114 imposes an early recombination block and RAD54 promotes a DMC1-independent DSB repair pathway. Genes to cells : devoted to molecular & cellular mechanisms *4*, 425-444.

Bishop, D.K., Park, D., Xu, L., and Kleckner, N. (1992). DMC1: a meiosis-specific yeast homolog of E. coli recA required for recombination, synaptonemal complex formation, and cell cycle progression. Cell *69*, 439-456.

Blagoev, B., Kratchmarova, I., Ong, S.E., Nielsen, M., Foster, L.J., and Mann, M. (2003). A proteomics strategy to elucidate functional protein-protein interactions applied to EGF signaling. Nature biotechnology *21*, 315-318.

Blom, N., Gammeltoft, S., and Brunak, S. (1999). Sequence and structure-based prediction of eukaryotic protein phosphorylation sites. Journal of molecular biology *294*, 1351-1362.

Boeke, J.D., Trueheart, J., Natsoulis, G., and Fink, G.R. (1987). 5-Fluoroorotic acid as a selective agent in yeast molecular genetics. Methods in enzymology *154*, 164-175.

Borde, V., Goldman, A.S., and Lichten, M. (2000). Direct coupling between meiotic DNA replication and recombination initiation. Science (New York, NY) *290*, 806-809.
Borde, V., Robine, N., Lin, W., Bonfils, S., Geli, V., and Nicolas, A. (2009). Histone H3 lysine 4 trimethylation marks meiotic recombination initiation sites. The EMBO journal *28*, 99-111.
Börner, G.V., Kleckner, N., and Hunter, N. (2004). Crossover/noncrossover differentiation, synaptonemal complex formation, and regulatory surveillance at the leptotene/zygotene transition of meiosis. Cell *117*, 29-45.
Brar, G.A., Kiburz, B.M., Zhang, Y., Kim, J.E., White, F., and Amon, A. (2006). Rec8 phosphorylation and recombination promote the step-wise loss of cohesins in meiosis. Nature *441*, 532-536.
Briggs, S.D., Xiao, T., Sun, Z.W., Caldwell, J.A., Shabanowitz, J., Hunt, D.F., Allis, C.D., and Strahl, B.D. (2002). Gene silencing: trans-histone regulatory pathway in chromatin. Nature *418*, 498.
Brown, M.S., Grubb, J., Zhang, A., Rust, M.J., and Bishop, D.K. (2015). Small Rad51 and Dmc1 Complexes Often Co-occupy Both Ends of a Meiotic DNA Double Strand Break. PLoS genetics *11*, e1005653.
Buonomo, S.B., Clyne, R.K., Fuchs, J., Loidl, J., Uhlmann, F., and Nasmyth, K. (2000). Disjunction of homologous chromosomes in meiosis I depends on proteolytic cleavage of the meiotic cohesin Rec8 by separin. Cell *103*, 387-398.
Busygina, V., Sehorn, M.G., Shi, I.Y., Tsubouchi, H., Roeder, G.S., and Sung, P. (2008). Hed1 regulates Rad51-mediated recombination via a novel mechanism. Genes & development *22*, 786-795.
Bzymek, M., Thayer, N.H., Oh, S.D., Kleckner, N., and Hunter, N. (2010). Double Holliday junctions are intermediates of DNA break repair. Nature *464*, 937-941.
Callender, T., Laureau, R., Wan, L., Chen, X., Sandhu, R., Laljee, S., Zhou, S., Suhandynata, R., Prugar, E., Gaines, W.A*., et al.* (in press). Mek1 downregulates Rad51 activity during yeast meiosis by phosphorylation of Hed1. PLoS genetics.
Callender, T.L., and Hollingsworth, N.M. (2010). Mek1 suppression of meiotic double-strand break repair is specific to sister chromatids, chromosome autonomous and independent of Rec8 cohesin complexes. Genetics *185*, 771-782.
Cao, L., Alani, E., and Kleckner, N. (1990). A pathway for generation and processing of double-strand breaks during meiotic recombination in S. cerevisiae. Cell *61*, 1089-1101.
Caplan, A.J., Cyr, D.M., and Douglas, M.G. (1992). YDJ1p facilitates polypeptide translocation across different intracellular membranes by a conserved mechanism. Cell *71*, 1143-1155.
Carballo, J.A., Johnson, A.L., Sedgwick, S.G., and Cha, R.S. (2008). Phosphorylation of the axial element protein Hop1 by Mec1/Tel1 ensures meiotic interhomolog recombination. Cell *132*, 758-770.
Caryl, A.P., Armstrong, S.J., Jones, G.H., and Franklin, F.C. (2000). A homologue of the yeast HOP1 gene is inactivated in the Arabidopsis meiotic mutant asy1. Chromosoma *109*, 62-71.
Castello, A., Fischer, B., Eichelbaum, K., Horos, R., Beckmann, B.M., Strein, C., Davey, N.E., Humphreys, D.T., Preiss, T., Steinmetz, L.M*., et al.* (2012). Insights into RNA biology from an atlas of mammalian mRNA-binding proteins. Cell *149*, 1393-1406.
Chai, B., Huang, J., Cairns, B.R., and Laurent, B.C. (2005). Distinct roles for the RSC and Swi/Snf ATP-dependent chromatin remodelers in DNA double-strand break repair. Genes & development *19*, 1656-1661.
Chambers, A.L., and Downs, J.A. (2012). The RSC and INO80 chromatin-remodeling complexes in DNA double-strand break repair. Progress in molecular biology and translational science *110*, 229-261.
Chen, S.H., Albuquerque, C.P., Liang, J., Suhandynata, R.T., and Zhou, H. (2010). A proteome-wide analysis of kinase-substrate network in the DNA damage response. The Journal of biological chemistry *285*, 12803-12812.

Chen, S.Y., Tsubouchi, T., Rockmill, B., Sandler, J.S., Richards, D.R., Vader, G., Hochwagen, A., Roeder, G.S., and Fung, J.C. (2008). Global analysis of the meiotic crossover landscape. Developmental cell *15*, 401-415.
Chen, X., Suhandynata, R.T., Sandhu, R., Rockmill, B., Mohibullah, N., Niu, H., Liang, J., Lo, H.C., Miller, D.E., Zhou, H.*, et al.* (2015). Phosphorylation of the Synaptonemal Complex Protein Zip1 Regulates the Crossover/Noncrossover Decision during Yeast Meiosis. PLoS biology *13*, e1002329.
Cheng, C.H., Lo, Y.H., Liang, S.S., Ti, S.C., Lin, F.M., Yeh, C.H., Huang, H.Y., and Wang, T.F. (2006). SUMO modifications control assembly of synaptonemal complex and polycomplex in meiosis of Saccharomyces cerevisiae. Genes & development *20*, 2067-2081.
Chu, S., and Herskowitz, I. (1998). Gametogenesis in yeast is regulated by a transcriptional cascade dependent on Ndt80. Molecular cell *1*, 685-696.
Chuang, C.N., Cheng, Y.H., and Wang, T.F. (2012). Mek1 stabilizes Hop1-Thr318 phosphorylation to promote interhomolog recombination and checkpoint responses during yeast meiosis. Nucleic acids research *40*, 11416-11427.
Cloud, V., Chan, Y.L., Grubb, J., Budke, B., and Bishop, D.K. (2012). Rad51 is an accessory factor for Dmc1-mediated joint molecule formation during meiosis. Science (New York, NY) *337*, 1222-1225.
Collins, I., and Newlon, C.S. (1994). Meiosis-specific formation of joint DNA molecules containing sequences from homologous chromosomes. Cell *76*, 65-75.
Couteau, F., Nabeshima, K., Villeneuve, A., and Zetka, M. (2004). A component of C. elegans meiotic chromosome axes at the interface of homolog alignment, synapsis, nuclear reorganization, and recombination. Current biology : CB *14*, 585-592.
Cyr, D.M., and Douglas, M.G. (1994). Differential regulation of Hsp70 subfamilies by the eukaryotic DnaJ homologue YDJ1. The Journal of biological chemistry *269*, 9798-9804.
Cyr, D.M., Lu, X., and Douglas, M.G. (1992). Regulation of Hsp70 function by a eukaryotic DnaJ homolog. The Journal of biological chemistry *267*, 20927-20931.
De Muyt, A., Jessop, L., Kolar, E., Sourirajan, A., Chen, J., Dayani, Y., and Lichten, M. (2012). BLM helicase ortholog Sgs1 is a central regulator of meiotic recombination intermediate metabolism. Molecular cell *46*, 43-53.
Dresser, M.E., Ewing, D.J., Conrad, M.N., Dominguez, A.M., Barstead, R., Jiang, H., and Kodadek, T. (1997). DMC1 functions in a Saccharomyces cerevisiae meiotic pathway that is largely independent of the RAD51 pathway. Genetics *147*, 533-544.
Dresser, M.E., and Giroux, C.N. (1988). Meiotic chromosome behavior in spread preparations of yeast. The Journal of cell biology *106*, 567-573.
Durocher, D., Taylor, I.A., Sarbassova, D., Haire, L.F., Westcott, S.L., Jackson, S.P., Smerdon, S.J., and Yaffe, M.B. (2000). The molecular basis of FHA domain:phosphopeptide binding specificity and implications for phospho-dependent signaling mechanisms. Molecular cell *6*, 1169-1182.
Eichenlaub-Ritter, U. (2012). Oocyte ageing and its cellular basis. The International journal of developmental biology *56*, 841-852.
Elia, A.E., Cantley, L.C., and Yaffe, M.B. (2003a). Proteomic screen finds pSer/pThr-binding domain localizing Plk1 to mitotic substrates. Science (New York, NY) *299*, 1228-1231.
Elia, A.E., Rellos, P., Haire, L.F., Chao, J.W., Ivins, F.J., Hoepker, K., Mohammad, D., Cantley, L.C., Smerdon, S.J., and Yaffe, M.B. (2003b). The molecular basis for phosphodependent substrate targeting and regulation of Plks by the Polo-box domain. Cell *115*, 83-95.
Elias, J.E., and Gygi, S.P. (2007). Target-decoy search strategy for increased confidence in large-scale protein identifications by mass spectrometry. Nat Methods *4*.
Enyenihi, A.H., and Saunders, W.S. (2003). Large-scale functional genomic analysis of sporulation and meiosis in Saccharomyces cerevisiae. Genetics *163*, 47-54.

Everley, P.A., Krijgsveld, J., Zetter, B.R., and Gygi, S.P. (2004). Quantitative cancer proteomics: stable isotope labeling with amino acids in cell culture (SILAC) as a tool for prostate cancer research. Molecular & cellular proteomics : MCP *3*, 729-735.
Falk, J.E., Chan, A.C., Hoffmann, E., and Hochwagen, A. (2010). A Mec1- and PP4-dependent checkpoint couples centromere pairing to meiotic recombination. Developmental cell *19*, 599-611.
Fan, C.Y., Ren, H.Y., Lee, P., Caplan, A.J., and Cyr, D.M. (2005). The type I Hsp40 zinc finger-like region is required for Hsp70 to capture non-native polypeptides from Ydj1. The Journal of biological chemistry *280*, 695-702.
Ficarro, S.B., McCleland, M.L., Stukenberg, P.T., Burke, D.J., Ross, M.M., Shabanowitz, J., Hunt, D.F., and White, F.M. (2002). Phosphoproteome analysis by mass spectrometry and its application to *Saccharomyces cerevisiae*. Nature biotechnology *20*, 301-305.
Flanagan, J.F., Mi, L.Z., Chruszcz, M., Cymborowski, M., Clines, K.L., Kim, Y., Minor, W., Rastinejad, F., and Khorasanizadeh, S. (2005). Double chromodomains cooperate to recognize the methylated histone H3 tail. Nature *438*, 1181-1185.
Fromont-Racine, M., Senger, B., Saveanu, C., and Fasiolo, F. (2003). Ribosome assembly in eukaryotes. Gene *313*, 17-42.
Gerik, K.J., Li, X., Pautz, A., and Burgers, P.M. (1998). Characterization of the two small subunits of Saccharomyces cerevisiae DNA polymerase delta. The Journal of biological chemistry *273*, 19747-19755.
Gobbini, E., Cesena, D., Galbiati, A., Lockhart, A., and Longhese, M.P. (2013). Interplays between ATM/Tel1 and ATR/Mec1 in sensing and signaling DNA double-strand breaks. DNA repair *12*, 791-799.
Goldfarb, T., and Lichten, M. (2010). Frequent and efficient use of the sister chromatid for DNA double-strand break repair during budding yeast meiosis. PLoS biology *8*, e1000520.
Goldstein, A.L., and McCusker, J.H. (1999). Three new dominant drug resistance cassettes for gene disruption in *Saccharomyces cerevisiae*. Yeast *15*, 1541-1553.
Govin, J., Dorsey, J., Gaucher, J., Rousseaux, S., Khochbin, S., and Berger, S.L. (2010). Systematic screen reveals new functional dynamics of histones H3 and H4 during gametogenesis. Genes & development *24*, 1772-1786.
Grandin, N., and Reed, S.I. (1993). Differential function and expression of Saccharomyces cerevisiae B-type cyclins in mitosis and meiosis. Molecular and cellular biology *13*, 2113-2125.
Greenwell, P.W., Kronmal, S.L., Porter, S.E., Gassenhuber, J., Obermaier, B., and Petes, T.D. (1995). TEL1, a gene involved in controlling telomere length in S. cerevisiae, is homologous to the human ataxia telangiectasia gene. Cell *82*, 823-829.
Gruhler, A., Olsen, J.V., Mohammed, S., Mortensen, P., Faergeman, N.J., Mann, M., and Jensen, O.N. (2005a). Quantitative phosphoproteomics applied to the yeast pheromone signaling pathway. Molecular & cellular proteomics : MCP *4*, 310-327.
Gruhler, A., Schulze, W.X., Matthiesen, R., Mann, M., and Jensen, O.N. (2005b). Stable isotope labeling of Arabidopsis thaliana cells and quantitative proteomics by mass spectrometry. Molecular & cellular proteomics : MCP *4*, 1697-1709.
Grushcow, J.M., Holzen, T.M., Park, K.J., Weinert, T., Lichten, M., and Bishop, D.K. (1999). *Saccharomyces cerevisiae* checkpoint genes *MEC1*, *RAD17* and *RAD24* are required for normal meiotic recombination partner choice. Genetics *153*, 607-620.
Harrison, J.C., and Haber, J.E. (2006). Surviving the breakup: the DNA damage checkpoint. Annual review of genetics *40*, 209-235.
Henderson, K.A., Kee, K., Maleki, S., Santini, P., and Keeney, S. (2006). Cyclin-dependent kinase directly regulates initiation of meiotic recombination. Cell *125:1321-1332*.
Herskowitz, I. (1988). Life cycle of the budding yeast Saccharomyces cerevisiae. Microbiological Reviews *52*, 536-553.

Ho, H.C., and Burgess, S.M. (2011). Pch2 acts through Xrs2 and Tel1/ATM to modulate interhomolog bias and checkpoint function during meiosis. PLoS genetics *7*, e1002351.
Hollingsworth, N.M., and Byers, B. (1989). HOP1: a yeast meiotic pairing gene. Genetics *121*, 445-462.
Hollingsworth, N.M., Goetsch, L., and Byers, B. (1990). The HOP1 gene encodes a meiosis-specific component of yeast chromosomes. Cell *61*, 73-84.
Hollingsworth, N.M., Ponte, L., and Halsey, C. (1995). *MSH5*, a novel MutS homolog, facilitates meiotic reciprocal recombination between homologs in *Saccharomyces cerevisiae* but not mismatch repair. Genes Dev *9*, 1728-1739.
Holt, L.J., Tuch, B.B., Villen, J., Johnson, A.D., Gygi, S.P., and Morgan, D.O. (2009). Global analysis of Cdk1 substrate phosphorylation sites provides insights into evolution. Science (New York, NY) *325*, 1682-1686.
Hooker, G.W., and Roeder, G.S. (2006). A Role for SUMO in meiotic chromosome synapsis. Current biology : CB *16*, 1238-1243.
Hunter, N., and Kleckner, N. (2001). The single-end invasion: an asymmetric intermediate at the double-strand break to double-holliday junction transition of meiotic recombination. Cell *106*, 59-70.
Jessop, L., Allers, T., and Lichten, M. (2005). Infrequent co-conversion of markers flanking a meiotic recombination initiation site in Saccharomyces cerevisiae. Genetics *169*, 1353-1367.
Jessop, L., and Lichten, M. (2008). Mus81/Mms4 endonuclease and Sgs1 helicase collaborate to ensure proper recombination intermediate metabolism during meiosis. Molecular cell *31*, 313-323.
Kadyk, L.C., and Hartwell, L.H. (1992). Sister chromatids are preferred over homologs as substrates for recombinational repair in Saccharomyces cerevisiae. Genetics *132*, 387-402.
Kao, L.R., Peterson, J., Ji, R., Bender, L., and Bender, A. (1996). Interactions between the ankyrin repeat-containing protein Akr1p and the pheromone response pathway in Saccharomyces cerevisiae. Molecular and cellular biology *16*, 168-178.
Kapitzky, L., Beltrao, P., Berens, T.J., Gassner, N., Zhou, C., Wuster, A., Wu, J., Babu, M.M., Elledge, S.J., Toczyski, D.*, et al.* (2010). Cross-species chemogenomic profiling reveals evolutionarily conserved drug mode of action. Molecular systems biology *6*, 451.
Kasten, M., Szerlong, H., Erdjument-Bromage, H., Tempst, P., Werner, M., and Cairns, B.R. (2004). Tandem bromodomains in the chromatin remodeler RSC recognize acetylated histone H3 Lys14. The EMBO journal *23*, 1348-1359.
Katis, V.L., Lipp, J.J., Imre, R., Bogdanova, A., Okaz, E., Habermann, B., Mechtler, K., Nasmyth, K., and Zachariae, W. (2010). Rec8 phosphorylation by casein kinase 1 and Cdc7-Dbf4 kinase regulates cohesin cleavage by separase during meiosis. Dev Cell *18*, 397-409.
Kaur, H., De Muyt, A., and Lichten, M. (2015). Top3-Rmi1 DNA single-strand decatenase is integral to the formation and resolution of meiotic recombination intermediates. Molecular cell *57*, 583-594.
Keeney, S., Giroux, C.N., and Kleckner, N. (1997). Meiosis-specific DNA double-strand breaks are catalyzed by Spo11, a member of a widely conserved protein family. Cell *88*, 375-384.
Kim, K.P., Weiner, B.M., Zhang, L., Jordan, A., Dekker, J., and Kleckner, N. (2010). Sister cohesion and structural axis components mediate homolog bias of meiotic recombination. Cell *143*, 924-937.
Kim, Y., Rosenberg, S.C., Kugel, C.L., Kostow, N., Rog, O., Davydov, V., Su, T.Y., Dernburg, A.F., and Corbett, K.D. (2014). The chromosome axis controls meiotic events through a hierarchical assembly of HORMA domain proteins. Developmental cell *31*, 487-502.
Klein, F., Mahr, P., Galova, M., Buonomo, S.B.C., Michaelis, C., Nairz, K., and Nasmyth, K. (1999). A central role for cohesins in sister chromatid cohesion, formation of axial elements and recombination during meiosis. Cell *98*, 91-103.
Kobayashi, M., Hirano, A., Kumano, T., Xiang, S.L., Mihara, K., Haseda, Y., Matsui, O., Shimizu, H., and Yamamoto, K. (2004). Critical role for chicken Rad17 and Rad9 in the cellular response to DNA damage and stalled DNA replication. Genes to cells : devoted to molecular & cellular mechanisms *9*, 291-303.

Kruger, M., Moser, M., Ussar, S., Thievessen, I., Luber, C.A., Forner, F., Schmidt, S., Zanivan, S., Fassler, R., and Mann, M. (2008). SILAC mouse for quantitative proteomics uncovers kindlin-3 as an essential factor for red blood cell function. Cell *134*, 353-364.
Kurzbauer, M.T., Uanschou, C., Chen, D., and Schlogelhofer, P. (2012). The recombinases DMC1 and RAD51 are functionally and spatially separated during meiosis in Arabidopsis. The Plant cell *24*, 2058-2070.
Lao, J.P., Oh, S.D., Shinohara, M., Shinohara, A., and Hunter, N. (2008). Rad52 promotes postinvasion steps of meiotic double-strand-break repair. Molecular cell *29*, 517-524.
Lauberth, S.M., Nakayama, T., Wu, X., Ferris, A.L., Tang, Z., Hughes, S.H., and Roeder, R.G. (2013). H3K4me3 interactions with TAF3 regulate preinitiation complex assembly and selective gene activation. Cell *152*, 1021-1036.
Laurent, B.C., Yang, X., and Carlson, M. (1992). An essential Saccharomyces cerevisiae gene homologous to SNF2 encodes a helicase-related protein in a new family. Molecular and cellular biology *12*, 1893-1902.
Lee, B.H., and Amon, A. (2003). Role of Polo-like kinase CDC5 in programming meiosis I chromosome segregation. Science (New York, NY) *300*, 482-486.
Lee, D.H., Sherman, M.Y., and Goldberg, A.L. (1996). Involvement of the molecular chaperone Ydj1 in the ubiquitin-dependent degradation of short-lived and abnormal proteins in Saccharomyces cerevisiae. Molecular and cellular biology *16*, 4773-4781.
Lee, K.S., Park, J.E., Asano, S., and Park, C.J. (2005). Yeast polo-like kinases: functionally conserved multitask mitotic regulators. Oncogene *24*, 217-229.
Leem, S.H., and Ogawa, H. (1992). The MRE4 gene encodes a novel protein kinase homologue required for meiotic recombination in Saccharomyces cerevisiae. Nucleic acids research *20*, 449-457.
Li, B., and Reese, J.C. (2001). Ssn6-Tup1 regulates RNR3 by positioning nucleosomes and affecting the chromatin structure at the upstream repression sequence. The Journal of biological chemistry *276*, 33788-33797.
Li, S., and Dass, C. (1999). Iron(III)-immobilized metal ion affinity chromatography and mass spectrometry for the purification and characterization of synthetic phosphopeptides. Analytical biochemistry *270*, 9-14.
Liu, P.C., and Thiele, D.J. (2001). Novel stress-responsive genes EMG1 and NOP14 encode conserved, interacting proteins required for 40S ribosome biogenesis. Molecular biology of the cell *12*, 3644-3657.
Liu, Y., Gaines, W.A., Callender, T., Busygina, V., Oke, A., Sung, P., Fung, J.C., and Hollingsworth, N.M. (2014). Down-regulation of Rad51 activity during meiosis in yeast prevents competition with Dmc1 for repair of double-strand breaks. PLoS genetics *10*, e1004005.
Liu, Y., and West, S.C. (2004). Happy Holliday: 40th anniversary of the Holliday junction. Nature reviews Molecular cell biology *5*, 937-944.
Lo, H.-C., Kunz, R.C., Marullo, A., Gygi, S.P., and Hollingsworth, N.M. (2012). Cdc7-Dbf4 is a gene-specific regulator of meiotic transcription in yeast. Mol Cell Bio *32*, 541-557.
Lo, H.-C., Wan, L., Rosebrock, A., Futcher, B., and Hollingsworth, N.M. (2008). Cdc7-Dbf4 regulates *NDT80* transcription as well as reductional segregation during budding yeast meiosis. Mol Biol Cell *19*.
Lo, H.C., and Hollingsworth, N.M. (2011). Using the semi-synthetic epitope system to identify direct substrates of the meiosis-specific budding yeast kinase, Mek1. Methods in molecular biology *745*, 135-149.
Longtine, M.S., McKenzie, A., 3rd, Demarini, D.J., Shah, N.G., Wach, A., Brachat, A., Philippsen, P., and Pringle, J.R. (1998). Additional modules for versatile and economical PCR-based gene deletion and modification in *Saccharomyces cerevisiae*. Yeast *14*, 953-961.

Longworth, J., Noirel, J., Pandhal, J., Wright, P.C., and Vaidyanathan, S. (2012). HILIC- and SCX-based quantitative proteomics of Chlamydomonas reinhardtii during nitrogen starvation induced lipid and carbohydrate accumulation. Journal of proteome research *11*, 5959-5971.
Lu, Z., and Cyr, D.M. (1998). The conserved carboxyl terminus and zinc finger-like domain of the co-chaperone Ydj1 assist Hsp70 in protein folding. The Journal of biological chemistry *273*, 5970-5978.
Lydall, D., Nikolsky, Y., Bishop, D.K., and Weinert, T. (1996). A meiotic recombination checkpoint controlled by mitotic checkpoint genes. Nature *383*, 840-843.
Lydeard, J.R., Jain, S., Yamaguchi, M., and Haber, J.E. (2007). Break-induced replication and telomerase-independent telomere maintenance require Pol32. Nature *448*, 820-823.
Lynn, A., Soucek, R., and Borner, G.V. (2007). ZMM proteins during meiosis: crossover artists at work. Chromosome research : an international journal on the molecular, supramolecular and evolutionary aspects of chromosome biology *15*, 591-605.
MacCoss, M.J., and Matthews, D.E. (2005). Quantitative MS for proteomics: teaching a new dog old tricks. Analytical chemistry *77*, 294a-302a.
Majka, J., and Burgers, P.M. (2003). Yeast Rad17/Mec3/Ddc1: a sliding clamp for the DNA damage checkpoint. Proceedings of the National Academy of Sciences of the United States of America *100*, 2249-2254.
Majka, J., Niedziela-Majka, A., and Burgers, P.M. (2006). The checkpoint clamp activates Mec1 kinase during initiation of the DNA damage checkpoint. Molecular cell *24*, 891-901.
Malkova, A., Swanson, J., German, M., McCusker, J.H., Housworth, E.A., Stahl, F.W., and Haber, J.E. (2004). Gene conversion and crossing over along the 405-kb left arm of Saccharomyces cerevisiae chromosome VII. Genetics *168*, 49-63.
Mandal, A.K., Nillegoda, N.B., Chen, J.A., and Caplan, A.J. (2008). Ydj1 protects nascent protein kinases from degradation and controls the rate of their maturation. Molecular and cellular biology *28*, 4434-4444.
Mann, M. (2006). Functional and quantitative proteomics using SILAC. Nature reviews Molecular cell biology *7*, 952-958.
Martin, D.G., Grimes, D.E., Baetz, K., and Howe, L. (2006). Methylation of histone H3 mediates the association of the NuA3 histone acetyltransferase with chromatin. Molecular and cellular biology *26*, 3018-3028.
Matos, J., Lipp, J.J., Bogdanova, A., Guillot, S., Okaz, E., Junqueira, M., Shevchenko, A., and Zachariae, W. (2008). Dbf4-dependent CDC7 kinase links DNA replication to the segregation of homologous chromosomes in meiosis I. Cell *135*, 662-678.
Matsuoka, S., Ballif, B.A., Smogorzewska, A., McDonald, E.R., 3rd, Hurov, K.E., Luo, J., Bakalarski, C.E., Zhao, Z., Solimini, N., Lerenthal, Y.*, et al.* (2007). ATM and ATR substrate analysis reveals extensive protein networks responsive to DNA damage. Science (New York, NY) *316*, 1160-1166.
McMahill, M.S., Sham, C.W., and Bishop, D.K. (2007). Synthesis-dependent strand annealing in meiosis. PLoS biology *5*, e299.
Middelhoven, W.J. (1964). THE PATHWAY OF ARGININE BREAKDOWN IN SACCHAROMYCES CEREVISIAE. Biochimica et biophysica acta *93*, 650-652.
Miller, T., Krogan, N.J., Dover, J., Erdjument-Bromage, H., Tempst, P., Johnston, M., Greenblatt, J.F., and Shilatifard, A. (2001). COMPASS: a complex of proteins associated with a trithorax-related SET domain protein. Proceedings of the National Academy of Sciences of the United States of America *98*, 12902-12907.
Miteva, Y.V., Budayeva, H.G., and Cristea, I.M. (2013). Proteomics-based methods for discovery, quantification, and validation of protein-protein interactions. Analytical chemistry *85*, 749-768.

Mok, J., Kim, P.M., Lam, H.Y., Piccirillo, S., Zhou, X., Jeschke, G.R., Sheridan, D.L., Parker, S.A., Desai, V., Jwa, M.*, et al.* (2010). Deciphering protein kinase specificity through large-scale analysis of yeast phosphorylation site motifs. Science signaling *3*, ra12.
Muller, H.J. (1916). The Mechanism of Crossing-Over. The American Naturalist *50*, 193-221.
Murakami, H., and Keeney, S. (2014). Temporospatial coordination of meiotic DNA replication and recombination via DDK recruitment to replisomes. Cell *158*, 861-873.
Nagaoka, S.I., Hassold, T.J., and Hunt, P.A. (2012). Human aneuploidy: mechanisms and new insights into an age-old problem. Nature reviews Genetics *13*, 493-504.
Nakajima, H., Toyoshima-Morimoto, F., Taniguchi, E., and Nishida, E. (2003). Identification of a consensus motif for Plk (Polo-like kinase) phosphorylation reveals Myt1 as a Plk1 substrate. The Journal of biological chemistry *278*, 25277-25280.
Nassif, N., Penney, J., Pal, S., Engels, W.R., and Gloor, G.B. (1994). Efficient copying of nonhomologous sequences from ectopic sites via P-element-induced gap repair. Molecular and cellular biology *14*, 1613-1625.
Neale, M.J., and Keeney, S. (2009). End-labeling and analysis of Spo11-oligonucleotide complexes in Saccharomyces cerevisiae. Methods in molecular biology (Clifton, NJ) *557*, 183-195.
Neiman, A.M. (2011). Sporulation in the budding yeast Saccharomyces cerevisiae. Genetics *189*, 737-765.
Ngo, G.H., Balakrishnan, L., Dubarry, M., Campbell, J.L., and Lydall, D. (2014). The 9-1-1 checkpoint clamp stimulates DNA resection by Dna2-Sgs1 and Exo1. Nucleic acids research *42*, 10516-10528.
Niu, H. (2007). Mek1 Regulates Partner CHoice during emiotic recombination in yeast. Ph D thesis, Stony Brook University.
Niu, H., Li, X., Job, E., Park, C., Moazed, D., Gygi, S.P., and Hollingsworth, N.M. (2007). Mek1 kinase is regulated to suppress double-strand break repair between sister chromatids during budding yeast meiosis. Molecular and cellular biology *27*, 5456-5467.
Niu, H., Wan, L., Baumgartner, B., Schaefer, D., Loidl, J., and Hollingsworth, N.M. (2005). Partner choice during meiosis is regulated by Hop1-promoted dimerization of Mek1. Molecular biology of the cell *16*, 5804-5818.
Niu, H., Wan, L., Busygina, V., Kwon, Y., Allen, J.A., Li, X., Kunz, R.C., Kubota, K., Wang, B., Sung, P.*, et al.* (2009). Regulation of meiotic recombination via Mek1-mediated Rad54 phosphorylation. Molecular cell *36*, 393-404.
Oh, S.D., Lao, J.P., Hwang, P.Y., Taylor, A.F., Smith, G.R., and Hunter, N. (2007). BLM ortholog, Sgs1, prevents aberrant crossing-over by suppressing formation of multichromatid joint molecules. Cell *130*, 259-272.
Ong, S.E., Blagoev, B., Kratchmarova, I., Kristensen, D.B., Steen, H., Pandey, A., and Mann, M. (2002). Stable isotope labeling by amino acids in cell culture, SILAC, as a simple and accurate approach to expression proteomics. Molecular & cellular proteomics : MCP *1*, 376-386.
Onodera, J., and Ohsumi, Y. (2005). Autophagy is required for maintenance of amino acid levels and protein synthesis under nitrogen starvation. The Journal of biological chemistry *280*, 31582-31586.
Padmore, R., Cao, L., and Kleckner, N.R. (1991). Temporal comparison of recombination and synaptonemal complex formation during meiosis in *Saccharomyces cerevisiae*. Cell *66*, 1239-1256.
Page, S.L., and Hawley, R.S. (2004). The genetics and molecular biology of the synaptonemal complex. Annual review of cell and developmental biology *20*, 525-558.
Pan, J., and Keeney, S. (2007). Molecular cartography: mapping the landscape of meiotic recombination. PLoS biology *5*, e333.
Pan, J., and Keeney, S. (2009). Detection of SPO11-oligonucleotide complexes from mouse testes. Methods in molecular biology (Clifton, NJ) *557*, 197-207.

Pangas, S.A., Yan, W., Matzuk, M.M., and Rajkovic, A. (2004). Restricted germ cell expression of a gene encoding a novel mammalian HORMA domain-containing protein. Gene expression patterns : GEP *5*, 257-263.
Panizza, S., Mendoza, M.A., Berlinger, M., Huang, L., Nicolas, A., Shirahige, K., and Klein, F. (2011). Spo11-accessory proteins link double-strand break sites to the chromosome axis in early meiotic recombination. Cell *146*, 372-383.
Pauling, M.H., McPheeters, D.S., and Ares, M., Jr. (2000). Functional Cus1p is found with Hsh155p in a multiprotein splicing factor associated with U2 snRNA. Molecular and cellular biology *20*, 2176-2185.
Petronczki, M., Siomos, M.F., and Nasmyth, K. (2003). Un menage a quatre: the molecular biology of chromosome segregation in meiosis. Cell *112*, 423-440.
PhoshoGRID (2015).
Posewitz, M.C., and Tempst, P. (1999). Immobilized gallium(III) affinity chromatography of phosphopeptides. Analytical chemistry *71*, 2883-2892.
Primig, M., Williams, R.M., Winzeler, E.A., Tevzadze, G.G., Conway, A.R., Hwang, S.Y., Davis, R.W., and Esposito, R.E. (2000). The core meiotic transcriptome in budding yeasts. Nature genetics *26*, 415-423.
Rockmill, B., and Roeder, G.S. (1991). A meiosis-specific protein kinase homolog required for chromosome synapsis and recombination. Genes & development *5*, 2392-2404.
Rose, M.D., Winston, F., and Heiter, P. (1990). Methods in Yeast Genetics: A laboratory course manual (Cold Spring Harbor: Cold Spring Harbor Laboratory Press).
Sanchez, Y., Desany, B.A., Jones, W.J., Liu, Q., Wang, B., and Elledge, S.J. (1996). Regulation of RAD53 by the ATM-like kinases MEC1 and TEL1 in yeast cell cycle checkpoint pathways. Science (New York, NY) *271*, 357-360.
Sardana, R., Zhu, J., Gill, M., and Johnson, A.W. (2014). Physical and functional interaction between the methyltransferase Bud23 and the essential DEAH-box RNA helicase Ecm16. Molecular and cellular biology *34*, 2208-2220.
Sasanuma, H., Hirota, K., Fukuda, T., Kakusho, N., Kugou, K., Kawasaki, Y., Shibata, T., Masai, H., and Ohta, K. (2008). Cdc7-dependent phosphorylation of Mer2 facilitates initiation of yeast meiotic recombination. Genes & development *22*, 398-410.
Schulze, J.M., Kane, C.M., and Ruiz-Manzano, A. (2010). The YEATS domain of Taf14 in Saccharomyces cerevisiae has a negative impact on cell growth. Molecular genetics and genomics : MGG *283*, 365-380.
Schulze, W.X., Deng, L., and Mann, M. (2005). Phosphotyrosine interactome of the ErbB-receptor kinase family. Molecular systems biology *1*, 2005.0008.
Schulze, W.X., and Mann, M. (2004). A novel proteomic screen for peptide-protein interactions. The Journal of biological chemistry *279*, 10756-10764.
Schwacha, A., and Kleckner, N. (1994). Identification of joint molecules that form frequently between homologs but rarely between sister chromatids during yeast meiosis. Cell *76*, 51-63.
Schwacha, A., and Kleckner, N. (1995). Identification of double Holliday junctions as intermediates in meiotic recombination. Cell *83*, 783-791.
Schwacha, A., and Kleckner, N. (1997). Interhomolog bias during meiotic recombination: meiotic functions promote a highly differentiated interhomolog-only pathway. Cell *90*, 1123-1135.
Schwartz, D., and Gygi, S.P. (2005). An iterative statistical approach to the identification of protein phosphorylation motifs from large-scale data sets. Nature biotechnology *23*, 1391-1398.
Shi, X., Kachirskaia, I., Walter, K.L., Kuo, J.H., Lake, A., Davrazou, F., Chan, S.M., Martin, D.G., Fingerman, I.M., Briggs, S.D*., et al.* (2007). Proteome-wide analysis in Saccharomyces cerevisiae identifies several PHD fingers as novel direct and selective binding modules of histone H3 methylated at either lysine 4 or lysine 36. The Journal of biological chemistry *282*, 2450-2455.

Shilatifard, A. (2012). The COMPASS family of histone H3K4 methylases: mechanisms of regulation in development and disease pathogenesis. Annual review of biochemistry *81*, 65-95.
Shin, M.E., Skokotas, A., and Winter, E. (2010). The Cdk1 and Ime2 protein kinases trigger exit from meiotic prophase in Saccharomyces cerevisiae by inhibiting the Sum1 transcriptional repressor. Molecular and cellular biology *30*, 2996-3003.
Shinohara, M., Hayashihara, K., Grubb, J.T., Bishop, D.K., and Shinohara, A. (2015). DNA damage response clamp 9-1-1 promotes assembly of ZMM proteins for formation of crossovers and synaptonemal complex. Journal of cell science *128*, 1494-1506.
Shinohara, M., Oh, S.D., Hunter, N., and Shinohara, A. (2008). Crossover assurance and crossover interference are distinctly regulated by the ZMM proteins during yeast meiosis. Nature genetics *40*, 299-309.
Shiomi, Y., Shinozaki, A., Nakada, D., Sugimoto, K., Usukura, J., Obuse, C., and Tsurimoto, T. (2002). Clamp and clamp loader structures of the human checkpoint protein complexes, Rad9-1-1 and Rad17-RFC. Genes to cells : devoted to molecular & cellular mechanisms *7*, 861-868.
Shonn, M.A., McCarroll, R., and Murray, A.W. (2000). Requirement of the spindle checkpoint for proper chromosome segregation in budding yeast meiosis. Science (New York, NY) *289*, 300-303.
Smith, A.V., and Roeder, G.S. (1997). The yeast Red1 protein localizes to the cores of meiotic chromosomes. The Journal of cell biology *136*, 957-967.
Sommermeyer, V., Beneut, C., Chaplais, E., Serrentino, M.E., and Borde, V. (2013). Spp1, a member of the Set1 Complex, promotes meiotic DSB formation in promoters by tethering histone H3K4 methylation sites to chromosome axes. Molecular cell *49*, 43-54.
Sourirajan, A., and Lichten, M. (2008). Polo-like kinase Cdc5 drives exit from pachytene during budding yeast meiosis. Genes & development *22*, 2627-2632.
Storlazzi, A., Xu, L., Cao, L., and Kleckner, N. (1995). Crossover and noncrossover recombination during meiosis: timing and pathway relationships. Proceedings of the National Academy of Sciences of the United States of America *92*, 8512-8516.
Sturtevant, A.H. (1913). A THIRD GROUP OF LINKED GENES IN DROSOPHILA AMPELOPHILA. Science (New York, NY) *37*, 990-992.
Subramanian, V.V., and Hochwagen, A. (2014). The meiotic checkpoint network: step-by-step through meiotic prophase. Cold Spring Harbor perspectives in biology *6*, a016675.
Suhandynata, R., Liang, J., Albuquerque, C.P., Zhou, H., and Hollingsworth, N.M. (2014). A method for sporulating budding yeast cells that allows for unbiased identification of kinase substrates using stable isotope labeling by amino acids in cell culture. G3 (Bethesda, Md) *4*, 2125-2135.
Suhandynata, R.T., Wan, L., Zhou, H., and Hollingsworth, N.M. (2016). Identification of Putative Mek1 Substrates during Meiosis in Saccharomyces cerevisiae Using Quantitative Phosphoproteomics. PloS one *11*, e0155931.
Sun, H., Treco, D., and Szostak, J.W. (1991). Extensive 3'-overhanging, single-stranded DNA associated with the meiosis-specific double-strand breaks at the ARG4 recombination initiation site. Cell *64*, 1155-1161.
Sun, Z., Fay, D.S., Marini, F., Foiani, M., and Stern, D.F. (1996). Spk1/Rad53 is regulated by Mec1-dependent protein phosphorylation in DNA replication and damage checkpoint pathways. Genes & development *10*, 395-406.
Sury, M.D., Chen, J.X., and Selbach, M. (2010). The SILAC fly allows for accurate protein quantification in vivo. Molecular & cellular proteomics : MCP *9*, 2173-2183.
Sym, M., and Roeder, G.S. (1994). Crossover interference is abolished in the absence of a synaptonemal complex protein. Cell *79*, 283-292.

Sym, M., and Roeder, G.S. (1995). Zip1-induced changes in synaptonemal complex structure and polycomplex assembly. The Journal of cell biology *128*, 455-466.
Tang, S., Wu, M.K., Zhang, R., and Hunter, N. (2015). Pervasive and essential roles of the Top3-Rmi1 decatenase orchestrate recombination and facilitate chromosome segregation in meiosis. Molecular cell *57*, 607-621.
Thacker, D., Mohibullah, N., Zhu, X., and Keeney, S. (2014). Homologue engagement controls meiotic DNA break number and distribution. Nature *510*, 241-246.
Thingholm, T.E., and Jensen, O.N. (2009). Enrichment and characterization of phosphopeptides by immobilized metal affinity chromatography (IMAC) and mass spectrometry. Methods in molecular biology (Clifton, NJ) *527*, 47-56, xi.
Thompson, A., Schafer, J., Kuhn, K., Kienle, S., Schwarz, J., Schmidt, G., Neumann, T., Johnstone, R., Mohammed, A.K., and Hamon, C. (2003). Tandem mass tags: a novel quantification strategy for comparative analysis of complex protein mixtures by MS/MS. Analytical chemistry *75*, 1895-1904.
Thompson, D.A., and Stahl, F.W. (1999). Genetic control of recombination partner preference in yeast meiosis. Isolation and characterization of mutants elevated for meiotic unequal sister-chromatid recombination. Genetics *153*, 621-641.
Thompson, E.A., and Roeder, G.S. (1989). Expression and DNA sequence of RED1, a gene required for meiosis I chromosome segregation in yeast. Molecular & general genetics : MGG *218*, 293-301.
Traven, A., and Heierhorst, J. (2005). SQ/TQ cluster domains: concentrated ATM/ATR kinase phosphorylation site regions in DNA-damage-response proteins. BioEssays : news and reviews in molecular, cellular and developmental biology *27*, 397-407.
Tsubouchi, H., and Roeder, G.S. (2006). Budding yeast Hed1 down-regulates the mitotic recombination machinery when meiotic recombination is impaired. Genes & development *20*, 1766-1775.
Tung, K.S., and Roeder, G.S. (1998). Meiotic chromosome morphology and behavior in zip1 mutants of Saccharomyces cerevisiae. Genetics *149*, 817-832.
Usui, T., Ogawa, H., and Petrini, J.H. (2001). A DNA damage response pathway controlled by Tel1 and the Mre11 complex. Molecular cell *7*, 1255-1266.
Vicente-Munoz, S., Romero, P., Magraner-Pardo, L., Martinez-Jimenez, C.P., Tordera, V., and Pamblanco, M. (2014). Comprehensive analysis of interacting proteins and genome-wide location studies of the Sas3-dependent NuA3 histone acetyltransferase complex. FEBS open bio *4*, 996-1006.
Villeneuve, A.M., and Hillers, K.J. (2001). Whence meiosis? Cell *106*, 647-650.
Wan, L., de los Santos, T., Zhang, C., Shokat, K., and Hollingsworth, N.M. (2004). Mek1 kinase activity functions downstream of *RED1* in the regulation of meiotic DSB repair in budding yeast. Mol Biol Cell *15*, 11-23.
Wan, L., Niu, H., Futcher, B., Zhang, C., Shokat, K.M., Boulton, S.J., and Hollingsworth, N.M. (2008). Cdc28-Clb5 (CDK-S) and Cdc7-Dbf4 (DDK) collaborate to initiate meiotic recombination in yeast. Genes & development *22*, 386-397.
Wan, L., Zhang, C., Shokat, K.M., and Hollingsworth, N.M. (2006). Chemical inactivation of Cdc7 kinase in budding yeast results in a reversible arrest that allows efficient cell synchronization prior to meiotic recombination. Genetics *174*, 1667-1774.
Webb, K.J., Laganowsky, A., Whitelegge, J.P., and Clarke, S.G. (2008). Identification of two SET domain proteins required for methylation of lysine residues in yeast ribosomal protein Rpl42ab. The Journal of biological chemistry *283*, 35561-35568.
Welch, M.D., and Drubin, D.G. (1994). A nuclear protein with sequence similarity to proteins implicated in human acute leukemias is important for cellular morphogenesis and actin cytoskeletal function in Saccharomyces cerevisiae. Molecular biology of the cell *5*, 617-632.

Wells, S.E., Neville, M., Haynes, M., Wang, J., Igel, H., and Ares, M., Jr. (1996). CUS1, a suppressor of cold-sensitive U2 snRNA mutations, is a novel yeast splicing factor homologous to human SAP 145. Genes & development *10*, 220-232.
White, E.J., Cowan, C., Cande, W.Z., and Kaback, D.B. (2004). In vivo analysis of synaptonemal complex formation during yeast meiosis. Genetics *167*, 51-63.
Wojtasz, L., Daniel, K., Roig, I., Bolcun-Filas, E., Xu, H., Boonsanay, V., Eckmann, C.R., Cooke, H.J., Jasin, M., Keeney, S.*, et al.* (2009). Mouse HORMAD1 and HORMAD2, two conserved meiotic chromosomal proteins, are depleted from synapsed chromosome axes with the help of TRIP13 AAA-ATPase. PLoS genetics *5*, e1000702.
Wu, H.Y., Ho, H.C., and Burgess, S.M. (2010). Mek1 kinase governs outcomes of meiotic recombination and the checkpoint response. Current biology : CB *20*, 1707-1716.
Wu, T.C., and Lichten, M. (1994). Meiosis-induced double-strand break sites determined by yeast chromatin structure. Science (New York, NY) *263*, 515-518.
Xaver, M., Huang, L., Chen, D., and Klein, F. (2013). Smc5/6-Mms21 prevents and eliminates inappropriate recombination intermediates in meiosis. PLoS genetics *9*, e1004067.
Xu, L., Ajimura, M., Padmore, R., Klein, C., and Kleckner, N. (1995). *NDT80*, a meiosis-specific gene required for exit from pachytene in *Saccharomyces cerevisiae*. Mol Cell Biol *15*, 6572-6581.
Xu, L., Weiner, B.M., and Kleckner, N. (1997). Meiotic cells monitor the status of the interhomolog recombination complex. Genes & development *11*, 106-118.
Yamashita, K., Shinohara, M., and Shinohara, A. (2004). Rad6-Bre1-mediated histone H2B ubiquitylation modulates the formation of double-strand breaks during meiosis. Proceedings of the National Academy of Sciences of the United States of America *101*, 11380-11385.
Zakharyevich, K., Ma, Y., Tang, S., Hwang, P.Y., Boiteux, S., and Hunter, N. (2010). Temporally and biochemically distinct activities of Exo1 during meiosis: double-strand break resection and resolution of double Holliday junctions. Molecular cell *40*, 1001-1015.
Zakharyevich, K., Tang, S., Ma, Y., and Hunter, N. (2012). Delineation of joint molecule resolution pathways in meiosis identifies a crossover-specific resolvase. Cell *149*, 334-347.
Zhang, Z., and Reese, J.C. (2005). Molecular genetic analysis of the yeast repressor Rfx1/Crt1 reveals a novel two-step regulatory mechanism. Molecular and cellular biology *25*, 7399-7411.
Zhou, H., Albuquerque, C.P., Liang, J., Suhandynata, R.T., and Weng, S. (2010). Quantitative phosphoproteomics: New technologies and applications in the DNA damage response. Cell Cycle *9*, 3479-3484.
Zubenko, G.S., Mitchell, A.P., and Jones, E.W. (1979). Septum formation, cell division, and sporulation in mutants of yeast deficient in proteinase B. Proceedings of the National Academy of Sciences of the United States of America *76*, 2395-2399.